COMPLUTENSE UNIVERSITY OF MADRID

FACULTY OF MATHEMATICAL SCIENCES

MASTER IN ADVANCED MATHEMATICS

MATHEMATICAL MODELING AND NUMERICAL SIMULATION OF THERMAL ABLATION TREATMENTS IN HEART ARRHYTHMIAS

MASTER'S THESIS

Author:
Aitor Amatriain Carballo

Directors:
Ignacio Parra Fabián
Gonzalo Rubio Calzado

UCM Tutor:
Miguel Ángel Herrero García

June 28, 2019

Abstract

Catheter ablation is a procedure that is used to treat cardiovascular diseases, specially arrhythmias. A catheter, that is inserted through a vein, is placed in the affected area of the heart, and an electric shock is applied in order to destroy the abnormal tissue. If the temperature of the cardiac tissue exceds a certain threshold stream pops occur, and this phenomenon can lead to serious complications. Therefore, a very helpful aspect consists of obtaining the temperature distribution in the cardiac tissue.

The number of studies centered in the mathematical modelization of the problem is limited, and the existing ones lack important sections as numerical scheme validations or certain correlation justifications. This is the reason why it is necessary to extend the preceding studies, the objective being to obtain results as realistic as possible. Taking into account the previous remarks, the main goal of this work is to take a first step towards analising the problem, considering a simple three-dimensional model; in particular, assuming rotational symmetry and approximating blood velocity by mean values. Moreover, making additional simplifications the problem can be reduced to a system of two parabolic equations and two elliptic equations, both of them subjected to compatibility conditions. The system is solved numerically by means of a spectral method.

With respect to the results, the temperature values that are obtained in standard conditions are coherent. Furthermore, a parametric study of the procedure is performed, together with an assessment of the importance of several assumptions made in the model. The results section concludes with an optimal control analysis of the system.

Resumen

La ablación con catéter es un procedimiento que se emplea para tratar enfermedades cardiovasculares, especialmente arritmias. Un catéter se inserta a través de una vena, se sitúa en el área afectada del corazón y se aplica una descarga eléctrica con el objetivo de inutilizar el tejido anormal. Si la temperatura del tejido cardíaco supera un valor umbral se producen burbujas de vapor, y este fenómeno puede dar lugar a serias complicaciones. Por consiguiente, un aspecto de gran utilidad reside en la obtención de la distribución de temperatura en el tejido cardíaco.

El número de trabajos centrados en la modelización matemática del problema es limitado, y los existentes carecen de apartados importantes como de validación de esquemas numéricos o de justificación de determinadas correlaciones. Es por ello por lo que es necesario ampliar los estudios previos, con el objetivo de obtener resultados lo más realistas posibles. Teniendo en cuenta las ideas anteriores, el propósito principal de este trabajo es el de dar un primer paso a la hora de analizar el problema, considerando un modelo tridimensional sencillo; en concreto, asumiendo simetría de revolución y aproximando la velocidad de la sangre por valores medios. Asimismo, realizando simplificaciones adicionales el problema puede reducirse a un sistema de dos ecuaciones parabólicas y dos ecuaciones elípticas, ambas sometidas a condiciones de compatibilidad. Dicho sistema se resuelve numéricamente por medio de un método espectral.

En lo que respecta los resultados, los valores de temperatura que se obtienen en condiciones estándar son coherentes. Además, se realiza un estudio paramétrico del procedimiento, junto con una valoración de la importancia que poseen varias de las hipótesis realizadas en el modelo. El apartado de resultados concluye con un análisis sobre el control óptimo del sistema.

Résumé

L'ablation par cathéter est une procédure utilisée pour traiter des maladies cardiovasculaires, spécialement des arythmies. Un cathéter est introduit à travers d'une veine, il est placée dans la zone affectée et une décharge électrique est apliquée dans l'objectif d'inutiliser le tissu anormal. Si la température du tissu cardiaque dépasse une certaine valeur seuil des bulles de vapeur sont générées, et ce phénomène peut conduire à graves complications. Par conséquent, un aspect de grande utilité réside dans l'obtention de la distribution de température dans le tissu cardiaque.

Le nombre de travaux axés sur la modélisation mathématique du problem es limité, et les existants manquent des sections importantes comme de validation des schémas numériques ou de justification de certaines corrélations. C'est pourquoi il est nécessaire d'élargir les études préliminaires, avec le principal but d'obtenir des résultats les plus réalistes possible. En tenant compte les idées ci-dessus, l'objectif principal de ce travail est de faire un primer pas pour l'analyse du problème, en considerant un modèle tridimensionnel simple; en particulier, en assumant symétrie rotationnelle et en rapprochant la vitesse du sang par valeurs mesurées. De plus, en effectuant des simplifications additionnels il est possible de réduire le problème a un système de deux équations paraboliques et deux elliptiques, les deux sujets à conditions de compatibilité. Ce système est résolu numériquement grâce à une méthode spectral.

En ce qui concerne les resultats, les valeurs de température qui sont obtenues dans des conditions standard sont cohérentes. En outre, une étude paramétrique de la procédure est réalisée, avec une évaluation de l'importance qui possèdent plusieurs hypothèses effectuées dans le modèle. La section résultats conclut avec un analyse sur la commande optimale du système.

Contents

Nomenclature

DIMENSIONAL VARIABLES

Symbol	Description	Units
$\vec{B}$	Magnetic field	T
$\vec{E}$	Electric field	N/C
e	Internal energy	J/kg
$\vec{f}_m$	Mass forces	m/s^2
$\vec{J}$	Current density	A/m^2
Q	Heat generated by an external source	W/m
q	Heat flux	W/m^2
r	Radial coordinate	m
T	Temperature	K
t	Time	s
V	Voltage	V
$\vec{v}$	Velocity	m/s
θ, φ	Polar coordinates	rad
ρ	Density	kg/m^3
τ	Viscous stress tensor	Pa/m
ω	Angular frequency	Hz

DIMENSIONLESS VARIABLES

Symbol	Description	Definition
s	Radial coordinate	r/ϵ
$\tilde{t}$	Time	$\alpha_{t_0} t/\varepsilon^2$
$\mathcal{V}$	Voltage	V/V_0
Θ	Temperature	$\dfrac{T - T_0}{T_e - T_0}$

DIMENSIONAL PARAMETERS

Symbol	Description	Units
c	Specific heat capacity	$\mathrm{J}/(\mathrm{kg}\cdot\mathrm{K})$
c	Speed of light	$\mathrm{m/s}$
h	Heat transfer coefficient	$\mathrm{W}/(\mathrm{m}^2\cdot\mathrm{K})$
k	Thermal conductivity	$\mathrm{W}/(\mathrm{m}\cdot\mathrm{K})$
T_e	Water boiling temperature	K
T_0	Human body temperature	K
t_d	Discharge time	s
V_0	Voltage amplitude	V
w	Perfusion frequency	Hz
α	Thermal diffusivity	m^2/s
ϵ_o	Vacuum permitivity	F/m
ε	Catheter radius	m
μ_o	Vacuum permeability	H/m
ρ_e	Charge density	C/m^3
σ	Electrical conductivity	S/m
ω	Catheter frequency	Hz

DIMENSIONLESS PARAMETERS

Symbol	Description	Definition
Bi	Biot number	$h\varepsilon/k$
$\tilde{c}_b$	Blood specific heat capacity	c_b/c_t
D	Derivation matrix	$-$
$\tilde{k}$	Heart tissue thermal conductivity	$\tilde{k}_0+\tilde{k}_1\Theta$
$\tilde{k}_b$	Blood thermal conductivity	k_b/k_0
$\tilde{k}_1$	Percentage increase of $\tilde{k}$	k_1/k_0
N	Chebyshev polynomial order	$-$
$\tilde{v}$	Velocity	$\varepsilon v/\alpha_b$
$\tilde{w}$	Perfusion frequency	$\rho_b c_b \varepsilon^2 w/k_0$
$\tilde{\alpha}_b$	Blood thermal diffusivity	$\tilde{k}_b/(\tilde{\rho}_b\tilde{c}_b)$

$\tilde{\rho}_b$	Blood density	ρ_b/ρ_t
$\tilde{\sigma}$	Heart tissue electrical conductivity	$\tilde{\sigma}_0 + \tilde{\sigma}_1\Theta$
$\tilde{\sigma}_b$	Blood electrical conductivity	σ_b/σ_0
$\tilde{\sigma}_0$	Heart tissue electrical conductivity at $T = T_0$	$\dfrac{\sigma_1 V_0^2}{k_0(T_e - T_0)}$
$\tilde{\sigma}_1$	Heart tissue percentage increase of electrical conductivity	$\sigma_1 V_0^2/k_0$

SUBINDEXES

Subindex	**Description**	**Units**
b	Blood	–
c	Catheter	–
m	Medium	–
t	Heart tissue	–
0	Initial time	–

FUNCTION SPACES

Space	**Definition**	**Exponent**
$C(\Omega)$	$\{f : \Omega \to \mathbb{R} \mid f \text{ is continuous}\}$	–
$C([0,\mathcal{T}];\Omega)$	$\{f : [0,\mathcal{T}] \to \Omega \mid f \text{ is continuous and } \|\|f\|\|_{C([0,\mathcal{T}];\Omega)} < \infty\}$	–
$C(\bar{\Omega})$	$\{f : \Omega \to \mathbb{R} \mid f \text{ is uniformly continuous}\}$	–
$C^k(\Omega)$	$\{f : \Omega \to \mathbb{R} \mid f \text{ is } k \text{ times continuously differentiable}\}$	$0 \leq k < \infty$
$C^\infty(\Omega)$	$\{f : \Omega \to \mathbb{R} \mid f \text{ is infinitely differentiable}\}$	–
$C_c^k(\Omega)$	$\{f \in C^k(\Omega) \mid f \text{ has compact support}\}$	$1 \leq k \leq \infty$
$D^\alpha f$	$\int_\Omega D^\alpha \psi \, \mathrm{d}x = (-1)^{\lvert\alpha\rvert} \int_\Omega D^\alpha f \phi \, \mathrm{d}x, \ \phi \in C_c^\infty(\Omega), \ f \in C^k(\Omega)$	$0 \leq \alpha \leq \infty, \ k \in \mathbb{Z}^+$
f'	$f' = g$ if $\int_0^{\mathcal{T}} \phi'(t) f(t) \, \mathrm{d}t = -\int_0^{\mathcal{T}} \phi(t) g(t) \, \mathrm{d}t \ \forall \phi \in C_c^\infty(0,\mathcal{T})$	$k \in \mathbb{Z}^+$
$H^k(\Omega)$	$W^{k,2}(\Omega)$	$k \in \mathbb{Z}^+$
$H^{1/2}(\Omega)$	$\{f \in L^2(\partial\Omega) \mid \exists \tilde{f} \in H^1(\Omega) : f = \mathrm{Tr}\ \tilde{f}\}$	–
$H_0^k(\Omega)$	$W_0^{k,2}(\Omega)$	$k \in \mathbb{Z}^+$
$H^{-1/2}(\Omega)$	Dual space of $H^{1/2}(\Omega)$	–
$H^{-1}(\Omega)$	Dual space of $H_0^1(\Omega)$	–
$H^k(0,\mathcal{T};\Omega)$	$W^{k,2}(0,\mathcal{T};\Omega)$	$k \in \mathbb{Z}^+$

$L^0(\Omega)$	$\{f : \Omega \to \mathbb{R} \mid f \text{ is Lebesgue measurable}\}$	–
$L^p(\Omega)$	$\{f : \Omega \to \mathbb{R} \mid f \in L^0(\Omega) \text{ and } \|\|f\|\|_{L^p(\Omega)} < \infty\}$	$1 \le p \le \infty$
$L^0(0,\mathcal{T};\Omega)$	$\{f : [0,\mathcal{T}] \to \Omega \mid f \text{ is Lebesgue measurable}\}$	
$L^p(0,\mathcal{T};\Omega)$	$\{f : [0,\mathcal{T}] \to \Omega \mid f \in L^0(0,\mathcal{T};\Omega) \text{ and } \|\|f\|\|_{L^p(0,\mathcal{T};\Omega)} < \infty\}$	$1 \le p \le \infty$
Tr f	$f\|_{\partial\Omega}$ if $f \in W^{1,p}(\Omega) \cap C(\bar{\Omega})$	$1 \le p \le \infty$
$W^{k,p}(\Omega)$	$\{f : \Omega \to \mathbb{R} \mid \forall \alpha,\ \|\alpha\| \le k,\ \|\|D^\alpha f\|\|_{L^p(\Omega)} < \infty\}$	$1 \le p \le \infty,\ k \in \mathbb{Z}^+$
$W_0^{k,p}(\Omega)$	$\{f : \Omega \to \mathbb{R} \mid f \in W^{k,p}(\Omega),\ \text{Tr } f = 0 \text{ on } \partial\Omega \text{ and } \partial\Omega \text{ is } C^1\}$	$1 \le p \le \infty,\ k \in \mathbb{Z}^+$
$W^{1,p}(0,\mathcal{T};\Omega)$	$\{f \in L^p(0,\mathcal{T};\Omega) \mid f' \text{ exists and } \|\|f\|\|_{L^p(0,\mathcal{T};\Omega)} < \infty\}$	$1 \le p \le \infty$

NORMS

Space	**Norm**	**Exponent**
$C(\Omega)$	$\sup_{x\in\Omega} \|f(x)\|$	–
$C([0,\mathcal{T}];\Omega)$	$\max_{0\le t\le\mathcal{T}} \|\|f(t)\|\| < \infty$	–
$C(\bar{\Omega})$	$\sup_{x\in\Omega} \|f(x)\|$	–
$C^k(\Omega)$	$\sum_{i=0}^k \sup_{x\in\Omega} \|f^{(i)}(x)\|$	$1 \le k < \infty$
$C^\infty(\Omega)$	$\sup_{x\in\Omega} \|f(x)\|$	–
$C_c^k(\Omega)$	$\sum_{i=0}^k \sup_{x\in\Omega} \|f^{(i)}(x)\|$	$1 \le k < \infty$
$H^{1/2}(\Omega)$	$\inf\{\|\|\tilde{f}\|\|_{H^1(\Omega)} \mid \text{Tr } \tilde{f} = f\}$	–
$L^p(\Omega)$	$\left(\int_\Omega \|f(x)\|^p \, \mathrm{d}x\right)^{1/p}$	$1 \le p < \infty$
$L^\infty(\Omega)$	$\text{ess sup}_{x\in\Omega} \|f(x)\|$	–
$L^p(0,\mathcal{T};\Omega)$	$\left(\int_0^\mathcal{T} \|\|f(t)\|\|^p \, \mathrm{d}t\right)^{1/p}$	$1 \le p < \infty$
$L^\infty(0,\mathcal{T};\Omega)$	$\text{ess sup}_{0\le t\le\mathcal{T}} \|\|f(t)\|\|$	–
$W^{k,p}(\Omega)$	$\left(\sum_{\|\alpha\|\le k} \int_\Omega \|D^\alpha f\|^p \, \mathrm{d}x\right)^{1/p}$	$1 \le p \le \infty,\ k \in \mathbb{Z}^+$
$W^{k,\infty}(\Omega)$	$\sum_{\|\alpha\|\le k} \text{ess sup}_\Omega \|D^\alpha f\|$	$k \in \mathbb{Z}^+$
$W_0^{k,p}(\Omega)$	$\left(\sum_{\|\alpha\|\le k} \int_\Omega \|D^\alpha f\|^p \, \mathrm{d}x\right)^{1/p}$	$1 \le p \le \infty,\ k \in \mathbb{Z}^+$
$W_0^{k,\infty}(\Omega)$	$\sum_{\|\alpha\|\le k} \text{ess sup}_\Omega \|D^\alpha f\|$	$k \in \mathbb{Z}^+$
$W^{1,p}(0,\mathcal{T};\Omega)$	$\left(\int_0^T \|\|f(t)\|\|^p + \|\|f'(t)\|\|^p \, \mathrm{d}t\right)^{1/p}$	$1 \le p < \infty$
$W^{1,\infty}(0,\mathcal{T};\Omega)$	$\text{ess sup}_{0\le t\le\mathcal{T}}(\|\|f(t)\|\| + \|\|f'(t)\|\|)$	–

Chapter 1

Introduction

Myocardial contraction and relaxation are produced through electrical impulses, which are transmitted by means of pacemaker cells. If they do not work correctly spurious oscillations can be produced, which can lead to cardiac diseases as arrhythmias.

A cardiac arrhythmia is a disorder of the heart rhythm. There exist different types of arrhythmias, depending on the affected zone and the changes in the heart rate, even though the most common one is atrial fibrillation. One of the indicators of atrial fibrillation is the absence of P-waves in the electrocardiogram, although in the cases that it is intermitent a modification in the wave morphology is produced, and further research is needed in order to perform an adequate diagnosis [Carlson, Johansson and Olsson, 2001].

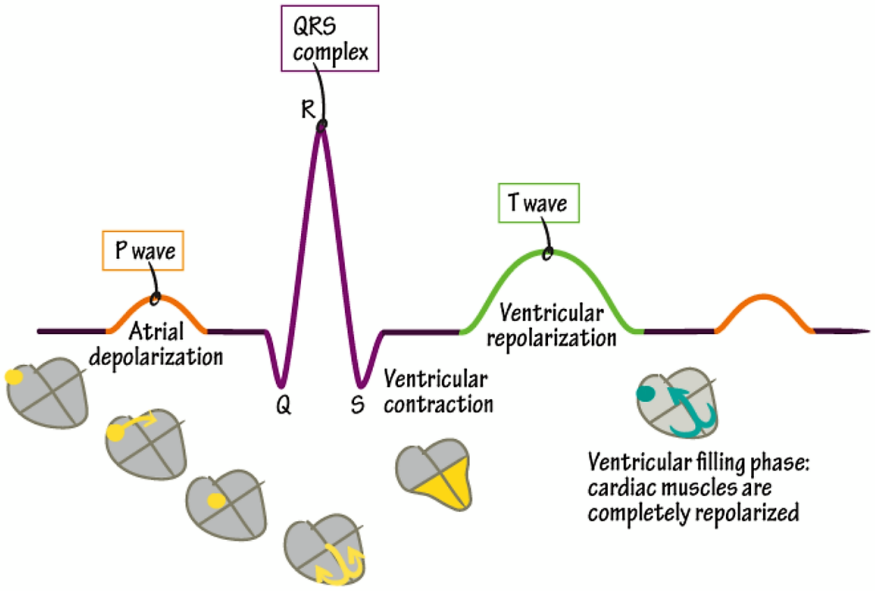

FIGURE 1.1: Waves of an electrocardiogram of a healthy patient [16].

The prevalence of atrial fibrillation in 2010 ranged from 2.7 to 6.1 million people in the USA, while in the European Union it was estimated that it was present in 8.8 million adults older than 55 years [Benjamin *et al.*, 2019]. Age accentuates the risk of suffering an arrhythmia, so this numbers rise every year as a consequence of the increase in life expectancy. Currently, atrial fibrillation is found in 9% of people over the age of 65.

The importance and the treatment of arrhythmias depends on the type of disorder and the patient. Focusing attention on cases that are not severe, until the 80s the only treatment consisted of lifetime medication. It was necessary to develop more effective and comfortable solutions for the patient, taking into account that there exist cases of intolerance to antiarrhythmic medication. This became a reality thanks to catheter ablation procedure, which has been recommended by experts in 2012 guidelines [Calkins *et al.*, 2012].

Catheters started to be employed in the 60s, the main objective being intracardiac stimulation [Joseph and Rajappan, 2011]. In particular, in 2000 it was shown that it was possible to induce arrhythmias by means of electrical stimulation, to subsequently carry out procedures of cardiac surgery [Durrer *et al.*, 1967]. Moreover, over the years it became clear that ablations were also an effective method to cure arrhythmias, by disabling the cells that do not work properly as a result of temperature rise. In this line, the first catheter ablation in humans was performed in 1981 by the american cardiologist Melvin Scheinman; the intervention was a complete success, and the same medical team performed subsequent ablations for treating, for example, the Wolff-Parkinson-White syndrome [Morady and Scheinman, 1984].

As a result of using continuous current, cases of interventions that caused severe damage to the cardiac tissue initially occured. This was due to the fact that high voltages were not easy to control, so continuous current was replaced by alternate current in the 90s [Jackman *et al.*, 1991]. This modification marked a major step forward because ablations can be conducted to conscious patients and lesions are more localised. However, catheter power and discharge time remained as the only adjustable parameters, so improvements in the design of catheters emerged at that time.

At the beginning of the 90s, the first catheter equipped with temperature sensors was designed [Langberg *et al.*, 1992]. Since constant power was employed in the catheters, the authors observed that the catheter tip heated up quickly until reaching a stationary state few seconds later. Based on this fact, the first catheter equipped with a control system was developed, with the objective of varying a more relevant parameter as the catheter tip temperature [Calkins *et al.*, 1994].

In 1998, the french cardiologist Michel Haïssaguerre analised the use of catheter ablation to treat atrial fibrillation [Haïssaguerre *et al.*, 1998]. By injecting adrenaline to the patient, in many cases it was possible to detect the zones that generated high-frequency oscillations, to later ablate them by means of the so-called pulmonary vein isolation. In 95-96% of the cases the zones were located at the beginning of the pulmonary veins, and the rate of success after 8 months was 62%.

One of the problems that arised with the previously mentioned procedure was pulmonary vein stenosis [Packer *et al.*, 2005], although the reported incidence in this study is variable, ranging from 4% and 42%. Nevertheless, several results from further studies about the electrical properties of the pulmonary veins [Kumagai *et al.*, 2004] enabled the development of new procedures, with the goal of isolating electrically the pulmonary vein [Ouyang *et al.*, 2004]. This became possible ablating adjacent zones, and, consequently, reducing the occurrence of the previous complication.

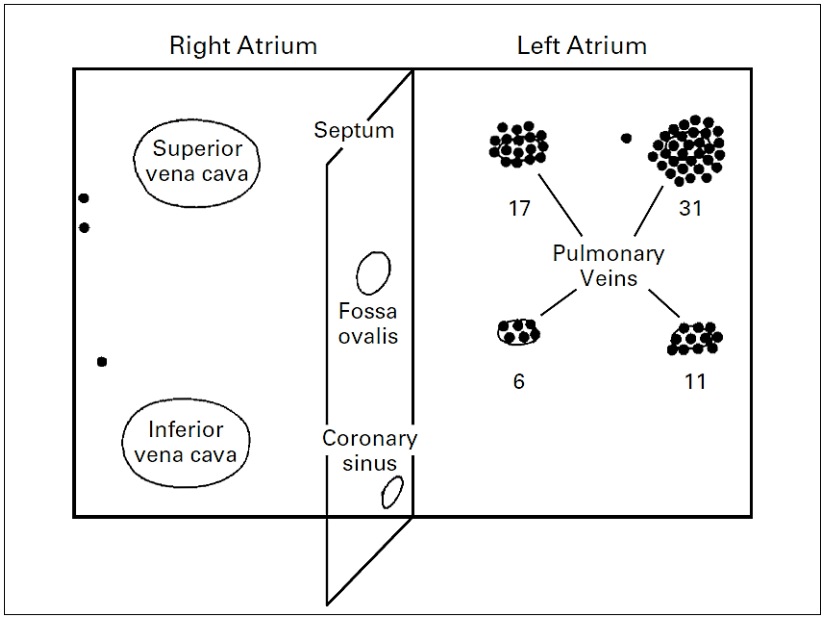

FIGURE 1.2: Generation zones of the atrial fibrillation [27].

Despite the fact that the new approach reduced the number of cases of pulmonary vein stenosis, in some patients (for example, when the esophagus is very close) it is obligatory to perform the ablation in the pulmonary vein [Almendral and Barrio-López, 2015]. For this reason, new investigations in this area have been conducted, deducing that occurrence is exceptional with the current techniques [Martín-Garre *et al.*, 2015].

As the number of interventions has increased, structural changes in the mediastine have been detected in the last 10 years [Zellerhopf *et al.*, 2010]. Even though the risk is lower than 1%, a complication that can occur is the development of an atrio-esophageal fistula, whose derived mortality rates are very high [Ghia *et al.*, 2009]. Researches based on catheter power reductions have been made, although esophagus lesions have continued to be detected [Rillig *et al.*, 2015], mainly due to the fact that the distance between the esophagus and the ablated zone is small in some people. In detail, a study conducted to 45 dead people concluded that in the 40% of the cases the distance between the endocardium and the esophagus was less than 5mm [Sánchez *et al.*, 2005].

The solution of the complications related to the esophagus came by means of the use of luminal temperature sensors, that is, measuring devices of the temperature inside the esophagus. Temperature variations are usually small, although values greater than 40°C can produce esophageal ulcers [Halm *et al.*, 2010]. It should also be taken into consideration that luminal temperature is not always the maximum temperature, as greater values of temperature can be achieved in the walls of the esophagus [Knecht *et al.*, 2017].

Another important matter that has been dealt with is if temperature sensors could be harmful for the esophagus, as a consequence of energy absorption [Deneke *et al.*, 2011]. However, recent studies have shown that esophageal temperature sensors are safe and necessary [Fasano *et al.*, 2016]. It has also been concluded that the maximum admisible response time of the sensors should be 4 seconds, with the aim of being capable of reacting safely to fast esophageal temperature variations [Anfuso, Corsi and Fasano, 2018].

Despite knowing the catheter tip temperature, if the contact force between the surface of the catheter and the cardiac tissue is reduced, heat transfer is not effective. On the contrary, if the force is high, the produced lesions can be too wide. This is the reason why it is being worked on contact-force-sensor-equipped catheters since the late 90s. In this line, first approaches were focused on computing the contact force by means of base impedance measures and catheter tip temperature data [Avitall *et al.*, 1997], although the accuracy of these methods has not been sufficiently validated.

Using constant-power catheters, further studies in dogs have analised the influence of the contact force in cardiac tissue temperature distribution [Yokoyama *et al.*, 2008]. This has been possible by introducing temperature sensors located at a distance of 3mm and 7mm from the catheter surface. Moreover, additional investigations have been conducted about the importance of the contact force between the catheter and the cardiac tissue [Kuck *et al.*, 2012], confirming that the data of the contact force allows the ablation to be more safe, and the possible complications decrease [Qi *et al.*, 2016].

With respect to to the mathematical modelization of the ablation procedure, previous studies have been made as [Kaouk *et al.*, 1996], [Tungjitkusolmun *et al.*, 2002] and [Schutt *et al.*, 2009]. However, those works have some shortcomings:

- The boundary conditions on the catheter-tissue and tissue-blood interfaces that are used are Robin-type, and the values of heat transfer coefficients are not justified.
- Nearly all the models are two-dimensional.
- In the majority of the articles it is not analised the temperature distribution in the zones where the esophagus can be located. In [Kaouk *et al*, 1996] a similar study is performed, even though temperatures greater than 40°C (the limit temperature at the esophagus) are considered.
- The effect of the contact force is not analised.
- Validated numerical schemes have not been observed.

The main objetive of this master thesis is to take a first step towards a future complete model, where [González-Suárez *et al.*, 2018] could serve as a good starting point. This will be done by considering a simple three-dimensional model and analising the effect of some parameters of the problem and the procedure. For that purpose, this work is divided into three sections: first of all, the statement of the problem (Chapter 2) consists of a mathematical model, accompanied by several hypotheses in order to obtain a numerically-solvable system of equations; secondly, the results corresponding to numerical simulations are presented (Chapter 3), and, finally, some conclusions and future work are drawn in Chapter 4.

Chapter 2

Statement of the problem

The problem to be solved consists of obtaining the temperature distribution in the cardiac tissue when an ablation is performed. The purpose of this chapter is to state the equations that model the behaviour of the blood and the cardiac tissue in order to achieve the goals set. To that end, firstly the system of equations in general form is presented (Section 2.1) as it is difficult to solve, some order-of-magnitude estimations and additional simplifications allow to obtain a numerically approachable system of equations in Section 2.2; then, the previous system of equations is stated in terms of dimensionless variables and parameters in Section 2.3, and, finally, numerical implementation and numerical scheme validation procedures are explained in Section [2.5.

2.1 Mathematical modeling.

The starting point in order to model the problem mathematically is the Figure 2.1, where two separated domains can be seen: the blood and the cardiac tissue.

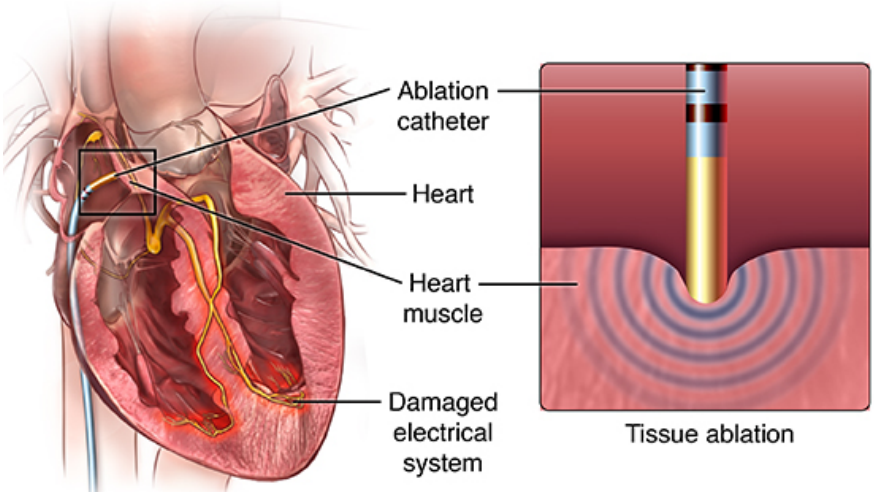

FIGURE 2.1: Catheter ablation procedure. Extracted from [54].

With respect to the equations, on the one side, the electrical problem is defined by means of Maxwell equations. Using the international system of units, these equations are as follows [Landau and Lifshitz, 1980]:

$$\begin{cases} \nabla \cdot \vec{E} = \dfrac{\rho_e}{\epsilon_o}; & (2.1) \\ \nabla \times \vec{E} = -\dfrac{\partial \vec{B}}{\partial t}; & (2.2) \\ \nabla \cdot \vec{B} = 0; & (2.3) \\ \nabla \times \vec{B} = \mu_o\Big(\vec{J} + \epsilon_o \dfrac{\partial \vec{E}}{\partial t}\Big), & (2.4) \end{cases}$$

where $\vec{E}$ is the electric field, $\vec{B}$ the magnetic field, $\vec{J}$ the current density, ρ_e the charge density, t time, $\mu_o = 4\pi \cdot 10^{-7}$ H/m the vacuum permeability and $\epsilon_o = 1/(\mu_o \mathtt{c}^2)$ F/m the vacuum permitivity, where $\mathtt{c}$ is the speed of light. Moreover, Ohm's law states the following relationship between the current density and the electric field:

$$\vec{J} = \sigma \vec{E}, \tag{2.5}$$

being σ the electrical conductivity.

The previous system of equations is completed with the Navier-Stokes equations in the blood [Landau and Lifshitz, 1987]:

$$\begin{cases} \dfrac{\partial \rho_b}{\partial t} + \nabla \cdot (\rho_b \vec{v}) = 0; & (2.6) \\ \rho_b \dfrac{\partial \vec{v}}{\partial t} + \rho_b \vec{v} \cdot \nabla \vec{v} = \nabla \cdot \tau + \rho_b \vec{f}_{mb}; & (2.7) \\ \rho_b \dfrac{\partial}{\partial t}\left(e_b + \dfrac{1}{2}v^2\right) + \vec{v} \cdot \nabla\left(e_b + \dfrac{1}{2}v^2\right) = \nabla \cdot (\tau \cdot \vec{v}) + \rho_b \vec{f}_m \cdot \vec{v} - \nabla \cdot \vec{q} + \vec{J} \cdot \vec{E} + Q, & (2.8) \end{cases}$$

and the equation of conservation of energy in the cardiac tissue:

$$\rho_t \frac{\partial e_t}{\partial t} = -\nabla \cdot \vec{q} + \vec{J} \cdot \vec{E} + Q, \tag{2.9}$$

where a term dependent of the current density has been added to the equation of conservation of energy, as a consequence of the electric field presence. With regard to the variables and the parameters involved, ρ is density, $\vec{v}$ velocity, $\vec{f}_m$ the mass forces, τ the viscous stress tensor, e the internal energy, q the heat flux and Q is the heat generated by an external source. The subindex b refers to the blood, while t denotes the cardiac tissue. The system of equations (2.1) - (2.9) has to be solved with the corresponding boundary and initial conditions.

2.2 Simplified model.

The numerical resolution of the previous system of equations is not an easy task in a general domain. Consequently, some hypotheses will be done in order to obtain a new numerically approachable system, with a reasonable computational cost.

2.2.1 Maxwell equations.

Order-of-magnitude analysis.

Taking (2.5) into account, the order of magnitude of each term of the equation (2.1) and (2.4) is estimated as follows:

$$\underbrace{\nabla \times \vec{E}}_{\frac{E}{L}} = -\underbrace{\frac{\partial \vec{B}}{\partial t}}_{B\omega} \tag{2.10}$$

$$\underbrace{\nabla \times \vec{B}}_{\frac{B}{L}} = \underbrace{\mu_o \vec{J}}_{\mu_o \sigma E} + \underbrace{\mu_o \epsilon_o \frac{\partial \vec{E}}{\partial t}}_{\mu_o \epsilon_o E \omega}, \tag{2.11}$$

where L is a characteristic length of the problem, in this case the catheter radius, $L \sim 10^{-3}$ m. Furthermore, ω is a characteristic frequency, for which the frequency of the potential generated by the catheter is chosen, $\omega \sim 10^6$ Hz. Finally, a typical electrical conductivity of human tissues, $\sigma \sim 1$ S/m will be considered. As $\mu_o \sim 10^{-7}$ and $\epsilon_o \sim 10^{-12}$, substituting the previous values in (2.11) yields the result:

$$\underbrace{\nabla \times \vec{B}}_{\frac{B}{L}} = \underbrace{\mu_o \vec{J}}_{10^{-7}E} + \underbrace{\mu_o \epsilon_o \frac{\partial \vec{E}}{\partial t}}_{10^{-13}E}, \tag{2.12}$$

that is, the first term on the right-hand side is 6 orders of magnitude greater than the second term on the right-hand side. Consequently, (2.4) is reduced to:

$$\nabla \times \vec{B} = \mu_o \vec{J}. \tag{2.13}$$

It is important to note that the term on the right-hand side of (2.13) is the driven force, as the source term of the equation of conservation of energy is proportional to $\vec{J}$ (see (2.8) and (2.9)). Consequently, this term cannot be neglected in the model. If $\nabla \times \vec{B}$ is negligible with respect to $\mu_o \vec{J}$, then $\vec{J} \approx 0$, so there would not be any source term in the equation of conservation of energy; that is, the effect of the electrical discharge produced by the catheter would not be considered. This fact allows to deduce that the values of both terms of the equation (2.13) have the same order of magnitude, that is:

$$\frac{B}{L} \sim \mu_o \sigma E \implies B \sim \mu_o \sigma E L. \tag{2.14}$$

Once a value for the characteristic magnetic field has been obtained, it can be substituted in the equation (2.10) to give

$$\underbrace{\nabla \times \vec{E}}_{\frac{E}{L}} = -\underbrace{\frac{\partial \vec{B}}{\partial t}}_{\mu_o \sigma E L \omega}, \tag{2.15}$$

so

$$\underbrace{\nabla \times \vec{E}}_{10^3 E} = - \underbrace{\frac{\partial \vec{B}}{\partial t}}_{10^{-4} E}, \tag{2.16}$$

and Maxwell-Faraday equation (2.2) can be simplified to:

$$\nabla \times \vec{E} = 0 \implies \vec{E} = \nabla V. \tag{2.17}$$

Then, applying the divergence operator to the equation (2.13):

$$\nabla \cdot (\nabla \times \vec{B}) = 0 = \mu_o (\nabla \cdot \vec{J}), \tag{2.18}$$

so, using (2.5) and (2.17), it is found that:

$$\nabla \cdot (\sigma \nabla V) = 0, \tag{2.19}$$

and Maxwell equations are simplified to (2.17) and (2.19).

2.2.2 Navier-Stokes equations.

Plasma constitutes 55% of the total volume of blood, while 92% of the total volume of plasma is water. In addition, as blood pressure is in the order of ambient pressure, it can be assumed that blood behaves like an incompressible fluid. Accordingly, it is a perfect liquid, so as in the case of the cardiac tissue, internal energy can be expressed as a function of temperature, T:

$$e = e_0 + cT, \tag{2.20}$$

where c is specific heat capacity and subidex 0 is referred as a reference state.

The components of the viscous stress tensor can be written in the way presented below:

$$\tau_{ij} = -p\delta_{ij} + \tau'_{ij}, \tag{2.21}$$

being δ_{ij} the Kronecker delta and τ' a new viscous stress tensor. It is important to note that blood does not behave as a newtonian fluid (i.e., stress tensor cannot be written as a function proportional to velocity gradient) [Bodnár, Sequeira and Prosi, 2011]. Thus, τ' does not have an inmediate expression as a function of velocity.

With regard to heat flux, if it is assumed that the fluid is statistically isotrope, Fourier's law is fulfilled:

$$\vec{q} = -k \nabla T, \tag{2.22}$$

where k is the thermal conductivity.

With the assumptions made so far and neglecting the effect of mass forces, the system of equations (2.6) - (2.9) now reads:

$$\begin{cases} \nabla \cdot \vec{v} = 0; & (2.23) \\ \rho_b \dfrac{\partial \vec{v}}{\partial t} + \rho_b \vec{v} \cdot \nabla \vec{v} = -\nabla p + \nabla \cdot \tau'; & (2.24) \\ \rho_b \dfrac{\partial}{\partial t}\left(c_b T_b + \dfrac{1}{2} v^2 \right) + \rho_b \vec{v} \cdot \nabla \left(c_b T_b + \dfrac{1}{2} v^2 \right) = \nabla \cdot (\tau \cdot \vec{v}) + \nabla \cdot (k_b \nabla T_b) + \vec{J} \cdot \vec{E}_b + Q; & (2.25) \\ \rho_t \dfrac{\partial (c_t T_t)}{\partial t} = \nabla \cdot (k_t \nabla T_t) + \vec{J}_t \cdot \vec{E}_t + Q. & (2.26) \end{cases}$$

The main goal of this work is to obtain the temperature distribution, so continuity and momentum equations will be disregarded. Therefore, on first consideration mean values of blood velocity will be introduced in the convective term of the equation of conservation of energy. Moreover, a linear model with respect to temperature is considered for the conductivities:

$$\sigma_t = \sigma_0 + \sigma_1 (T_t - T_0); \quad (2.27)$$

$$k_t = k_0 + k_1 (T_t - T_0). \quad (2.28)$$

With regard to the heat Q, it is zero in the blood, and it can be modeled as a sum of different components in the cardiac tissue:

$$Q = Q_m + Q_p = Q_m - w \rho_b c_b (T_t - T_b). \quad (2.29)$$

In the previous relation, Q_m is the heat generated by metabolic processes, while Q_p takes into account blood perfusion effects, where w is the perfusion frequency. It is worth noting that Q_q is much greater than Q_m [Berjano, 2006], so the system of equations (2.23) - (2.26) becomes:

$$\begin{cases} \rho_t c_t \dfrac{\partial T_t}{\partial t} = \nabla \cdot (k_t \nabla T_t) + \sigma_t ||\nabla V_t||^2 - w \rho_b c_b (T_t - T_b); & (2.30) \\ \rho_b c_b \dfrac{\partial T_b}{\partial t} + \rho_b c_b \vec{v} \cdot \nabla T_b = k_b \Delta T_b + \sigma_b ||\nabla V_b||^2, & (2.31) \end{cases}$$

where constant blood heat capacity and thermal conductivity have been assumed, and Ohm's (2.5) and Gauss' (2.17) laws have been used in the current density-dependent term.

2.2.3 Initial and boundary conditions.

Using spherical coordinates and assuming rotational symmetry, that is, $\partial / \partial \psi = 0$, as a first approximation a two-dimensional model will be considered, as the one from Figure 2.2. Ω is the domain of the problem and $r(\partial \Omega_{i2}) \to \infty$, $i = 1, 2$.

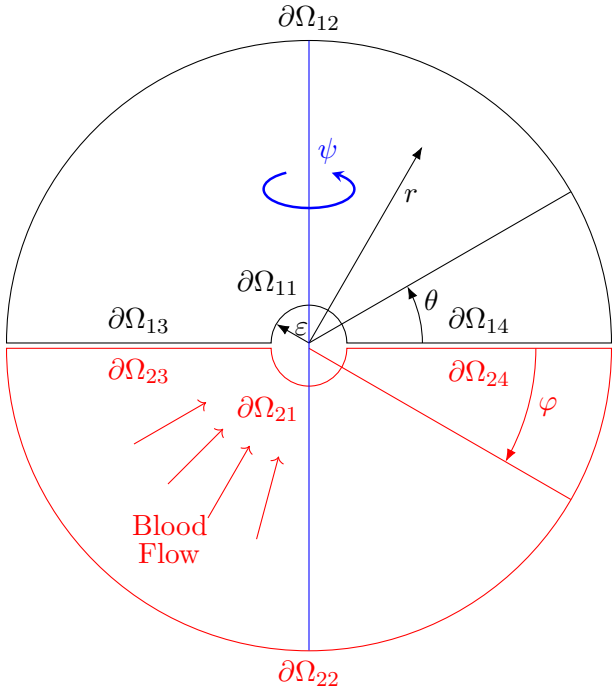

FIGURE 2.2: Domain of the problem.

As can be viewed in the previous figure, the domain has the shape of a ring, after eliminating the effect of the cylindrical component of the catheter. Moreover, r is the radial coordinate, while θ y φ are the polar coordinates in the cardiac tissue and in the blood, respectively.

Initial conditions.

Initial values for cardiac tissue and blood temperatures have to be established. It will be considered that both values are the same and equal to human body temperature, T_0:

$$T_t = T_0 \quad \text{on } \Omega_1 \times \{t = 0\}; \tag{2.32}$$
$$T_b = T_0 \quad \text{on } \Omega_2 \times \{t = 0\}. \tag{2.33}$$

Boundary conditions.

Firstly, it will be assumed that when $r \to \infty$ voltage is zero, while the temperature in both mediums is equal to human body temperature:

$$T_t = T_0 \text{ and } V_t = 0 \quad \text{on } \partial\Omega_{12} \times (0, \mathcal{T}); \tag{2.34}$$
$$T_b = T_0 \text{ and } V_b = 0 \quad \text{on } \partial\Omega_{22} \times (0, \mathcal{T}), \tag{2.35}$$

where $\mathcal{T}$ is the simulation time.

Secondly, it is assumed that the catheter is refrigerated, so its surface temperature is constant and equal to human body temperature, that is:

$$T_t = T_0 \quad \text{on } \partial\Omega_{11} \times (0, \mathcal{T}); \tag{2.36}$$
$$T_b = T_0 \quad \text{on } \partial\Omega_{21} \times (0, \mathcal{T}). \tag{2.37}$$

With respect to the voltage, AC current is used, so, in principle, the boundary conditions should be

$$V_t = V_0 \sin(\omega t) \quad \text{on } \partial\Omega_{11} \times (0, \mathcal{T}); \tag{2.38}$$
$$V_b = V_0 \sin(\omega t) \quad \text{on } \partial\Omega_{21} \times (0, \mathcal{T}). \tag{2.39}$$

Nevertheless, as $\omega \sim 10^6$, the time step required to solve the equations is too small. As a consequence, RMS value will be used, that is:

$$V_t = \frac{V_0}{\sqrt{2}} \quad \text{on } \partial\Omega_{11} \times (0, \mathcal{T}); \tag{2.40}$$
$$V_b = \frac{V_0}{\sqrt{2}} \quad \text{on } \partial\Omega_{21} \times (0, \mathcal{T}). \tag{2.41}$$

Finally, it is necessary to add four compatibility conditions on the cardiac tissue-blood interface: two for the thermal problem and other two for the electrical problem. This will be done, on the one side, imposing temperature and voltage equality:

$$T_t = T_b \text{ and } V_t = V_b \quad \text{on } (\partial\Omega_{13} \cup \partial\Omega_{14}) \times (0, \mathcal{T}), \tag{2.42}$$

while the remaining conditions consist of heat flux equality and voltage function differentiability:

$$k_t \frac{\partial T_t}{\partial \nu_t} = k_b \frac{\partial T_b}{\partial \nu_b} \text{ and } \frac{\partial V_t}{\partial \nu_t} = \frac{\partial V_b}{\partial \nu_b} \quad \text{on } (\partial\Omega_{23} \cup \partial\Omega_{24}) \times (0, \mathcal{T}), \tag{2.43}$$

where $\Omega_{13} = \Omega_{23}$ and $\Omega_{14} = \Omega_{24}$. In terms of spatial coordinates, the previous conditions are equivalent to:

$$k_t \frac{\partial T_t}{\partial \theta} = -k_b \frac{\partial T_b}{\partial \varphi} \text{ and } \frac{\partial V_t}{\partial \theta} = -\frac{\partial V_b}{\partial \varphi} \quad \text{on } (\partial\Omega_{23} \cup \partial\Omega_{24}) \times (0, \mathcal{T}). \tag{2.44}$$

Thus, taking into account (2.27) and (2.28), the system of equations that has to be solved is:

$$\begin{cases} \rho_t c_t \dfrac{\partial T_t}{\partial t} = \nabla \cdot (k_t \nabla T_t) + \sigma_t ||\nabla V_t||^2 - w \rho_b c_b (T_t - T_b) & \text{in } \Omega_1 \times (0, \mathcal{T}); \quad (2.45) \\ T_t = T_0 \quad \text{on } (\partial\Omega_{11} \cup \partial\Omega_{12}) \times (0, \mathcal{T}); & (2.46) \\ T_t = T_0 \quad \text{on } \Omega_1 \times \{t = 0\}. & (2.47) \end{cases}$$

$$\begin{cases} \nabla \cdot (\sigma \nabla V_t) = 0 \quad \text{in } \Omega_1 \times (0, \mathcal{T}); & (2.48) \\ V_t = \dfrac{V_0}{\sqrt{2}} \quad \text{on } \partial\Omega_{11} \times (0, \mathcal{T}); & (2.49) \\ V_t = 0 \quad \text{on } \partial\Omega_{12} \times (0, \mathcal{T}). & (2.50) \end{cases}$$

$$\begin{cases} \rho_b c_b \dfrac{\partial T_b}{\partial t} + \rho_b c_b \vec{v} \cdot \nabla T_b = k_b \Delta T_b + \sigma_b ||\nabla V_b||^2 \quad \text{in } \Omega_2 \times (0, \mathcal{T}); & (2.51) \\ T_b = T_0 \quad \text{on } (\partial\Omega_{21} \cup \partial\Omega_{22}) \times (0, \mathcal{T}); & (2.52) \\ T_b = T_0 \quad \text{on } \Omega_2 \times \{t = 0\}. & (2.53) \end{cases}$$

$$\begin{cases} \Delta V_b = 0 \quad \text{in } \Omega_2 \times (0, \mathcal{T}); & (2.54) \\ V_b = \dfrac{V_0}{\sqrt{2}} \quad \text{on } \partial\Omega_{21} \times (0, \mathcal{T}); & (2.55) \\ V_b = 0 \quad \text{on } \partial\Omega_{22} \times (0, \mathcal{T}). & (2.56) \end{cases}$$

$$T_t = T_b \text{ and } V_t = V_b \quad \text{on } (\partial\Omega_{13} \cup \partial\Omega_{14}) \times (0, \mathcal{T}); \tag{2.57}$$

$$k_t \frac{\partial T_t}{\partial \theta} = -k_b \frac{\partial T_b}{\partial \varphi} \text{ and } \frac{\partial V_t}{\partial \theta} = -\frac{\partial V_b}{\partial \varphi} \quad \text{on } (\partial\Omega_{23} \cup \partial\Omega_{24}) \times (0, \mathcal{T}). \tag{2.58}$$

$$\begin{cases} \sigma_t = \sigma_0 + \sigma_1 (T_t - T_0) \quad \text{in } \Omega_1 \times (0, \mathcal{T}); & (2.59) \\ k_t = k_0 + k_1 (T_t - T_0) \quad \text{in } \Omega_1 \times (0, \mathcal{T}); & (2.60) \end{cases}$$

2.3 Nondimensionalization of the equations.

2.3.1 Equations in the cardiac tissue.

First of all, assuming $T_b = T_0$ only in the perfusion term:

$$\rho_t c_t \frac{\partial T_t}{\partial t} = \nabla \cdot \Big([k_0 + k_1 (T_t - T_0)] \nabla T_t \Big) + [\sigma_0 + \sigma_1 (T_t - T_0)] \|\nabla V_t\|^2 - w \rho_b c_b (T_t - T_0). \tag{2.61}$$

Secondly, the dimensionless temperature, voltage, radial coordinate and time are defined as follows:

$$\Theta_t = \frac{T_t - T_0}{T_e - T_0}; \quad \mathcal{V}_t = \frac{V_t}{V_0}; \quad s = \frac{r}{\varepsilon}; \quad \tilde{t} = \frac{\alpha_{t_0}}{\varepsilon^2} t. \tag{2.62}$$

In the previous relations T_e is the water boiling temperature, V_0 the voltage amplitude, ε the catheter radius and α_{t_0} the thermal conductivity of the cardiac tissue at $T_t = T_0$. In terms of this variables and making use of (2.59) and (2.60), equation (2.61) becomes:

$$\begin{aligned} \frac{k_0 (T_e - T_0)}{\varepsilon^2} \frac{\partial \Theta_t}{\partial \tilde{t}} =& \frac{1}{\varepsilon^2} \nabla \cdot \Big([k_0 + k_1 (T_e - T_0) \Theta_t] (T_e - T_0) \nabla \Theta_t \Big) + \\ &+ \frac{1}{\varepsilon^2} [\sigma_0 + \sigma_1 (T_e - T_0) \Theta_t] V_0^2 \|\nabla \mathcal{V}_t\|^2 - w \rho_b c_b (T_e - T_0) \Theta_t. \end{aligned} \tag{2.63}$$

The previous equation is multiplied by $\varepsilon^2 / (k_0 (T_e - T_0))$ to give:

$$\begin{aligned}\frac{\partial \Theta_t}{\partial \tilde{t}} =& \frac{1}{k_0(T_e - T_0)} \nabla \cdot \Big([k_0 + k_1(T_e - T_0)\Theta_t](T_e - T_0)\nabla \Theta_t \Big) + \\ &+ \frac{1}{k_0(T_e - T_0)} [\sigma_0 + \sigma_1(T_e - T_0)\Theta] V_0^2 \|\nabla \mathcal{V}_t\|^2 - \frac{\rho_b c_b \varepsilon^2}{k_0} w \Theta_t.\end{aligned} \tag{2.64}$$

Defining the following dimensionless parameters:

$$\tilde{k}_1 = \frac{k_1}{k_0}; \quad \tilde{\sigma}_0 = \frac{\sigma_0 V_0^2}{k_0(T_e - T_0)}; \quad \tilde{\sigma}_1 = \frac{\sigma_1 V_0^2}{k_0}; \quad \tilde{w} = \frac{\rho_b c_b \varepsilon^2 w}{k_0}, \tag{2.65}$$

equation (2.64) reads:

$$\frac{\partial \Theta_t}{\partial \tilde{t}} = \nabla \cdot (\tilde{k}_t \nabla \Theta_t) + \tilde{\sigma}_t \|\nabla \mathcal{V}_t\|^2 - \tilde{w} \Theta_t, \tag{2.66}$$

where

$$\tilde{\sigma}_t = \tilde{\sigma}_0 + \tilde{\sigma}_1 \Theta; \tag{2.67}$$

$$\tilde{k}_t = 1 + \tilde{k}_1 \Theta. \tag{2.68}$$

The initial and boundary conditions of the equation of conservation of energy (2.46) - (2.47) can be written in terms of the dimensionless temperature:

$$\Theta_t = 0. \tag{2.69}$$

Furthermore, using the dimensionless voltage (2.62) and electrical conductivity (2.67), the elliptic equation (2.48) is:

$$\nabla \cdot (\tilde{\sigma}_t \nabla \mathcal{V}_t) = 0, \tag{2.70}$$

and its corresponding boundary conditions (2.49) - (2.50) take the form:

$$\mathcal{V}_t = \frac{1}{\sqrt{2}} \quad \text{on } \partial\Omega_{11} \times (0, \mathcal{T}); \tag{2.71}$$

$$\mathcal{V}_t = 0 \quad \text{on } \partial\Omega_{12} \times (0, \mathcal{T}), \tag{2.72}$$

2.3.2 Equations in the blood.

In this case, new dimensionless variables have to be defined:

$$\Theta_b = \frac{T_b - T_0}{T_e - T_0}; \quad \mathcal{V}_b = \frac{V_b}{V_0}, \tag{2.73}$$

so (2.51) can be rewritten as follows:

$$\frac{k_0 \rho_b c_b (T_e - T_0)}{\rho_t c_t \varepsilon^2} \frac{\partial \Theta_b}{\partial \tilde{t}} + \frac{\rho_b c_b (T_e - T_0)}{\varepsilon} \vec{v} \cdot \nabla \Theta_b = \frac{k_b (T_e - T_0)}{\varepsilon^2} \Delta \Theta_b + \frac{\sigma_b V_0^2}{\varepsilon^2} \|\nabla \mathcal{V}_b\|^2. \tag{2.74}$$

Multiplying the previous equation by $\varepsilon^2/(k_0(T_e - T_0))$:

$$\frac{\rho_b c_b}{\rho_t c_t}\frac{\partial \Theta_b}{\partial \tilde{t}} + \frac{k_b}{k_0}\frac{\varepsilon}{\alpha_b}\vec{v}\cdot\nabla\Theta_b = \frac{k_b}{k_0}\Delta\Theta_b + \frac{\sigma_b V_0^2}{k_0(T_e - T_0)}\|\nabla\mathcal{V}_b\|^2. \tag{2.75}$$

Finally, introducing new parameters:

$$\tilde{\rho}_b = \frac{\rho_b}{\rho_t}; \quad \tilde{c}_b = \frac{c_b}{c_t}; \quad \tilde{v} = \frac{\varepsilon v}{\alpha_b}; \quad \tilde{k}_b = \frac{k_b}{k_0}; \quad \tilde{\sigma}_b = \frac{\sigma_b V_0^2}{k_b(T_e - T_0)}; \quad \tilde{\alpha}_b = \frac{\tilde{k}_b}{\tilde{\rho}_b\tilde{c}_b}, \tag{2.76}$$

(2.75) takes the form:

$$\frac{\partial \Theta_b}{\partial \tilde{t}} + \tilde{\alpha}_b\tilde{v}\nabla\Theta_b = \tilde{\alpha}_b\Delta\Theta_b + \tilde{\alpha}_b\tilde{\sigma}_b\|\nabla\mathcal{V}_b\|^2, \tag{2.77}$$

and the corresponding boundary conditions (2.52) and (2.53):

$$\Theta_b = 0. \tag{2.78}$$

In order to conclude with the nondimensionalization of the equations in the blood, the elliptic equation (2.54) can be rewritten as

$$\Delta\mathcal{V}_b = 0, \tag{2.79}$$

and the boundary conditions (2.55) and (2.56):

$$\mathcal{V}_b = \frac{1}{\sqrt{2}} \quad \text{on } \partial\Omega_{21}\times(0,\mathcal{T}); \tag{2.80}$$

$$\mathcal{V}_b = 0 \quad \text{on } \partial\Omega_{22}\times(0,\mathcal{T}). \tag{2.81}$$

2.3.3 Compatibility equations.

Using the previous definitions, the compatibility conditions (2.57) and (2.58) become:

$$\Theta_t = \Theta_b \text{ and } \mathcal{V}_t = \mathcal{V}_b \quad \text{on } (\partial\Omega_{13}\cup\partial\Omega_{14})\times(0,\mathcal{T}); \tag{2.82}$$

$$\tilde{k}_t\frac{\partial\Theta_t}{\partial\theta} = -\tilde{k}_b\frac{\partial\Theta_b}{\partial\varphi} \text{ and } \frac{\partial\mathcal{V}_t}{\partial\theta} = -\frac{\partial\mathcal{V}_b}{\partial\varphi} \quad \text{on } (\partial\Omega_{23}\cup\partial\Omega_{24})\times(0,\mathcal{T}). \tag{2.83}$$

Finally, the system of equations in terms of dimensionless variables and parameters reads:

$$\begin{cases} \dfrac{\partial\Theta_t}{\partial\tilde{t}} = \nabla\cdot(\tilde{k}_t\nabla\Theta_t) + \tilde{\sigma}_t\|\nabla\mathcal{V}_t\|^2 - \tilde{w}\Theta_t \quad \text{in } \Omega_1\times(0,\mathcal{T}); & (2.84)\\ \Theta_t = 0 \quad \text{on } (\partial\Omega_{11}\cup\partial\Omega_{12})\times(0,\mathcal{T}); & (2.85)\\ \Theta_t = 0 \quad \text{on } \Omega_1\times\{t=0\}. & (2.86) \end{cases}$$

$$\begin{cases} \nabla \cdot (\tilde{\sigma}_t \nabla \mathcal{V}_t) = 0 \quad \text{in } \Omega_1 \times (0, \mathcal{T}); & (2.87) \\ \mathcal{V}_t = \dfrac{1}{\sqrt{2}} \quad \text{on } \partial\Omega_{11} \times (0, \mathcal{T}); & (2.88) \\ \mathcal{V}_t = 0 \quad \text{on } \partial\Omega_{12} \times (0, \mathcal{T}). & (2.89) \end{cases}$$

$$\begin{cases} \dfrac{\partial \Theta_b}{\partial \tilde{t}} + \tilde{\alpha}_b \tilde{v} \nabla \Theta_b = \tilde{\alpha}_b \Delta \Theta_b + \tilde{\alpha}_b \tilde{\sigma}_b \|\nabla \mathcal{V}_b\|^2 \quad \text{in } \Omega_2 \times (0, \mathcal{T}); & (2.90) \\ \Theta_b = 0 \quad \text{on } (\partial\Omega_{21} \cup \partial\Omega_{22}) \times (0, \mathcal{T}); & (2.91) \\ \Theta_b = 0 \quad \text{on } \Omega_2 \times \{t = 0\}; & (2.92) \end{cases}$$

$$\begin{cases} \Delta \mathcal{V}_b = 0 \quad \text{in } \Omega_2 \times (0, \mathcal{T}); & (2.93) \\ \mathcal{V}_b = \dfrac{1}{\sqrt{2}} \quad \text{on } \partial\Omega_{21} \times (0, \mathcal{T}); & (2.94) \\ \mathcal{V}_b = 0 \quad \text{on } \partial\Omega_{22} \times (0, \mathcal{T}); & (2.95) \end{cases}$$

$$\Theta_t = \Theta_b \text{ and } \mathcal{V}_t = \mathcal{V}_b \quad \text{on } (\partial\Omega_{13} \cup \partial\Omega_{14}) \times (0, \mathcal{T}); \tag{2.96}$$

$$\tilde{k}_t \frac{\partial \Theta_t}{\partial \theta} = -\tilde{k}_b \frac{\partial \Theta_b}{\partial \varphi} \text{ and } \frac{\partial \mathcal{V}_t}{\partial \theta} = -\frac{\partial \mathcal{V}_b}{\partial \varphi} \quad \text{on } (\partial\Omega_{23} \cup \partial\Omega_{24}) \times (0, \mathcal{T}). \tag{2.97}$$

$$\tilde{\sigma}_t = \tilde{\sigma}_0 + \tilde{\sigma}_1 \Theta; \tag{2.98}$$

$$\tilde{k}_t = 1 + \tilde{k}_1 \Theta. \tag{2.99}$$

2.4 Numerical implementation.

With the objective of solving numerically the system of equations (2.84) - (2.99), first of all, the terms of the equations (2.84) and (2.87) will be developed. Taking into account (2.98) and (2.99):

$$\frac{\partial \Theta_t}{\partial \tilde{t}} = \tilde{k}_t \Delta \Theta_t + \tilde{k}_1 ||\nabla \Theta_t||^2 + \tilde{\sigma}_t \|\nabla \mathcal{V}_t\|^2 - \tilde{w} \Theta_t; \tag{2.100}$$

$$\tilde{\sigma}_t \Delta \mathcal{V}_t + \tilde{\sigma}_1 \nabla \Theta_t \cdot \nabla \mathcal{V}_t = 0; \tag{2.101}$$

$$\frac{\partial \Theta_b}{\partial \tilde{t}} + \tilde{\alpha}_b \tilde{v} \nabla \Theta_b = \tilde{\alpha}_b \Delta \Theta_b + \tilde{\alpha}_b \tilde{\sigma}_b \|\nabla \mathcal{V}_b\|^2; \tag{2.102}$$

$$\Delta \mathcal{V}_b = 0. \tag{2.103}$$

The second step will be to obtain the expressions of the gradient and the laplacian in spherical coordinates [Higuera *et al.*, 2005]. Taking spherical symmetry into account:

$$\nabla \Gamma_k = \frac{\partial \Gamma_k}{\partial s} \hat{\boldsymbol{s}} + \frac{1}{s} \frac{\partial \Gamma_k}{\partial \phi} \hat{\boldsymbol{\phi}}; \quad \Delta \Gamma_k = \frac{\partial^2 \Gamma_k}{\partial s^2} + \frac{1}{s^2} \frac{\partial^2 \Gamma_k}{\partial \phi^2} + \frac{2}{s} \frac{\partial \Gamma_k}{\partial s} + \frac{1}{\tan \phi} \frac{\partial \Gamma_k}{\partial \phi}, \tag{2.104}$$

being, from here on, $\Gamma = \Theta$ or $\mathcal{V}$, $k = t$ or b and $\phi = \theta$ or φ, as appropriate.

The spatial discretization is performed in terms of Chebyshev polynomials of order N, whose definition and properties can be found in [Boyd, 2000]. Hence, voltage and temperature values are storaged in a $N \times N$ matrix:

$$\Gamma_k = \begin{bmatrix} \Gamma_{k_{11}} & \Gamma_{k_{12}} & \dots & \Gamma_{k_{1N}} \\ \Gamma_{k_{21}} & \Gamma_{k_{22}} & \dots & \Gamma_{k_{2N}} \\ \vdots & \vdots & \ddots & \vdots \\ \Gamma_{k_{N1}} & \Gamma_{k_{N2}} & \dots & \Gamma_{k_{NN}} \end{bmatrix}, \tag{2.105}$$

In terms of Chebyshev polynomials, the derivatives that appear in (2.104) are defined as follows:

$$\frac{\partial \Gamma_{k_{ij}}}{\partial s} = \sum_{m=1}^{N} D_{s_{im}} \Gamma_{k_{mj}}; \quad \frac{\partial \Gamma_{k_{ij}}}{\partial \phi} = \sum_{m=1}^{N} D_{\phi_{jm}} \Gamma_{k_{im}}; \tag{2.106}$$

$$\frac{\partial^2 \Gamma_{k_{ij}}}{\partial s^2} = \sum_{m=1}^{N} D^2_{s_{im}} \Gamma_{k_{mj}}; \quad \frac{\partial^2 \Gamma_{k_{ij}}}{\partial \phi^2} = \sum_{m=1}^{N} D^2_{\phi_{jm}} \Gamma_{k_{im}}, \tag{2.107}$$

where i is referred to the radial coordinate and j to the polar coordinate. Furthermore, D_s and D_ϕ are the derivation matrices with respect to the dimensionless radial and polar coordinates, respectively:

$$D_l = \begin{bmatrix} D_{l_{11}} & D_{l_{12}} & \dots & D_{l_{1N}} \\ D_{l_{21}} & D_{l_{22}} & \dots & D_{l_{2N}} \\ \vdots & \vdots & \ddots & \vdots \\ D_{l_{N1}} & D_{l_{N2}} & \dots & D_{l_{NN}} \end{bmatrix}, \tag{2.108}$$

being $D_l^2 = D_l \cdot D_l$, $l = s$ or ϕ.

With respect to the algorithms to compute derivation matrices, these have been extracted from [Kopriva, 2009]. Nevertheless, it has to be noted that in that reference the derivation matrices related to Chebyshev polynomials are obtained, that is, the ones defined on the interval $(-1, 1)$. In the current problem the domain is expanded in both coordinates, where $\phi \in (0, \pi)$ and $s \in (1, \infty)$. Consequently, in the case of the radial direction, Chebyshev rational polynomials are employed.

Accordingly, a relationship between the derivation matrices corresponding to the polynomials defined on the intervals $(-1, 1)$, $(0, \pi)$ y $(1, \infty)$ has to be set. For that purpose, the following mappings are defined:

$$\begin{aligned} f : (-1, 1) &\to (0, \pi) \\ u &\mapsto s = \frac{\pi(s+1)}{2}; \end{aligned} \tag{2.109}$$

$$\begin{aligned} g : (-1, 1) &\to (1, \infty) \\ u &\mapsto \phi = \frac{1+s}{1-s}, \end{aligned} \tag{2.110}$$

and partial derivatives:

$$\frac{\partial}{\partial s} = \frac{\partial u}{\partial s}\frac{\partial}{\partial u} = \frac{1}{2(u-1)^2}\frac{\partial}{\partial u}; \quad \frac{\partial}{\partial \phi} = \frac{\partial u}{\partial \phi}\frac{\partial}{\partial u} = \frac{2}{\pi}\frac{\partial}{\partial u}. \tag{2.111}$$

On the basis of the above, if D_u is the derivation matrix corresponding to Chebyshev polynomials defined on the interval $(-1, 1)$, the matrices D_s y D_ϕ can be obtained as a consequence of (2.111):

$$D_s = \frac{1}{2(u-1)^2} D_u; \quad D_\phi = \frac{2}{\pi} D_u. \tag{2.112}$$

Once the spatial discretization has been done, the last step involves obtaining the system of $2N^2$ linear algebraic equations for the elliptic equations (2.101) and (2.103):

$$Ax = B, \tag{2.113}$$

and the N-component vectors for the parabolic equations (2.100) and (2.102).

2.4.1 Elliptic equations.

With respect to the elliptic equations, new $N^2 \times N^2$ matrices are computed ($\tilde{D}_\phi$ and $\tilde{D}_s$) with the aim of facilitating the algebraic equation implementation.

$$\tilde{D}_\phi = \begin{bmatrix} \begin{bmatrix} D_{\phi_{11}} & 0 & \dots & 0 \\ 0 & D_{\phi_{11}} & \dots & 0 \\ \vdots & \vdots & \ddots & \vdots \\ 0 & 0 & \dots & D_{\phi_{11}} \end{bmatrix} & \dots & \begin{bmatrix} D_{\phi_{1N}} & 0 & \dots & 0 \\ 0 & D_{\phi_{1N}} & \dots & 0 \\ \vdots & \vdots & \ddots & \vdots \\ 0 & 0 & \dots & D_{\phi_{1N}} \end{bmatrix} \\ \vdots & \ddots & \vdots \\ \begin{bmatrix} D_{\phi_{N1}} & 0 & \dots & 0 \\ 0 & D_{\phi_{N1}} & \dots & 0 \\ \vdots & \vdots & \ddots & \vdots \\ 0 & 0 & \dots & D_{\phi_{N1}} \end{bmatrix} & \dots & \begin{bmatrix} D_{\phi_{NN}} & 0 & \dots & 0 \\ 0 & D_{\phi_{NN}} & \dots & 0 \\ \vdots & \vdots & \ddots & \vdots \\ 0 & 0 & \dots & D_{\phi_{NN}} \end{bmatrix} \end{bmatrix}.$$

$$\tilde{D}_s = \left[\begin{array}{c|c|c|c} D_s & 0 & \dots & 0 \\ \hline 0 & D_s & \dots & 0 \\ \hline \vdots & \vdots & \ddots & \vdots \\ \hline 0 & 0 & \dots & D_s \end{array}\right];$$

Making use of the matrices $\tilde{D}_\phi$ and $\tilde{D}_s$, the equivalent matrix of the equation (2.101) is A_t, whose components are:

$$A_{t_{ij}} = \left(\tilde{\sigma}_0+\tilde{\sigma}_1\tilde{\Theta}_i\right)\left(\tilde{D}^2_{s_{ij}}+\frac{1}{\tilde{s}_i^2}\tilde{D}^2_{\theta_{ij}}+\frac{2}{\tilde{s}_i}\tilde{D}_{s_{ij}}+\frac{1}{\tan\tilde{\theta}_i}\tilde{D}_{\theta_{ij}}\right)+\tilde{\sigma}_1\tilde{\Theta}_{t_i}\left((\tilde{D}_{s_{ij}})^2+\frac{1}{\tilde{s}_i^2}(\tilde{D}_{\theta_{ij}})^2\right), \quad (2.114)$$

where $\tilde{s}_i = \tilde{s}_p$ y $\tilde{\theta}_i = \tilde{\theta}_q$, being $p = i \bmod N$. Moreover, if $\mathrm{int}(x)$ denotes the integer part function of x:

$$q = \begin{cases} \mathrm{int}(i/N)+1 & \text{if} \quad 1 \le i \le N-1; \quad (2.115) \\ \mathrm{int}(i/N) & \text{if} \quad i \ge N. \quad (2.116) \end{cases}$$

Meanwhile, the equivalent matrix of the equation (2.103) is A_b, whose components are:

$$A_{b_{ij}} = \tilde{D}^2_{s_{ij}} + \frac{1}{\tilde{s}_i^2}\tilde{D}^2_{\tilde{\varphi}_{ij}} + \frac{2}{\tilde{s}_i}\tilde{D}_{s_{ij}} + \frac{1}{\tan\tilde{\varphi}_i}\tilde{D}_{\varphi_{ij}}. \quad (2.117)$$

As both elliptic equations are coupled, the matrix of the complete system is defined:

$$A = \left[\begin{array}{c|c} A_t & A_{t_{aux}} \\ \hline A_{b_{aux}} & A_b \end{array}\right],$$

although it remains to apply the boundary and compatibility conditions.

Boundary conditions.

The boundary conditions (2.88), (2.89), (2.94) and (2.95) are imposed by cancelling all of the values of the correspondent line, except the component where $i = j$, which takes the value 1. That is, in the case of (2.88):

$$A_{t_{ij}} = \begin{cases} 1 & \text{if} \quad i,j = 1+(p-1)N,\ p \in \mathbb{Z}^+; \quad (2.118) \\ 0 & \text{if} \quad i = 1+(p-1)N,\ p \in \mathbb{Z}^+,\ j \ne i, \quad (2.119) \end{cases}$$

while

$$B_{t_i} = 1 \ \text{ if } \ i = 1+(p-1)n,\ p \in \mathbb{Z}^+, \quad (2.120)$$

being

$$B = \left[\frac{B_t}{B_b}\right].$$

With regard to (2.89):

$$A_{t_{ij}} = \begin{cases} 1 & \text{if} \quad i,j = (p-1)N,\ p \in \mathbb{Z}^+; \quad (2.121) \\ 0 & \text{if} \quad i = (p-1)N,\ p \in \mathbb{Z}^+,\ j \neq i. \quad (2.122) \end{cases}$$

The values of the components of the matrix and the vector are the same in the case of the boundary conditions in the blood:

$$A_{b_{ij}} = \begin{cases} 1 & \text{if} \quad i,j = 1 + (p-1)N,\ p \in \mathbb{Z}^+; \quad (2.123) \\ 0 & \text{if} \quad i = 1 + (p-1)N,\ p \in \mathbb{Z}^+,\ j \neq i; \quad (2.124) \end{cases}$$

$$B_{b_i} = 1 \ \text{ if } \ i = 1 + (p-1)N,\ p \in \mathbb{Z}^+, \quad (2.125)$$

$$A_{b_{ij}} = \begin{cases} 1 & \text{if} \quad i,j = (p-1)N,\ p \in \mathbb{Z}^+; \quad (2.126) \\ 0 & \text{if} \quad i = (p-1)N,\ p \in \mathbb{Z}^+,\ j \neq i. \quad (2.127) \end{cases}$$

The compatibility conditions (2.96) and (2.97) are implemented by following an analogous procedure. Firstly, the second condition of (2.96) is applied in the matrices A_t and $A_{t_{aux}}$:

$$A_{t_{ij}} = \begin{cases} 1 & \text{if} \quad i \text{ is such that } q(i) = 1 \text{ or } N,\ j = i; \quad (2.128) \\ 0 & \text{if} \quad i \text{ is such that } q(i) = 1 \text{ or } N,\ j \neq i. \quad (2.129) \end{cases}$$

$$A_{t_{aux_{ij}}} = \begin{cases} -1 & \text{if} \quad i \text{ is such that } q(i) = 1 \text{ or } N,\ j = i; \quad (2.130) \\ 0 & \text{if} \quad i \text{ is such that } q(i) = 1 \text{ or } N,\ j \neq i. \quad (2.131) \end{cases}$$

being q the subindex defined in (2.115) and (2.116). The second condition of (2.97) is applied in the matrices A_b and $A_{b_{aux}}$:

$$A_{b_{ij}} = \begin{cases} D_{\theta_{1p}} & \text{if} \quad i \text{ is such that } q(i) = 1,\ j = (p-1)N+1, ..., pN,\ p \in \mathbb{Z}^+; \quad (2.132) \\ D_{\theta_{Np}} & \text{if} \quad i \text{ is such that } q(i) = N,\ j = (p-1)N+1, ..., pN,\ p \in \mathbb{Z}^+; \quad (2.133) \\ 0 & \text{if} \quad i \text{ is such that } q(i) = 1,\ j \neq (p-1)N+1, ..., pN,\ p \in \mathbb{Z}^+; \quad (2.134) \\ 0 & \text{if} \quad i \text{ is such that } q(i) = N,\ j \neq (p-1)N+1, ..., pN,\ p \in \mathbb{Z}^+. \quad (2.135) \end{cases}$$

$$A_{b_{ij}} = \begin{cases} D_{\varphi_{1p}} & \text{if} \quad i \text{ is such that } q(i) = 1,\ j = (p-1)N+1, ..., pN,\ p \in \mathbb{Z}^+; \quad (2.136) \\ D_{\varphi_{Np}} & \text{if} \quad i \text{ is such that } q(i) = N,\ j = (p-1)N+1, ..., pN,\ p \in \mathbb{Z}^+; \quad (2.137) \\ 0 & \text{if} \quad i \text{ is such that } q(i) = 1,\ j \neq (p-1)N+1, ..., pN,\ p \in \mathbb{Z}^+; \quad (2.138) \\ 0 & \text{if} \quad i \text{ is such that } q(i) = N,\ j \neq (p-1)N+1, ..., pN,\ p \in \mathbb{Z}^+. \quad (2.139) \end{cases}$$

with $p = i \bmod N$.

Finally, from an $N \times N$ matrix, voltage and temperature become a column vector of N^2 components, $\tilde{\mathcal{V}}$ and $\tilde{\Theta}$:

$$\tilde{\Gamma} = \begin{bmatrix} \tilde{\Gamma}_1 = \Gamma_{11} \\ \vdots \\ \tilde{\Gamma}_N = \Gamma_{N1} \\ \tilde{\Gamma}_{N+1} = \Gamma_{12} \\ \vdots \\ \tilde{\Gamma}_{2N} = \Gamma_{N2} \\ \vdots \\ \tilde{\Gamma}_{(N-1)N+1} = \Gamma_{1N} \\ \vdots \\ \tilde{\Gamma}_{N^2} = \Gamma_{NN} \end{bmatrix},$$

being $x = \tilde{\Gamma}$.

Once the system of $2N^2$ linear algebraic equations has been obtained, it is solved using an algorith based on LU factorization with partial pivoting by means of the LAPACK library (see [43]), in particular the DGESV subroutine.

2.4.2 Parabolic equations.

Taking into account (2.104), (2.106) and (2.107), the system of equations (2.101) and (2.103) is written:

$$\begin{aligned} \frac{\partial \Theta_{t_{ij}}}{\partial \tilde{t}} =& (\tilde{k}_0 + \tilde{k}_1 \Theta_{t_{ij}}) \Bigg(\sum_{m=1}^{N} \Big(D^2_{s_{im}} + \frac{2}{s} D_{s_{im}} \Big) \Theta_{t_{mj}} + \\ &+ \sum_{m=1}^{N} \Big(\frac{1}{s_i^2} D^2_{\theta_{jm}} + \frac{1}{\tan\theta_j} D_{\theta_{jm}} \Big) \Theta_{t_{im}} + \\ &+ \tilde{k}_1 \Big(\sum_{m=1}^{N} D_{s_{im}} \Theta_{t_{mj}} + \sum_{m=1}^{N} \frac{1}{s_i} D_{\theta_{jm}} \Theta_{t_{im}} \Big)^2 + \\ &+ (\tilde{\sigma}_0 + \tilde{\sigma}_1 \Theta_{t_{ij}}) \Big(\sum_{m=1}^{N} D_{s_{im}} \mathcal{V}_{t_{mj}} + \sum_{r=1}^{N} \frac{1}{s_i} D_{\theta_{jm}} \mathcal{V}_{t_{im}} \Big)^2 - \tilde{w} \Theta_{t_{ij}}; \end{aligned} \tag{2.140}$$

$$\begin{aligned} \frac{\partial \Theta_{b_{ij}}}{\partial \tilde{t}} =& - \tilde{\alpha}_b v \Big(\sum_{m=1}^{N} D_{s_{im}} \Theta_{b_{mj}} + \sum_{m=1}^{N} \frac{1}{s_i} D_{\theta_{jm}} \Theta_{b_{im}} \Big) + \\ &+ \tilde{\alpha}_b \Bigg(\sum_{m=1}^{N} \Big(D^2_{s_{im}} + \frac{2}{s} D_{s_{im}} \Big) \Theta_{b_{mj}} + \sum_{m=1}^{N} \Big(\frac{1}{s_i^2} D^2_{\theta_{jm}} + \frac{1}{\tan\theta_j} D_{\theta_{jm}} \Big) \Theta_{b_{im}} \Bigg) + \\ &+ \tilde{\alpha}_b \tilde{\sigma}_b \Big(\sum_{m=1}^{N} D_{s_{im}} \mathcal{V}_{b_{mj}} + \sum_{m=1}^{N} \frac{1}{s_i} D_{\theta_{jm}} \mathcal{V}_{b_{im}} \Big)^2, \end{aligned} \tag{2.141}$$

while the resolution of the system of $2N^2$ ordinary differential equations is carried out using a 4th order Runge-Kutta scheme.

Boundary conditions.

Boundary conditions are applied after solving the system of equations. In the case of (2.85):

$$\Theta_{t_{1j}} = \Theta_{t_{Nj}} = 0, \quad j = 1, ..., N \ , \tag{2.142}$$

while (2.91) reads:

$$\Theta_{b_{1j}} = \Theta_{b_{Nj}} = 0, \quad j = 1, ..., N. \tag{2.143}$$

Compatibility conditions.

First of all, (2.96) is numerically implemented by computing mean temperatures on both sides of the interface:

$$\Theta_{m1_j} = \frac{\Theta_{t_{1j}} + \Theta_{b_{1j}}}{2}; \quad \Theta_{mN_j} = \frac{\Theta_{t_{Nj}} + \Theta_{b_{Nj}}}{2}; \quad j = 1, ..., N \ , \tag{2.144}$$

and imposing that both temperature values are equal to the mean value, that is:

$$\Theta_{t_{1j}} = \Theta_{b_{1j}} = \Theta_{m1_j}; \quad \Theta_{t_{Nj}} = \Theta_{b_{Nj}} = \Theta_{mN_j}; \quad j = 1, ..., N. \tag{2.145}$$

With respect to fluxes, reasoning is analogous. A new flux is defined,

$$\begin{aligned} q_{m1_i} &= \frac{\tilde{k}\frac{\partial \Theta_t}{\partial \theta}\Big|_{\Omega_{14}} - \tilde{k}_b \frac{\partial \Theta_b}{\partial \varphi}\Big|_{\Omega_{24}}}{2} = \frac{\tilde{k}\sum\limits_{m=1}^{N} D_{\theta_{1m}}\Theta_{t_{im}} - \tilde{k}_b \sum\limits_{m=1}^{N} D_{\varphi_{1m}}\Theta_{b_{im}}}{2}; \quad i = 1, ..., N; \\ q_{mN_i} &= \frac{\tilde{k}\frac{\partial \Theta_t}{\partial \theta}\Big|_{\Omega_{13}} - \tilde{k}_b \frac{\partial \Theta_b}{\partial \varphi}\Big|_{\Omega_{23}}}{2} = \frac{\tilde{k}\sum\limits_{m=1}^{N} D_{\theta_{Nm}}\Theta_{t_{im}} - \tilde{k}_b \sum\limits_{m=1}^{N} D_{\varphi_{Nm}}\Theta_{b_{im}}}{2}; \quad i = 1, ..., N, \end{aligned} \tag{2.146}$$

and, finally:

$$\begin{aligned} \tilde{k}\sum_{m=1}^{N} D_{\theta_{1m}}\Theta_{t_{im}} = -\tilde{k}_b \sum_{m=1}^{N} D_{\varphi_{1m}}\Theta_{b_{im}} = q_{m1_i}; \quad i = 1, ..., N; \\ \tilde{k}\sum_{m=1}^{N} D_{\theta_{Nm}}\Theta_{t_{im}} = -\tilde{k}_b \sum_{m=1}^{N} D_{\varphi_{Nm}}\Theta_{b_{im}} = q_{mN_i}; \quad i = 1, ..., N. \end{aligned} \tag{2.147}$$

2.5 Validation of the numerical scheme.

The last step after numerically simulating the system of equations (2.84) - (2.99) is to validate the numerical scheme used to solve it. This is performed by means of a manufactured solution; that is, an analytical solution that is introduced in the original system of equations and gives rise to a new system, where source terms appear. If the difference between analytical and numerical

solutions is less than a critical value, it is possible to conclude that the used numerical scheme is correct.

The proposed analytical solutions are as follows:

$$\hat{\Theta}_t(s,\tilde{t},\theta) = \frac{\tilde{t}}{\tilde{t}_1}\,\mathrm{sech}\left(\frac{s-b}{\tilde{t}+\tilde{\omega}^{-1}}\right)\sin\theta; \tag{2.148}$$

$$\hat{\mathcal{V}}_t(s,\theta) = \frac{e^{-s^2}}{s}\sin^2\theta; \tag{2.149}$$

$$\hat{\Theta}_b(s,\tilde{t},\varphi) = \frac{\tilde{t}}{\tilde{t}_1}\,\mathrm{sech}\left(\frac{s-b}{\tilde{t}+\tilde{\omega}^{-1}}\right)\sin^2\varphi; \tag{2.150}$$

$$\hat{\mathcal{V}}_b(s,\varphi) = \frac{e^{-s^2}}{s^2}\sin^2\varphi; \tag{2.151}$$

where b, $\tilde{\omega}$ and $\tilde{t}_1$ are parameters whose value will be specified later. It has to be noted that similar functions to the expected results have been chosen, with the goal of simulating a system of equations as realistic as possible. Introducing the previous expressions in (2.84) - (2.99) leads to:

$$\begin{cases} \dfrac{\partial\hat{\Theta}_t}{\partial\tilde{t}} = \nabla\cdot(\tilde{k}\nabla\hat{\Theta}_t) + \tilde{\sigma}\|\nabla\hat{\mathcal{V}}_t\|^2 - \tilde{w}\hat{\Theta}_t + f_1(s,\theta,\tilde{t}) \quad \text{in } \Omega_1\times(0,\mathcal{T}); & (2.152)\\ \hat{\Theta}_t = \dfrac{\tilde{t}}{\tilde{t}_1}\,\mathrm{sech}\left(\dfrac{1-b}{\tilde{t}+\tilde{\omega}^{-1}}\right)\sin\theta \quad \text{on } \partial\Omega_{11}\times(0,\mathcal{T}); & (2.153)\\ \hat{\Theta}_t = 0 \quad \text{on } \partial\Omega_{12}\times(0,\mathcal{T}); & (2.154)\\ \hat{\Theta}_t = 0 \quad \text{on } \Omega_1\times\{t=0\}. & (2.155) \end{cases}$$

$$\begin{cases} \nabla\cdot(\tilde{\sigma}\nabla\hat{\mathcal{V}}_t) = f_2(s,\theta) \quad \text{in } \Omega_1\times(0,\mathcal{T}); & (2.156)\\ \hat{\mathcal{V}}_t = \dfrac{\sin^2\theta}{e} \quad \text{on } \partial\Omega_{11}\times(0,\mathcal{T}); & (2.157)\\ \hat{\mathcal{V}}_t = 0 \quad \text{on } \partial\Omega_{12}\times(0,\mathcal{T}). & (2.158) \end{cases}$$

$$\begin{cases} \dfrac{\partial\hat{\Theta}_b}{\partial\tilde{t}} + \tilde{\alpha}_b\tilde{v}\nabla\hat{\Theta}_b = \tilde{\alpha}_b\Delta\hat{\Theta}_b + \tilde{\alpha}_b\tilde{\sigma}_b\|\nabla\hat{\mathcal{V}}_b\|^2 + f_3(s,\varphi,\hat{t}) \quad \text{in } \Omega_2\times(0,\mathcal{T}); & (2.159)\\ \hat{\Theta}_b = \dfrac{\tilde{t}}{\tilde{t}_1}\,\mathrm{sech}\left(\dfrac{1-b}{\tilde{t}+\tilde{\omega}^{-1}}\right)\sin^2\varphi \quad \text{on } \partial\Omega_{21}\times(0,\mathcal{T}); & (2.160)\\ \hat{\Theta}_b = 0 \quad \text{on } \partial\Omega_{22}\times(0,\mathcal{T}); & (2.161)\\ \hat{\Theta}_b = 0 \quad \text{on } \Omega_2\times\{t=0\}; & (2.162) \end{cases}$$

$$\begin{cases} \Delta\hat{\mathcal{V}}_b = f_4(s,\theta,\tilde{t}) \quad \text{in } \Omega_2\times(0,\mathcal{T}); & (2.163)\\ \hat{\mathcal{V}}_b = \dfrac{\sin^2\varphi}{e} \quad \text{on } \partial\Omega_{21}\times(0,\mathcal{T}); & (2.164)\\ \hat{\mathcal{V}}_b = 0 \quad \text{on } \partial\Omega_{22}\times(0,\mathcal{T}); & (2.165) \end{cases}$$

$$\hat{\Theta}_t = \hat{\Theta}_b \text{ and } \hat{\mathcal{V}}_t - \hat{\mathcal{V}}_b = f_5(s) \quad \text{on } (\partial\Omega_{13} \cup \partial\Omega_{14}) \times (0, \mathcal{T}); \tag{2.166}$$

$$\tilde{k}\frac{\partial \hat{\Theta}_t}{\partial \theta} + \tilde{k}_b \frac{\partial \hat{\Theta}_b}{\partial \varphi} = f_6(s,\tilde{t}) \text{ y } \frac{\partial \hat{\mathcal{V}}_t}{\partial \theta} + \frac{\partial \hat{\mathcal{V}}_b}{\partial \varphi} = f_7(s) \quad \text{on } (\partial\Omega_{23} \cup \partial\Omega_{24}) \times (0, \mathcal{T}). \tag{2.167}$$

$$\tilde{\sigma}_t = \tilde{\sigma}_0 + \tilde{\sigma}_1 \Theta; \tag{2.168}$$

$$\tilde{k}_t = 1 + \tilde{k}_1 \Theta. \tag{2.169}$$

In order to have an explicit value for $f_1,\ f_2,\ f_3,\ f_4,\ f_5, f_6$ and f_7, it is found that:

$$\frac{\partial \hat{\Theta}_t}{\partial \tilde{t}} = \frac{1}{\tilde{t}_1}\left(\tilde{t}\frac{(s-b)\tanh\left(\frac{s-b}{\tilde{\omega}^{-1}+\tilde{t}}\right)}{(\tilde{\omega}^{-1}+\tilde{t})^2} + 1\right)\operatorname{sech}\left(\frac{s-b}{\tilde{\omega}^{-1}+\tilde{t}}\right)\sin\theta; \tag{2.170}$$

$$\frac{\partial \hat{\Theta}_t}{\partial s} = -\frac{\tilde{t}}{\tilde{t}_1}\frac{\tanh\left(\frac{s-b}{\tilde{\omega}^{-1}+\tilde{t}}\right)\operatorname{sech}\left(\frac{s-b}{\tilde{\omega}^{-1}+\tilde{t}}\right)}{\tilde{\omega}^{-1}+\tilde{t}}\sin\theta; \quad \frac{\partial \hat{\Theta}_t}{\partial \theta} = \frac{\tilde{t}}{\tilde{t}_1}\operatorname{sech}\left(\frac{s-b}{\tilde{t}+\tilde{\omega}^{-1}}\right)\cos\theta \tag{2.171}$$

$$\frac{\partial^2 \hat{\Theta}_t}{\partial s^2} = \frac{\tilde{t}}{\tilde{t}_1}\frac{\operatorname{sech}\left(\frac{s-b}{\tilde{\omega}^{-1}+\tilde{t}}\right)\left[\tanh^2\left(\frac{s-b}{\tilde{\omega}^{-1}+\tilde{t}}\right) - \operatorname{sech}^2\left(\frac{s-b}{\tilde{\omega}^{-1}+\tilde{t}}\right)\right]}{(\tilde{\omega}^{-1}+\tilde{t})^2}\sin\theta; \tag{2.172}$$

$$\frac{\partial^2 \hat{\Theta}_t}{\partial \theta^2} = \frac{\tilde{t}}{\tilde{t}_1}\operatorname{sech}\left(\frac{s-b}{\tilde{t}+\tilde{\omega}^{-1}}\right)\sin\theta. \tag{2.173}$$

$$\frac{\partial \hat{\mathcal{V}}_t}{\partial s} = -\frac{e^{-s^2}(2s^2+1)}{s^2}\sin^2\theta; \quad \frac{\partial \hat{\mathcal{V}}_t}{\partial \theta} = \frac{e^{-s^2}}{s}\sin(2\theta); \tag{2.174}$$

$$\frac{\partial^2 \hat{\mathcal{V}}_t}{\partial s^2} = \frac{2e^{-s^2}(2s^4+s^2+1)}{s^3}\sin^2\theta; \quad \frac{\partial^2 \hat{\mathcal{V}}_t}{\partial \theta^2} = \frac{2e^{-s^2}}{s}\cos(2\theta). \tag{2.175}$$

$$\frac{\partial \hat{\Theta}_b}{\partial \tilde{t}} = \frac{1}{\tilde{t}_1}\left(\tilde{t}\frac{(s-b)\tanh\left(\frac{s-b}{\tilde{\omega}^{-1}+\tilde{t}}\right)}{(\tilde{\omega}^{-1}+\tilde{t})^2} + 1\right)\operatorname{sech}\left(\frac{s-b}{\tilde{\omega}^{-1}+\tilde{t}}\right)\sin^2\varphi; \tag{2.176}$$

$$\frac{\partial \hat{\Theta}_b}{\partial s} = -\frac{\tilde{t}}{\tilde{t}_1}\frac{\tanh\left(\frac{s-b}{\tilde{\omega}^{-1}+\tilde{t}}\right)\operatorname{sech}\left(\frac{s-b}{\tilde{\omega}^{-1}+\tilde{t}}\right)}{\tilde{\omega}^{-1}+\tilde{t}}\sin^2\varphi; \quad \frac{\partial \hat{\Theta}_b}{\partial \varphi} = \frac{\tilde{t}}{\tilde{t}_1}\operatorname{sech}\left(\frac{s-b}{\tilde{t}+\tilde{\omega}^{-1}}\right)\sin(2\varphi); \tag{2.177}$$

$$\frac{\partial^2 \hat{\Theta}_b}{\partial s^2} = \frac{\tilde{t}}{\tilde{t}_1}\frac{\operatorname{sech}\left(\frac{s-b}{\tilde{\omega}^{-1}+\tilde{t}}\right)\left[\tanh^2\left(\frac{s-b}{\tilde{\omega}^{-1}+\tilde{t}}\right) - \operatorname{sech}^2\left(\frac{s-b}{\tilde{\omega}^{-1}+\tilde{t}}\right)\right]}{(\tilde{\omega}^{-1}+\tilde{t})^2}\sin^2\varphi; \tag{2.178}$$

$$\frac{\partial^2 \hat{\Theta}_b}{\partial \varphi^2} = \frac{\tilde{t}}{\tilde{t}_1}\operatorname{sech}\left(\frac{s-b}{\tilde{t}+\tilde{\omega}^{-1}}\right)\cos(2\varphi); \tag{2.179}$$

$$\frac{\partial \hat{\mathcal{V}}_b}{\partial s} = -\frac{2e^{-s^2}(s^2+1)}{s^3}\sin 2\varphi; \quad \frac{\partial \hat{\mathcal{V}}_b}{\partial \varphi} = \frac{e^{-s^2}}{s^2}\sin(2\varphi); \tag{2.180}$$

$$\frac{\partial^2 \hat{\mathcal{V}}_b}{\partial s^2} = \frac{2e^{-s^2}(2s^4+3s^2+3)}{s^4}\sin^2\varphi; \quad \frac{\partial^2 \hat{\mathcal{V}}_b}{\partial \varphi^2} = \frac{2e^{-s^2}}{s^2}\cos(2\varphi). \tag{2.181}$$

2.5.1 Results.

Before presenting the results, it is necessary to set values for all the parameters involved in the system (2.152) - (2.169). Those values can be found in Table 2.1.

Symbol	**Parameter**	**Definition**	**Value**
b	Parameter	–	0
$\tilde{c}_b$	Heart specific heat capacity	c_b/c_t	1.344
$\mathrm{d}\tilde{t}$	Time step	–	$2.5 \cdot 10^{-5}$
$\tilde{k}_b$	Blood thermal conductivity	k_b/k_0	1.019
$\tilde{k}_1$	Percentage increase of $\tilde{k}$	k_1/k_0	$1.16 \cdot 10^{-3}$
$\tilde{t}_1$	Time parameter	–	0.1
$\tilde{v}$	Velocity	$\varepsilon v/\alpha_b$	853.771
$\tilde{\rho}_b$	Blood density	ρ_b/ρ_t	1
$\tilde{\sigma}_0$	Heart tissue electrical conductivity at T_0	$\dfrac{\sigma_1 V_0^2}{k_0(T_e - T_0)}$	5.859
$\tilde{\sigma}_1$	Tissue increase of electrical conductivity	$\sigma_1 V_0^2/k_0$	14.765
$\tilde{\omega}$	Parameter	–	$1 \cdot 10^{-2}$

TABLE 2.1: Dimensionless parameters.

It remains to study the influence of the value of the order of Chebyshev polynomials, N. As N increases, the difference between the analyical and the numerical solution should decrease. For that purpose, it has been decided to use $||\cdot||_{L^\infty}$ to analise the validity of the results. If the subindex "an" denotes the analytical solution, "num" the numerical solution and δ the comitted error, that is:

$$\delta = ||\hat{\Theta}_{\text{num}} - \hat{\Theta}_{\text{an}}||_{L^\infty(\Omega)}, \tag{2.182}$$

Table [2.2] shows the value of δ for several values of N at $\tilde{t} = \tilde{t}_1$.

N	δ
10	$5.8 \cdot 10^{-5}$
15	$1.6 \cdot 10^{-5}$
20	$6.9 \cdot 10^{-6}$
25	$3.3 \cdot 10^{-6}$

TABLE 2.2: Influence of the order of Chebyshev polynomials.

In all cases the error is in the order of 10^{-5} or less, and as N increased, δ decreases, so this allows to conclude that the employed numerical scheme is correct.

Chapter 3

Results

In this chapter the results obtained by solving numerically the system of equations (2.84) - (2.99) are discussed. For that purpose, firstly the order of Chebyshev polynomials is chosen, taking three properties of the solutions as reference; secondly, a parametric study of the ablation procedure is performed in Section 3.1; Section 3.2 consists of an analysis about the importance of several parameters linked to the mathematical model presented before, and, finally, an optimal control analysis of the system is presented (Section 3.3).

First of all, Table 3.1 shows the values of the dimensional parameters.

Symbol	**Parameter**	**Value**	**Units**	**Reference**
c_b	Blood specific heat capacity	4180	$\mathrm{J/(kg \cdot K)}$	[24]
c_t	Tissue specific heat capacity	4111	$\mathrm{J/(kg \cdot K)}$	[24]
$\mathrm{d}t$	Time step	$2.475 \cdot 10^{-4}$	s	–
k_b	Blood thermal conductivity	0.541	$\mathrm{W/(m \cdot K)}$	[24]
k_0	Tissue thermal conductivity at T_0	0.531	$\mathrm{W/(m \cdot K)}$	[55]
k_1	Tissue increase of thermal conductivity	0.0014	–	[55]
T_0	Human body temperature	37	°C	–
t_d	Discharge time	60	s	–
V_0	Voltage amplitude	28	V	–
v	Blood velocity	4.5	m/s	[5]
w	Perfusion frequency	0.017	Hz	[20]
ε	Catheter radius	$1.3 \cdot 10^{-3}$	m	[5]
ρ_b	Blood density	1000	$\mathrm{kg/m^3}$	[24]
ρ_t	Tissue density	1000	$\mathrm{kg/m^3}$	[**?**]
σ_0	Tissue electrical conductivity at T_0	0.5	S/m	[53]
σ_1	Tissue increase of electrical conductivity	0.02	–	[21]

Table 3.1: Dimensional parameters.

Taking into account the previous values, the dimensionless parameters listed in Table 3.2 applies.

Symbol	**Parameter**	**Definition**	**Value**
$\tilde{c}_b$	Blood specific heat capacity	c_b/c_t	1.344
$\mathrm{d}\tilde{t}$	Time step	–	$2.5 \cdot 10^{-5}$
$\tilde{k}_b$	Blood thermal conductivity	k_b/k_0	1.019
$\tilde{k}_1$	Tissue increase of $\tilde{k}$	k_1/k_0	$1.162 \cdot 10^{-1}$
$\tilde{t}_d$	Discharge time	$\alpha_{t_0} t_d/\varepsilon^2$	6.056
$\tilde{v}$	Velocity	$\varepsilon v/\alpha_b$	853.771
$\tilde{w}$	Perfusion frequency	$\rho_b c_b \varepsilon^2 w/k_0$	0.226
$\tilde{\rho}_b$	Blood density	ρ_b/ρ_t	1
$\tilde{\sigma}_0$	Tissue electrical conductivity at T_0	$\dfrac{\sigma_1 V_0^2}{k_0(T_e - T_0)}$	5.859
$\tilde{\sigma}_1$	Tissue increase of $\tilde{\sigma}$	$\sigma_1 V_0^2/k_0$	14.765

TABLE 3.2: Dimensionless parameters.

Once the values of the parameters are set, as a first result the influence of the order of Chebyshev polynomials will be analised, with the goal of knowing from which value of N the obtained values represent correctly the main features of the real solution. For that purpose, 3 numbers will be examined: the maximum temperature, T_{max}, the distance to the catheter surface where T_{max} is reached, r_{max}, and the safe radius, r_{safe}; that is, the distance to the catheter surface from which temperature is lower than 40°C.

$\boldsymbol{N}$	$\boldsymbol{T_{max}}$ **(°C)**	$\boldsymbol{r_{max}}$ **(mm)**	$\boldsymbol{r_{safe}}$ **(mm)**
11	69.069	0.794	6.813
15	68.481	0.792	6.724
19	68.415	0.790	6.721
23	68.405	0.790	6.720

TABLE 3.3: Influence of the order of Chebyshev polynomials.

The previous table shows that as the order of the polynomials is increased, all three values tend to a certain value. Values of N greater than 15 produce small differences, so it has been decided to choose $N = 15$. This is because the current model is approximate, and the commited error is greater than the one that is obtained by taking $N = 15$ and not $N = 23$, for example.

Moreover, as the number of algebraic equations that has to be solved after spatially-discretizing the elliptic equations scales with N^2 (see Section 2.4), the computational cost raises in a very important way by increasing the order of the polynomial.

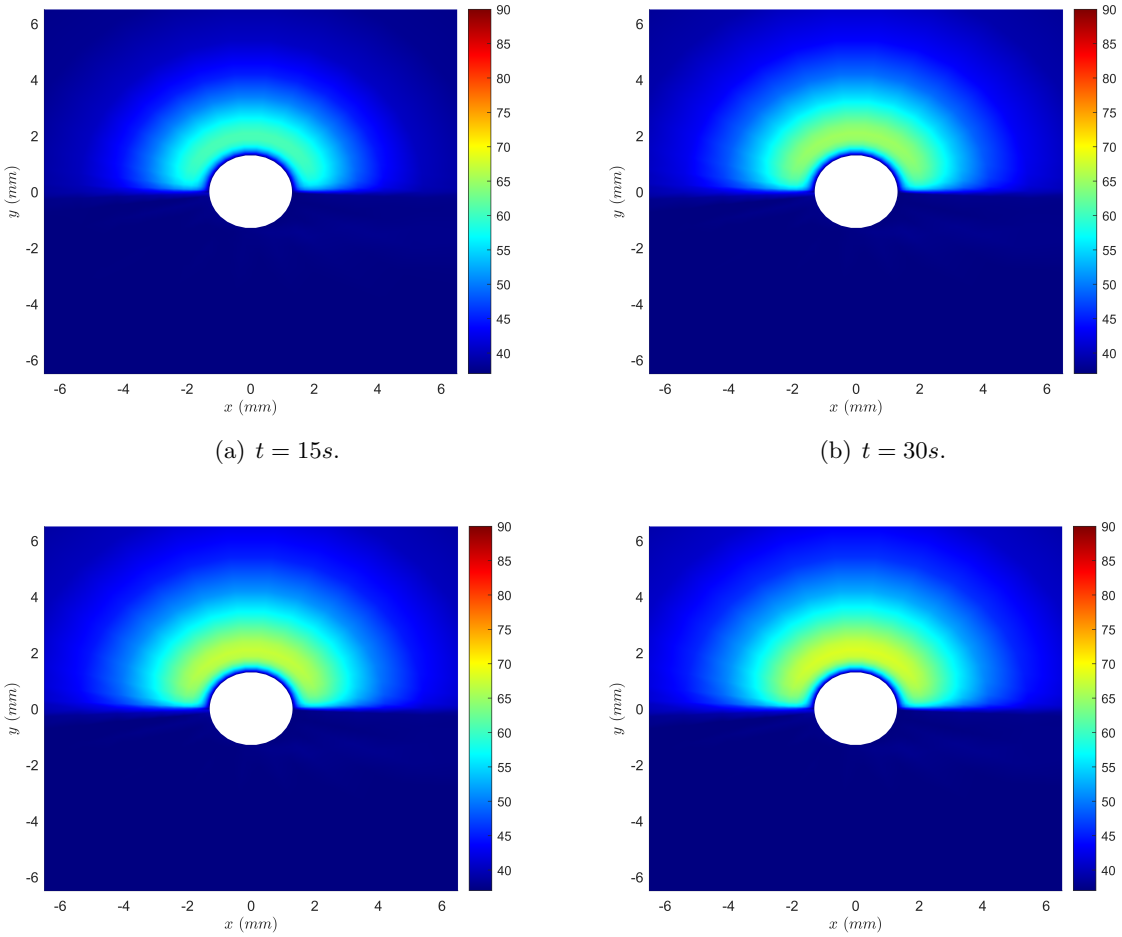

(a) $t = 15s$. (b) $t = 30s$.

(c) $t = 45s$. (d) $t = 60s$.

FIGURE 3.1: Temperature distribution in °C.

Figure 3.1 shows that the temperature distribution is nearly symmetrical. Moreover, as Table 3.3 shows maximum temperature is far from dangerous values, even though the safe radius is too big, as it has been pointed out that the esophagus can be at a distance of 5mm to the endocardium. Maximum blood temperature, 46.592°C, is reached on the blood-tissue interface at a distance of 1.034mm to the catheter surface.

3.1 Influence of the parameters of the procedure.

Focusing attention on the ablation procedure, four parameters involved in the model can be modified: the catheter radius, the amplitude of the voltage, the discharge time and the contact force. The influence of the first three of them will be discussed in this section, while the

effect of the contact force will be left for future research. This is because it involves important modifications in the numerical resolution, specially in the spatial discretization, as the geometry of the domain becomes more complicated.

It has to be noted that, from now on, the value of the integral of the temperature distribution in the cardiac tissue is also analised, even though it will not be taken into account in the section related to the influence of the catheter radius, as the domain is not the same in each case. The integral is performed using the trapezoidal rule; the precision of the method is not clear, as the domain is almost infinite and the number of points is modest, but it will serve as a comparation between different conditions.

3.1.1 Amplitude of the voltage and discharge time.

On the one hand, given the similarity of the graph at $t = 45$s and $t = 60$s, Table 3.4 illustrates the variation in the three values analised previously and the integral of the temperature distribution. The variations in maximum temperature and its location are negligible, while the safe radius increases significantly as time increases; that is, the zones far from the catheter surface are the ones that suffer significant temperature changes.

t (s)	T_{max} (°C)	r_{max} (mm)	r_{safe} (mm)	$\int_{\Omega_1} T_t \, dx$ (K ·m ^{2})
45	67.396	0.780	6.301	0.676
60	68.481	0.792	6.724	0.678
75	69.116	0.798	6.995	0.679

TABLE 3.4: Influence of the discharge time ($V_0 = 28$V).

In view of the above, if the amplitude of the voltage, V_0, is also modified, it can be verified in Table 3.5 that lower values of V_0 produce temperature distributions that are more concentrated near the catheter. Consequently, if the esophagus is near the endocardium, the best choice will be to lower the voltage amplitude and the discharge time as required.

t (s)	V_0 (V)	T_{max} (°C)	r_{max} (mm)	r_{safe} (mm)	$\int_{\Omega_1} T_t \, dx$ (K ·m ^{2})
30	29	67.789	0.756	5.820	0.676
60	28	68.481	0.792	6.724	0.678
90	27	66.782	0.803	6.924	0.677

TABLE 3.5: Influence of the voltage amplitude.

3.1.2 Catheter radius.

The last parameter of the procedure that can be modified is catheter radius. As the catheter has to be inserted through a vein, there will be a maximum permissible value, while the catheter is

not supposed to be too small because of design limitations. As a consequence, Table 3.6 shows the effect of small variations in the value of catheter radius, and enables to deduce that higher values produce higher safe radii, while the value of the maximum temperature decreases and its location increases. The effect is just the opposite if ε is lowered. These results are obtained because of the heat transfer between the blood and the cardiac tissue, as catheter radius is proportional to dimensionless blood velocity and perfusion frequency. The importance of both terms will be analised later, in order to give a clear explanation of the differences observed below.

ε (mm)	T_{max} (°C)	r_{max} (mm)	r_{safe} (mm)
1.1	72.123	0.704	6.551
1.3	68.481	0.792	6.724
1.5	65.569	0.876	6.885

TABLE 3.6: Influence of the catheter radius.

3.2 Influence of the parameters of the model.

In order to obtain the system of equations (2.84) - (2.99), several assumptions have been made. The choice is not inmediate in some cases, so it is necessary to evaluate the importance of each one in the results. For that purpose, in this section four hypotheses will be analised: the temperature-dependency of the thermal and electrical conductivities in Section 3.2.1, the presence of the perfusion term in Section 3.2.2, the value of blood velocity in Section 3.2.3 and the importance of the equation of conservation of energy in the blood in Section 3.2.4.

3.2.1 Temperature-dependency of the thermal and electrical conductivities.

In the previous chapter, the followed approach has consisted of a linear model with respect to temperature for both conductivities. However, in the case of the electrical conductivity, this is not the only model that has been proposed previously. Furthermore, if $\sigma = \sigma_0$ the problem becomes more simple, as the equation (2.87) - (2.89) is reduced to the Laplace equation. Drawing attention to the thermal conductivity, it is not clear that such an small value for k_1 (see Table 3.1) produces modifications with respect to the constant-thermal-conductivity model.

k_1	T_{max} (°C)	r_{max} (mm)	r_{safe} (mm)	$\int_{\Omega_1} T_t \, dx$ (K ·m ^{2})
0	68.498	0.790	6.722	0.678
0.0014	68.481	0.792	6.724	0.678

TABLE 3.7: Influence of the thermal conductivity model.

On the one hand, as it can be seen in Table 3.7, the differences between the case of constant thermal conductivity and the one proposed in the model are negligible.

On the other hand, there exists an additional approach for the electrical conductivity, where $\sigma_1 = 0.015$ and not $\sigma_1 = 0.02$ [González-Suarez *et al*, 2016]. It has to be remarked that the current model is actually a linearization from

$$\sigma(T) = \sigma_0 e^{\sigma_1 (T - T_0)} \tag{3.1}$$

[Duck, 1990], and serves as a first-approximation study.

σ_1	T_{max} (°C)	r_{max} (mm)	r_{safe} (mm)	$\int_{\Omega_1} T_t \, dx$ (K ·m ^{2})
0	62.077	0.797	5.753	0.669
0.015	67.039	0.793	6.508	0.676
0.02	68.481	0.792	6.724	0.678

TABLE 3.8: Influence of the electrical conductivity model.

Based on the values presented in Table 3.8, the difference between $\sigma_1 = 0.015$ and $\sigma_1 = 0.02$ is not important. However, it is necessary to consider a temperature-dependent electrical conductivity, as the maximum temperature and the safe radius in the case of $\sigma_1 = 0$ are a major deviation wih respect to temperature-dependent models. Lower values of T_{max} are caused as a consequence of the fact that the source term arising in the equation of conservation of energy is proportional to σ, and r_{safe} is higher due to the absence of σ in the elliptic equation; that is, σ acts in this equation as k in the equation of conservation of energy: as σ decreases, voltage distribution is more concentrated in the surroudings of the origin.

3.2.2 Perfusion term.

Blood perfusion is the process where blood passes from the circulatory system to an organ or tissue through capillaries, in order to supply oxygen. In the case of catheter ablation, this process is also a cooling process, as blood temperature is lower than the temperature of the cardiac tissue. Consequently, a term arises in the equation of conservation of energy, and, in principle, it is not clear if it is dominant or not. Several publications neglect it as [Tungjitkusolmun *et al.*, 2002] and [González-Suárez *et al.*, 2018], while other authors consider it [Fasano *et al.*, 2016].

Perfusion term	T_{max} (°C)	r_{max} (mm)	r_{safe} (mm)	$\int_{\Omega_1} T_t \, dx$ (K ·m ^{2})
✓	68.481	0.792	6.724	0.678
✗	78.682	0.899	8.509	0.693

TABLE 3.9: Influence of the perfusion term.

Table [3.9] proves that blood perfusion is an effective method to prevent from important temperature variations in the cardiac tissue, so perfusion term cannot be neglected in the current model. This is because blood temperature is supposed to be equal to 37°C inside the cardiac

tissue, so the difference between tissue and blood temperatures is big and heat transfer caused by blood perfusion is important. If the temperature of the cardiac tissue increases, the cooling process becomes more effective, and this is the reason why r_{safe} is higher in the case of the absence of the perfusion term. Moreover, as the dimensionless perfusion frequency is proportional to ε^2 (see Table 3.2), this proves the fact that higher catheter radius cause smaller values of maximum cardiac tissue temperature.

Despite the fact that the inclusion of the perfusion term seems to be an important improvement, it may not be necessarily true that blood temperature remains constant, so further investigations are needed in order to improve the accuracy of the results.

3.2.3 Value of blood velocity.

In order to obtain the previous results, medium blood flow has been considered (see [Benchimol, Desser and Gartlan, 1975]). The next table shows the influence of the chosen mean blood velocity, and tells that higher values produce lower values of temperature in the cardiac tissue, as expected. Nevertheless, the differences are not substantial.

v (m/s)	T_{max} (°C)	r_{max} (mm)	r_{safe} (mm)	$\int_{\Omega_1} T_t \, dx$ (K ·m ^{2})
2.5	69.496	0.792	6.730	0.680
4.5	68.481	0.792	6.724	0.678
8.5	68.472	0.792	6.722	0.676

Table 3.10: Influence of blood velocity I.

To conclude, the maximum temperature achieved on the blood-tissue interface in each case can be seen in Table 3.11. The differences are important, even though the only parameter that is significantly affected is the value of the integral of the temperature distribution.

v (m/s)	$T_{max}(\theta = 0)$ (°C)	$r_{max}(\theta = 0)$ (mm)
2.5	47.757	0.912
4.5	46.592	1.034
8.5	44.982	1.192

Table 3.11: Influence of blood velocity II.

3.2.4 Importance of the equation of conservation of energy in the blood.

As variations in blood velocity do not induce substantial changes in the temperature distribution, it has been decided to study if the presence of the equation of conservation of energy is important in the model presented in the previous chapter. Table 3.12 shows that it can be neglected in an approximate model, as the differences in the previously analised values are not significant. It is

worth noting that the value of the integral of the temperature distribution is lower in the case of the reduced model, as the temperature on the interface is greater than 37°C, as it has been shown in Table 3.11.

Energy equation	T_{max} (°C)	r_{max} (mm)	r_{safe} (mm)	$\int_{\Omega_1} T_t \, dx$ (K ·m ^{2})
✓	68.481	0.792	6.724	0.678
✗	68.264	0.791	6.709	0.657

TABLE 3.12: Importance of the equation of conservation of energy in the blood.

3.3 Optimal control analysis.

As has already been remarked in the first chapter, control systems for catheter temperature have been developed [Calkins *et al.*, 1994]. In connection with the mathematical modelization of the problem, there exist studies where control systems have been proposed for the cardiac tissue temperature in contact with the catheter [Haemerich and Webster, 2005], specifically PID-type controls. The previous method has also been validated by other investigators [González-Suárez *et al.*, 2018], even though there have been no studies where the maximum temperature on the cardiac tissue is controlled. Consequently, an interesting feature will be to do this control.

One of the objectives of this work is to lay the foundations for a more complex future analysis of the problem, considering a three dimensional model without symmetry assumptions. However, in the case of developing a control system, the computational cost would be too high, so attention will be focused in designing a control system for the two dimensional model. In particular, a prior objective consists of solving the equations only in the cardiac tissue, making use of modified boundary conditions on the catheter-tissue and tissue-blood interfaces that are explained below.

The basis for the two-dimensional model is the approach followed in this work, that is, the rotational symmetry assumption. Nevertheless, it is not necessarily true that catheter temperature is equal to human body temperature, so Robin boundary conditions are required in order to modelise correctly the heat transfer between the catheter and the cardiac tissue. It has to be noted that Robin-type boundary conditions can also be applied on the cardiac tissue-blood interface, with the objective of not solving the equation of conservation of energy in the blood. So, following [Tungjitkusolmun *et al.*, 2002] or [Schutt *et al.*, 2009]:

$$k_t \frac{\partial T_t}{\partial \nu} + h_{tc}(T_t - T_0) = 0 \quad \text{on } \partial\Omega_{11} \times (0, \mathcal{T}); \tag{3.2}$$

$$k_t \frac{\partial T_t}{\partial \nu} + h_{tb}(T_t - T_0) = 0 \quad \text{on } (\partial\Omega_{13} \cup \Omega_{14}) \times (0, \mathcal{T}), \tag{3.3}$$

where h_{tc} and h_{tb} are the heat transfer coefficients between the cardiac tissue and the catheter and between the tissue and the blood, respectively. Currently, the available values are not validated, so it is not possible to ensure that the previous boundary conditions represent correctly real effects. As a consequence, it has been decided not to use them in the present study.

Once improved models are performed and heat transfer coefficients are validated, another important step consists of developing a control system for the maximum temperature achieved in the cardiac tissue. However, first of all it has to be analised if it is possible to design such a control system. For that purpose, a optimal-control study will be performed.

Another assumption consists of considering that voltage is known on the interface between the blood and the cardiac tissue ($\mathcal{V}(s) \approx 1/s$). Thus, modifying Dirichlet boundary conditions (2.85) and (2.91) by Robin boundary conditions (3.2) and (3.3), assuming that blood temperature is equal to T_0 and neglecting the perfusion term, the system of equations takes the following form:

$$\begin{cases} \Theta_t - \nabla \cdot (k(\Theta)\nabla\Theta) = \sigma(\Theta)|\nabla\mathcal{V}|^2 \quad \text{in } \Omega_1 \times (0,\mathcal{T}); & (3.4) \\ \dfrac{\partial\Theta}{\partial\nu} + \mathrm{Bi}(\Theta)\Theta = 0 \quad \text{on } \partial\Omega_1 \times (0,\mathcal{T}); & (3.5) \\ \Theta = \Theta_0 \quad \text{on } \Omega_1 \times \{t=0\}; & (3.6) \\ \nabla \cdot (\sigma(\Theta)\nabla\mathcal{V}) = 0 \quad \text{in } \Omega_1 \times (0,\mathcal{T}); & (3.7) \\ \mathcal{V} = \mathcal{V}_0 \quad \text{on } \partial\Omega_1 \times (0,\mathcal{T}), & (3.8) \end{cases}$$

where Biot number has been introduced, after nondimensionalising the boundary conditions (3.2) and (3.3):

$$\mathrm{Bi} = \frac{h\varepsilon}{\tilde{k}}. \tag{3.9}$$

3.3.1 Existence and uniqueness.

In order to obtain the existence and uniqueness of the system of equations (3.4) - (3.8), an extension of the article of S.N. Antontsev and M. Chipot [Antontsev and Chipot, 1994] will be done. The proof is divided into three parts:

1. Extension of the theory of parabolic linear equations, including the the case of Robin boundary conditions.
2. Assuming that $\sigma = \sigma(s)$ and $k = k(s)$, where s is a function with certain properties, proof of the existence and uniqueness of que equation (3.4) with the boundary conditions (3.5) and initial condition (3.6) and the equation (3.7) with the boundary condition (3.8).
3. Proof of $s = \Theta$, and, consequently, the existence and uniqueness of the system of equations (3.4) - (3.8).

Extension of the theory of linear parabolic equations.

The starting point for this section is the theory of existence and uniqueness of linear parabolic equations of the book from L.C. Evans [Evans, 2010] located at §7.1, where Dirichlet boundary conditions are considered. The goal of this section is to obtain the same results of existence and uniqueness, but in the more general case with Robin boundary conditions.

From now on, $\Omega = \Omega_1$. If Ω is an open and bounded set of $\mathbb{R}^n$, $\partial\Omega$ is C^1 and $\mathcal{T} > 0$, the next problem will be considered:

$$\begin{cases} u_t + Lu = f \quad \text{in } \Omega \times (0, \mathcal{T}); & (3.10) \\ \dfrac{\partial u}{\partial \nu} + hu = w \quad \text{on } \partial\Omega \times (0, \mathcal{T}); & (3.11) \\ u = g \quad \text{on } \Omega \times \{t = 0\}, & (3.12) \end{cases}$$

where $f \in L^2(0, \mathcal{T}; (H^1(\Omega_{\mathcal{T}}))^*)$, $g \in L^2(\Omega)$, $h \in L^2(0, \mathcal{T}; L^\infty(\partial\Omega))$ and $w \in L^2(0, \mathcal{T}; H^{-1/2}(\partial\Omega))$ are known. $(H^1(\Omega_{\mathcal{T}})))^*$ is the dual space of $H^1(\Omega)$, while $H^{-1/2}(\partial\Omega)$ is the dual space of $H^{1/2}(\partial\Omega)$ and $\Omega_T = \Omega \times (0, \mathcal{T})$. Weak solutions will be $u \in L^2(0, \mathcal{T}; H^1(\Omega))$. Moreover, L is, at each time, a second order differential operator:

$$Lu = -\sum_{i,j=1}^{n} (a^{ij}(x,t)u_{x_i})_{x_j} + \sum_{i=1}^{n} b^i(x,t)u_{x_i} + c(x,t)u, \tag{3.13}$$

where

$$a^{ij}, b^i, c \in L^\infty(\Omega_{\mathcal{T}}) \quad (i, j = 1, ..., n). \tag{3.14}$$

Before passing to define the bilinear form associated to the operator L, the weak formulation of the problem will be written. For that purpose, the equation (3.10) is multiplied by a function $v \in H^1(\Omega)$ and integrating by parts yields the result:

$$\begin{aligned} \int_\Omega u'v \, \mathrm{d}x + \int_\Omega \sum_{i,j=1}^{n} a^{ij} u_{x_i} v_{x_j} + \sum_{i=1}^{n} b^i(x,t)u_{x_i}v + c(x,t)uv \, \mathrm{d}x + \int_{\partial\Omega} h(\mathrm{Tr}\ u)(\mathrm{Tr}\ v) \, \mathrm{d}S = \\ = \int_\Omega fv \, \mathrm{d}x + \int_{\partial\Omega} w(\mathrm{Tr}\ v) \, \mathrm{d}S, \end{aligned} \tag{3.15}$$

where Green's formula has been used, including the boundary condition in the weak formulation of the problem. Moreover, the symbol $' = \mathrm{d}/\mathrm{d}t$ and

$$\begin{aligned} \mathrm{Tr} : H^1(\Omega) &\to L^2(\partial\Omega) \\ \mathrm{Tr}\ u &= u|_{\partial\Omega} \end{aligned} \tag{3.16}$$

is the trace operator, defined at each time $0 \leq t \leq \mathcal{T}$.

From the equation (3.15), the following symmetric bilinear form associated to the operator L is defined:

$$B[u, v; t] = \int_\Omega \sum_{i,j=1}^{n} a^{ij} u_{x_i} v_{x_j} + \sum_{i=1}^{n} b^i(x,t)u_{x_i}v + c(x,t)uv \, \mathrm{d}x + \int_{\partial\Omega} h(\mathrm{Tr}\ u)(\mathrm{Tr}\ v) \, \mathrm{d}S. \tag{3.17}$$

With all the previous considerations, now it is possible to present the problem whose existence and uniqueness of weak solutions is looked for:

Definition. *It is said that a function*

$$u \in L^2(0,\mathcal{T};H^1(\Omega)),\ with\ u' \in L^2(0,\mathcal{T};(H^1(\Omega))^*) \tag{3.18}$$

is a weak solution of the parabolic initial/boundary-value problem (3.10) - (3.12) if

$$\text{(i) } \langle u', v\rangle + B[u', v; t] = (f, v) \tag{3.19}$$

for all $v \in H^1(\Omega)$,

$$\text{(ii) } u(0) = g \tag{3.20}$$

and

$$\text{(iii) } \frac{\partial u}{\partial \nu} + hu = w \quad on\ \partial\Omega \times (0,T). \tag{3.21}$$

In addition,

$$u \in C(0,\mathcal{T};L^2(\Omega)) \tag{3.22}$$

as a consequence of Theorem 3 (Evans, §5.9.2).

Theorem. *There exists a unique weak solution for the problem (3.10) - (3.12).*

Proof. If it is shown that the bilinear form defined in (3.17) is coercive and bounded, the proof of the theorem is the same as the one that is made on the book of R. Dautray and J.L. Lions [Dautray and Lions, 2000], §18.3.3, Theorem 2.

With the objective of proving the boundedness, at each time $0 < t < \mathcal{T}$:

$$\begin{aligned} B[u,v;t] \leq \sum_{i,j=1}^{n} ||a^{ij}||_{L^\infty(\Omega)} \int_\Omega |\nabla u|\ |\nabla v|\ \mathrm{d}x + \sum_{i=1}^{n} ||b^i||_{L^\infty(\Omega)} \int_\Omega |\nabla u|\ |v|\ \mathrm{d}x + \\ + ||c||_{L^\infty(\Omega)} \int_\Omega |u|\ |v|\ \mathrm{d}x + ||h||_{L^\infty(\partial\Omega)} \int_{\partial\Omega} |\mathrm{Tr}\ u||\mathrm{Tr}\ v|\ \mathrm{d}x. \end{aligned} \tag{3.23}$$

Then, taking into account the Cauchy-Schwarz inequality, it is satisfied:

$$\begin{aligned} B[u,v;t] \leq \sum_{i,j=1}^{n} ||a^{ij}||_{L^\infty(\Omega)} ||\nabla u||_{L^2(\Omega;\mathbb{R}^n)} ||\nabla v||_{L^2(\Omega;\mathbb{R}^n)} + \\ + \sum_{i=1}^{n} ||b^i||_{L^\infty(\Omega)} ||\nabla u||_{L^2(\Omega;\mathbb{R}^n)} ||v||_{L^2(\Omega)} + ||c||_{L^\infty(\Omega)} ||u||_{L^2(\Omega)} ||v||_{L^2(\Omega)} + \\ + ||h||_{L^\infty(\partial\Omega)} ||\mathrm{Tr}\ u||_{L^2(\Omega)} ||\mathrm{Tr}\ v||_{L^2(\Omega)}, \end{aligned} \tag{3.24}$$

and using the trace theorem (Evans, §5.5, Theorem 1) it follows that:

$$\begin{aligned} B[u,v;t] \leq & \sum_{i,j=1}^{n} ||a^{ij}||_{L^\infty(\Omega)} ||\nabla u||_{L^2(\Omega;\mathbb{R}^n)} ||\nabla v||_{L^2(\Omega;\mathbb{R}^n)} + \\ & + \sum_{i=1}^{n} ||b^i||_{L^\infty(\Omega)} ||\nabla u||_{L^2(\Omega)} ||v||_{L^2(\Omega)} + ||c||_{L^\infty(\Omega)} ||u||_{L^2(\Omega)} ||v||_{L^2(\Omega)} + \\ & + C||h||_{L^\infty(\partial\Omega)} ||u||_{H^1(\Omega)} ||v||_{H^1(\Omega)} \leq \\ \leq & \alpha ||u||_{H^1(\Omega)} ||v||_{H^1(\Omega)}, \end{aligned} \tag{3.25}$$

which proves the result.

In the case of the coercivity, it has to be proved that there exists a constant $\beta > 0$ such that:

$$\beta ||u||^2_{H^1(\Omega)} \leq B[u,u;t] \quad \text{for all } u \in H^1(\Omega). \tag{3.26}$$

It will be assumed that the previous condition is not satisfied. So there exists an $N \in \mathbb{N}$ with the property of that for all $n \geq N$ a sequence $u_n \in H^1(\Omega)$ can be defined, and it satisfies

$$||u_n||^2_{H^1(\Omega)} > nB[u_n, u_n; t]. \tag{3.27}$$

Now let $v_n = u_n / ||u_n||_{H^1(\Omega)}$. Then, $||v_n||_{H^1(\Omega)} = 1$, so:

$$B[v_n, v_n; t] < \frac{1}{n} \quad \text{for all } n \geq N. \tag{3.28}$$

As $\{v_n\}$ is bounded in $H^1(\Omega)$, Rellich-Kondrachov compactness theorem (Evans, §5.7, Theorem 1) can be applied to deduce that $\{v_n\}$ has a subsequence $\{v_{n_k}\}$ converging to a $v \in L^2(\Omega)$.

Now, using (3.28) it is deduced that:

$$\begin{aligned} \int_\Omega \sum_{i,j=1}^{n} a^{ij} v_{n_k x_i} v_{n_k x_j} = & C \sum_{i,j=1}^{n} ||a^{ij}||_{L^\infty(\Omega)} \int_\Omega |\nabla v_{n_k}|^2 \, \mathrm{d}x = \\ = & C||\nabla v_{n_k}||^2_{L^2(\Omega;\mathbb{R}^n)} < \frac{1}{n_k}, \quad 0 < C \leq 1, \end{aligned} \tag{3.29}$$

that is, $Dv_{n_k} \to 0$ in $L^2(\Omega)$. Thus, for all $\phi \in C_0^\infty(\Omega)$:

$$\int_\Omega v \nabla \phi \, \mathrm{d}x = \lim_{k\to\infty} \int_\Omega v_{n_k} \nabla \phi \, \mathrm{d}x = - \lim_{k\to\infty} \int_\Omega \nabla v_{n_k} \phi \, \mathrm{d}x = 0, \tag{3.30}$$

where the dominated convergence theorem has been used. Hence, $v \in H^1(\Omega)$ and $\nabla v = 0$, that is, $v_{n_k} \to v$ in $H^1(\Omega)$. As $||v_{n_k}||_{H^1(\Omega)} = 1$ for all k, also $||v||_{H^1(\Omega)} = 1$.

Next, following the same reasoning as in (3.29):

$$C||\mathrm{Tr}\ v_{n_k}||^2_{L^2(\partial\Omega)} < \frac{1}{n_k}, \quad 0 < C \leq 1, \tag{3.31}$$

and as the trace operator is bounded, there exists a constant C' such that:

$$\begin{aligned} ||\text{Tr } v||_{L^2(\partial\Omega)} &= ||\text{Tr } v + \text{Tr } v_{n_k} - \text{Tr } v_{n_k}||_{L^2(\partial\Omega)} \leq \\ &\leq ||\text{Tr } v - \text{Tr } v_{n_k}||_{L^2(\partial\Omega)} + ||\text{Tr } v_{n_k}||_{L^2(\partial\Omega)} < \\ &< \frac{1}{Cn_k} + C'||v - v_{n_k}||_{H^1(\Omega)}, \end{aligned} \tag{3.32}$$

after using the triangular inequality. Setting $k \to \infty$ it is concluded that Tr v in $L^2(\partial\Omega)$.

With the previous demonstrations, it has been proved that $v \in H^1(\Omega)$ and $\nabla v = \text{Tr } v = 0$. $\nabla v = 0$ implies that v is constant in Ω, so it is continuous in Ω. As the trace of a continuous function is the value of that function at the boundary, if the trace is 0, that means $v = 0$. This contradicts the fact that $||v||_{H^1(\Omega)} = 1$, so $B[u, v; t]$ is coercive.

□

Existence and uniqueness of both equations separately.

First of all, a function $s \in L^2(0, \mathcal{T}; L^2(\Omega))$ with Tr $s \in L^2(0, \mathcal{T}; L^2(\partial\Omega))$ is considered. Moreover:

$$\mathcal{V}_0 \in L^\infty(0, \mathcal{T}; W^{1,\infty}(\Omega)) \text{ with } \sigma\mathcal{V}_0\nabla\mathcal{V}_0 \in L^\infty(0, \mathcal{T}; H^1(\partial\Omega)) \text{ and } \nabla(\sigma\mathcal{V}_0\nabla\mathcal{V}_0)|_{\partial\Omega} = 0; \tag{3.33}$$

$$k \text{ continuous with respect to } s, \quad 0 < k_1 \leq k \leq k_2 < \infty; \tag{3.34}$$

$$\sigma \text{ linear with respect to } s, \qquad 0 < \sigma_1 \leq \sigma \leq \sigma_2 < \infty; \tag{3.35}$$

$$\text{Bi continuous with respect to } s, \quad 0 < \text{Bi}_1 \leq \text{Bi} \leq \text{Bi}_2 < \infty, \tag{3.36}$$

where k_1, σ_1, Bi_1, k_2, σ_2 and Bi_2 are positive constants, so $k, \sigma \in L^\infty(0, \mathcal{T}; L^\infty(\Omega))$ and $\text{Bi} \in L^\infty(0, \mathcal{T}; L^\infty(\partial\Omega))$.

Elliptic equation.

In this section the equation (3.7) with the boundary condition (3.8) will be studied:

$$\begin{cases} \nabla \cdot (\sigma\nabla\mathcal{V}) = 0 \quad \text{in } \Omega \times (0, \mathcal{T}), & (3.37) \\ \mathcal{V} = \mathcal{V}_0 \quad \text{on } \partial\Omega \times (0, \mathcal{T}). & (3.38) \end{cases}$$

Firstly, it is interesting to do a change of variable that transforms the boundary condition (3.38) into an homogeneous one. For that purpose, a new variable is defined:

$$\Upsilon = \mathcal{V} - \mathcal{V}_0, \tag{3.39}$$

so the equation (3.7) - (3.8) becomes:

$$\begin{cases} \nabla \cdot (\sigma\nabla\Upsilon) = f \quad \text{in } \Omega \times (0, \mathcal{T}), & (3.40) \\ \Upsilon = 0 \quad \text{on } \partial\Omega \times (0, \mathcal{T}), & (3.41) \end{cases}$$

where $f = -\nabla \cdot (\sigma\nabla\mathcal{V}_0)$. Solutions as $\Upsilon \in H_0^1(\Omega)$ wil be looked for at each time $0 < t < \mathcal{T}$. With the aim of showing the existence and uniqueness of the previous equation, the associated

differential operator is defined:

$$L\Upsilon = -\nabla \cdot (\sigma \nabla \mathcal{V}), \tag{3.42}$$

while the bilinear form is

$$B[\Upsilon, v; t] = \int_\Omega \sigma \nabla \Upsilon \cdot \nabla v \, \mathrm{d}x, \quad \forall v \in H_0^1(\Omega). \tag{3.43}$$

On the one side, f satisfies:

$$\langle f, v \rangle = -\int_\Omega \nabla \cdot (\sigma \nabla \mathcal{V}_0) v \, \mathrm{d}x = -\int_\Omega \sigma \nabla \mathcal{V}_0 \cdot \nabla v \, \mathrm{d}x, \quad \forall v \in H_0^1(\Omega), \tag{3.44}$$

that is, the weak formulation of the problem (3.40) - (3.41) is as follows:

$$\int_\Omega \sigma \nabla \Upsilon \cdot \nabla v \, \mathrm{d}x = -\int_\Omega \sigma \nabla \mathcal{V}_0 \cdot \nabla v \, \mathrm{d}x, \quad \forall v \in H_0^1(\Omega). \tag{3.45}$$

Furthermore:

$$\int_\Omega |\sigma \nabla \mathcal{V}_0|^2 \, \mathrm{d}x \leq ||\sigma^2||_{L^\infty(\Omega)} |||\nabla \mathcal{V}_0|^2||_{L^\infty(\Omega)} \int_\Omega \, \mathrm{d}x < \infty, \tag{3.46}$$

so $\sigma \nabla \mathcal{V}_0 \in L^2(\Omega)$, and using the characterization of the space $H^{-1}(\Omega)$ (Evans, §5.9.1, Theorem 1) it is deduced that $f \in H^{-1}(\Omega)$ at each time $0 < t < \mathcal{T}$.

On the other side, as $\sigma \in L^\infty(\Omega)$ and the bilinear form from (3.43) is bounded and is coercive, Lax-Milgram theorem (Evans, §6.2.1, Theorem 1) applies, so there exists a unique weak solution $\Upsilon \in H_0^1(\Omega)$ for the problem (3.40) - (3.41), which is equivalent to state that there exists a unique weak solution $\mathcal{V} \in H^1(\Omega)$.

Assuming that $\mathcal{V}$ is measurable in t, the maximum principle can be used (§8.1, Theorem 8.1 from [Gilbarg and Trudinger, 2010]), so:

$$||\mathcal{V}||_{L^\infty(\Omega)} \leq ||\mathcal{V}_0||_{L^\infty(\partial\Omega)}. \tag{3.47}$$

In addition, multiplying the equation (3.37) by $\mathcal{V} - \mathcal{V}_0$ yields the result:

$$\int_\Omega \nabla \cdot (\sigma \nabla \mathcal{V})(\mathcal{V} - \mathcal{V}_0) \, \mathrm{d}x = \int_\Omega \sigma \nabla \mathcal{V} \cdot \nabla (\mathcal{V} - \mathcal{V}_0) \, \mathrm{d}x = 0. \tag{3.48}$$

Finally:

$$\sigma_1 \int_\Omega |\nabla \mathcal{V}|^2 \, \mathrm{d}x \leq \left| \int_\Omega \sigma \nabla \mathcal{V} \cdot \nabla \mathcal{V}_0 \, \mathrm{d}x \right| \leq \sigma_2 \int_\Omega |\nabla \mathcal{V}| \, |\nabla \mathcal{V}_0| \, \mathrm{d}x, \tag{3.49}$$

and using the Cauchy-Schwarz inequelity:

$$\sigma_1 \int_\Omega |\nabla \mathcal{V}|^2 \, \mathrm{d}x < \infty \Longrightarrow \mathcal{V} \in L^\infty(0, \mathcal{T}; H^1(\Omega) \cap L^\infty(\Omega)). \tag{3.50}$$

Parabolic equation.

In this section, the following parabolic equation will be analised:

$$\begin{cases} \Theta_t - \nabla \cdot (k\nabla\Theta) = \sigma|\nabla\mathcal{V}|^2 \quad \text{in } \Omega \times (0,\mathcal{T}); & (3.51) \\ \dfrac{\partial\Theta}{\partial\nu} + \text{Bi } \Theta = 0 \quad \text{on } \partial\Omega \times (0,\mathcal{T}); & (3.52) \\ \Theta = \Theta_0 \quad \text{on } \Omega \times \{t=0\}. & (3.53) \end{cases}$$

Comparing (3.51) - (3.53) with (3.4) - (3.6), it is clear that $\Theta_0 \in L^2(\Omega)$ and $h/k \in L^\infty(0,\mathcal{T};\partial\Omega)$. With regard to f, it has to be proved that $\sigma|\nabla\mathcal{V}|^2 \in L^2(0,T;(H^1(\Omega_\mathcal{T}))^*)$. As $H_0^1(\Omega_\mathcal{T}) \subset H^1(\Omega_\mathcal{T})$, this implies that $H^{-1}(\Omega_\mathcal{T}) \subset (H^1(\Omega_\mathcal{T}))^*$, so it suffices to show that $\sigma|\nabla\mathcal{V}|^2 \in L^2(0,\mathcal{T};H^{-1}(\Omega_\mathcal{T}))$. First of all, the following inequality is satisfied:

$$\nabla \cdot (\sigma\mathcal{V}\nabla\mathcal{V}) = \sigma|\nabla\mathcal{V}|^2 + \nabla \cdot (\sigma\nabla\mathcal{V}) = \sigma|\nabla\mathcal{V}|^2, \tag{3.54}$$

where (3.37) has been used in order to eliminate the second term. Therefore, if $v \in H_0^1(\Omega)$:

$$\int_\Omega \sigma|\nabla\mathcal{V}|^2 v \, \mathrm{d}x = \int_\Omega \nabla \cdot (\sigma\mathcal{V}\nabla\mathcal{V}) v \, \mathrm{d}x = \int_\Omega \sigma\mathcal{V}\nabla\mathcal{V} \cdot \nabla v \, \mathrm{d}x. \tag{3.55}$$

As $\sigma \in L^\infty(0,\mathcal{T};L^\infty(\Omega))$ and $\mathcal{V} \in L^\infty(0,\mathcal{T};H^1(\Omega) \cap L^\infty(\Omega))$:

$$\int_\Omega |\sigma\mathcal{V}\nabla\mathcal{V}|^2 \, \mathrm{d}x \leq ||\sigma^2||_{L^\infty(\Omega)} ||\mathcal{V}^2||_{L^\infty(\Omega)} \int_\Omega |\nabla\mathcal{V}|^2 \, \mathrm{d}x < \infty, \tag{3.56}$$

so $\sigma\mathcal{V}\nabla\mathcal{V} \in L^2(0,\mathcal{T};(L^2(\Omega_\mathcal{T}))^*)$, and making use again of the characterization of the space $H^{-1}(\Omega)$ it follows that $\sigma|\nabla\mathcal{V}|^2 \in L^2(0,\mathcal{T};(H^1(\Omega_\mathcal{T}))^*)$. Now, the differential operator takes the following form:

$$L\Theta = -\nabla \cdot (k\nabla\Theta), \tag{3.57}$$

and the associated bilinear form:

$$B[\Theta, v; t] = \int_\Omega k\nabla\Theta \cdot \nabla v \, \mathrm{d}x + \int_{\partial\Omega} \text{Bi}(\text{Tr } \Theta)(\text{Tr } v) \, \mathrm{d}S, \quad v \in H^1(\Omega), \tag{3.58}$$

which has the same form as Lu defined in (3.13). Thus, the conditions of the section [3.3.1] are fulfilled, and applying the Theorem it is deduced that the problem (3.51) - (3.53) has a unique weak solution. Moreover, the weak formulation reads:

$$\int_\Omega \Theta' v \, \mathrm{d}x + \int_\Omega k\nabla\Theta \cdot \nabla v \, \mathrm{d}x + \int_{\partial\Omega} \text{Bi}(\text{Tr } \Theta)(\text{Tr } v) \, \mathrm{d}S = \int_\Omega \sigma\mathcal{V}\nabla\mathcal{V} \cdot \nabla v \, \mathrm{d}x, \ \ \forall v \in H^1(\Omega). \tag{3.59}$$

Existence and uniqueness of the system of equations.

Integrating with respect to t in the weak formulation (3.59) and considering $v = \Theta$:

$$\begin{aligned}
\frac{1}{2}||\Theta||^2_{L^2(\Omega)} + k_1 \int_0^t ||\nabla\Theta||^2_{L^2(\Omega;\mathbb{R}^n)}\ \mathrm{d}t \leq \frac{1}{2}||\Theta||^2_{L^2(\Omega)}\ \mathrm{d}t + \int_0^t k||\nabla\Theta||^2_{L^2(\Omega;\mathbb{R}^n)}\ \mathrm{d}t = \\
= \frac{1}{2}||\Theta(0)||^2_{L^2(\Omega)} - \int_0^t \int_\Omega \sigma\mathcal{V}\nabla\mathcal{V}\cdot\nabla\Theta\ \mathrm{d}x\ \mathrm{d}t - \\
+ \int_0^t \int_{\partial\Omega} \frac{\partial(\sigma\mathcal{V}\nabla\mathcal{V})}{\partial\nu}\mathrm{Tr}\ \Theta\ \mathrm{d}S\ \mathrm{d}t - \\
- \int_0^t \mathrm{Bi}||\mathrm{Tr}\ \Theta||^2_{L^2(\partial\Omega)}\ \mathrm{d}t \leq \\
\leq \frac{1}{2}||\Theta(0)||^2_{L^2(\Omega)} - \int_0^t \int_\Omega \sigma\mathcal{V}\nabla\mathcal{V}\cdot\nabla\Theta\ \mathrm{d}x\ \mathrm{d}t + \\
+ \int_0^t ||\nabla(\sigma\mathcal{V}\nabla\mathcal{V})||_{L^2(\partial\Omega;\mathbb{R}^n)}||\mathrm{Tr}\ \Theta||_{L^2(\partial\Omega)}\ \mathrm{d}t - \\
- \int_0^t \mathrm{Bi}||\mathrm{Tr}\ \Theta||^2_{L^2(\partial\Omega)}\ \mathrm{d}t \leq \\
\leq \frac{1}{2}||\Theta(0)||^2_{L^2(\Omega)} + \\
+ ||\sigma||_{L^\infty(\Omega)}||\mathcal{V}||_{L^\infty(\Omega)} \int_0^t \int_\Omega |\nabla\mathcal{V}|\cdot|\nabla\Theta|\ \mathrm{d}x\ \mathrm{d}t + \\
+ C_1||\sigma\mathcal{V}\nabla\mathcal{V}||_{H^1(\partial\Omega;\mathbb{R}^n)} \int_0^t ||\Theta||_{H^1(\Omega)}\ \mathrm{d}t + \\
+ C_2||\mathrm{Bi}||_{L^\infty(\Omega)} \int_0^t ||\Theta||^2_{H^1(\Omega)}\ \mathrm{d}t,
\end{aligned} \tag{3.60}$$

where the trace theorem has been used, and also the fact that $\sigma\mathcal{V}_0\nabla\mathcal{V}_0 \in H^1(\partial\Omega)$ as a consequence of the hypothesis (3.33). Finally, making use of the Cauchy-Schwarz inequality yields the result:

$$\begin{aligned}
\frac{1}{2}||\Theta||^2_{L^2(\Omega)} + k_1 \int_0^t ||\nabla\Theta||^2_{L^2(\Omega;\mathbb{R}^n)}\ \mathrm{d}t \leq \frac{1}{2}||\Theta(0)||^2_{L^2(\Omega)} + \\
+ C_1 \int_0^t ||\nabla\mathcal{V}||_{L^2(\Omega;\mathbb{R}^n)}||\nabla\Theta||_{L^2(\Omega;\mathbb{R}^n)}\ \mathrm{d}t + \\
+ C_2 \int_0^t ||\Theta||_{H^1(\Omega)}\ \mathrm{d}t + C_3 \int_0^t ||\Theta||^2_{H^1(\Omega)}\ \mathrm{d}t \leq \\
\leq \frac{1}{2}||\Theta(0)||^2_{L^2(\Omega)} + \frac{k_1}{2} \int_0^t ||\nabla\mathcal{V}||^2_{L^2(\Omega;\mathbb{R}^n)}\ \mathrm{d}t + \\
+ \frac{C_1}{2k_1} \int_0^t ||\nabla\Theta||^2_{L^2(\Omega;\mathbb{R}^n)}\ \mathrm{d}t + \\
+ C_2 \int_0^t ||\Theta||_{H^1(\Omega)}\ \mathrm{d}t + \\
+ C_3 \int_0^t ||\Theta||^2_{H^1(\Omega)}\ \mathrm{d}t,
\end{aligned} \tag{3.61}$$

so

$$\frac{1}{2}||\Theta||^2_{L^2(\Omega)} + k_1 \int_0^t ||\nabla\Theta||^2_{L^2(\Omega;\mathbb{R}^n)}\ \mathrm{d}t < \infty, \tag{3.62}$$

that is:

$$||u_t||_{L^2(0,\mathcal{T};(H^1(\Omega))^*)} < \infty. \tag{3.63}$$

Now, a mapping is defined:

$$\begin{aligned} F : L^2(0,\mathcal{T};L^2(\Omega)) &\to L^2(0,\mathcal{T};H^1(\Omega)) \subset\subset L^2(0,\mathcal{T};L^2(\Omega)) \\ s &\mapsto \Theta. \end{aligned} \tag{3.64}$$

If R is taken sufficiently large, F leaves invariant $B(0,R;L^2(0,\mathcal{T};L^2(\Omega)))$. Moreover, it is well-known that the following inmersion between the following spaces

$$\{\Theta \in L^2(0,\mathcal{T};H^1(\Omega)) \mid \Theta_t \in L^2(0,\mathcal{T};(H^1(\Omega))^*)\} \tag{3.65}$$

and $L^2(0,\mathcal{T};L^2(\Omega))$ is compact as a consequence of the Rellich-Kondrachov theorem. Now a sequence $s_n \in L^2(0,\mathcal{T};L^2(\Omega))$ is considered such that:

$$s_n \to s \ \text{ in } B(0,R;L^2(0,\mathcal{T};L^2(\Omega))), \tag{3.66}$$

and also $\mathcal{V}_n,\ f_n = \nabla\cdot(\sigma\mathcal{V}_n\nabla\mathcal{V}_n)$ and $\Theta_n = F(s_n)$. It has to be proved that

$$\Theta_n \to \Theta = F(s) \ \text{ in } B(0,R;L^2(0,\mathcal{T};L^2(\Omega))). \tag{3.67}$$

For that purpose, substracting the equation that satisfies Θ_n to the one that satisfies Θ and considering $v = \Theta_n - \Theta_n$, after integrating with respect to t in the weak formulation of the problem (3.59) gives the result:

$$\begin{aligned} &\frac{1}{2}||\Theta_n-\Theta||^2_{L^2(\Omega)} + k_1\int_0^t ||\nabla(\Theta_n-\Theta)||^2_{L^2(\Omega;\mathbb{R}^n)}\ \mathrm{d}t + h_1\int_0^t ||\mathrm{Tr}\ (\Theta_n-\Theta)||^2_{L^2(\partial\Omega)}\ \mathrm{d}t \le \\ &\le \frac{1}{2}||\Theta_n-\Theta||^2_{L^2(\Omega)} + \int_0^t\int_\Omega k(s_n)|\nabla(\Theta_n-\Theta)|^2\ \mathrm{d}x\ \mathrm{d}t + \\ &\quad + \int_0^t\int_{\partial\Omega} \mathrm{Bi}(s_n)|\mathrm{Tr}\ (\Theta_n-\Theta)|^2\ \mathrm{d}t = \\ &= \int_0^t\int_\Omega (k(s)-k(s_n))\nabla\Theta\cdot\nabla(\Theta_n-\Theta)\ \mathrm{d}x\ \mathrm{d}t + \int_0^t \langle f_n - f, \Theta_n-\Theta\rangle\ \mathrm{d}t + \\ &\quad + \int_0^t\int_{\partial\Omega}(\mathrm{Bi}(s)-\mathrm{Bi}(s_n))(\mathrm{Tr}\ \Theta)(\mathrm{Tr}\ (\Theta_n-\Theta))\ \mathrm{d}t = \\ &= I_1 + I_2 + I_3. \end{aligned} \tag{3.68}$$

Then, making use of the Young inequality the following estimations are obtained:

$$
\begin{aligned}
|I_1| &= \left| \int_0^t \int_\Omega (k(s) - k(s_n)) \nabla\Theta \cdot \nabla(\Theta_n - \Theta) \, \mathrm{d}x \, \mathrm{d}t \right| \leq \\
&\leq \frac{k_1}{4} \int_0^t ||\nabla(\Theta_n - \Theta)||^2_{L^2(\Omega;\mathbb{R}^n)} \, \mathrm{d}t + \frac{1}{k_1} \int_0^t ||(k(s) - k(s_n))\nabla\Theta||^2_{L^2(\Omega;\mathbb{R}^n)} \, \mathrm{d}t.
\end{aligned} \tag{3.69}
$$

$$
\begin{aligned}
|I_2| &= \left| \int_0^t \int_\Omega -(\sigma(s_n)\mathcal{V}_n\nabla\mathcal{V}_n - \sigma(s)\mathcal{V}\nabla\mathcal{V}) \cdot \nabla(\Theta_n - \Theta) \, \mathrm{d}x + \right. \\
&\quad \left. + \int_{\partial\Omega} \frac{\partial(\sigma(s_n)\mathcal{V}_n\nabla\mathcal{V}_n - \sigma\mathcal{V}\nabla\mathcal{V})}{\partial\nu} (\mathrm{Tr}\ (\Theta_n - \Theta)) \, \mathrm{d}S \, \mathrm{d}t \right| \leq \\
&\leq \left| \int_0^t \int_\Omega -(\sigma(s_n)\mathcal{V}_n\nabla\mathcal{V}_n - \sigma(s)\mathcal{V}\nabla\mathcal{V}) \cdot \nabla(\Theta_n - \Theta) \, \mathrm{d}x \, \mathrm{d}t \right| + \\
&\quad + \left| \int_{\partial\Omega} \frac{\partial(\sigma(s_n)\mathcal{V}_n\nabla\mathcal{V}_n - \sigma\mathcal{V}\nabla\mathcal{V})}{\partial\nu} (\mathrm{Tr}\ (\Theta_n - \Theta)) \, \mathrm{d}S \, \mathrm{d}t \right| \leq \\
&\leq \frac{k_1}{4} \int_0^t ||\nabla(\Theta_n - \Theta)||^2_{L^2(\Omega;\mathbb{R}^n)} \, \mathrm{d}t + \frac{1}{k_1} \int_0^t ||\sigma(s_n)\mathcal{V}_n\nabla\mathcal{V}_n - \sigma(s)\mathcal{V}\nabla\mathcal{V}||^2_{L^2(\Omega;\mathbb{R}^n)} \, \mathrm{d}t + \\
&\quad + \frac{\varepsilon}{2} \int_0^t ||\mathrm{Tr}\ (\Theta_n - \Theta)||^2_{L^2(\partial\Omega)} \, \mathrm{d}t + \\
&\quad + \frac{1}{2\varepsilon} \int_0^t ||\nabla(\sigma(s_n)\mathcal{V}_n\nabla\mathcal{V}_n - \sigma(s)\mathcal{V}\nabla\mathcal{V})||^2_{L^2(\partial\Omega;\mathbb{R}^n)} \, \mathrm{d}t.
\end{aligned} \tag{3.70}
$$

$$
\begin{aligned}
|I_3| &= \left| \int_0^t (\mathrm{Bi}(s) - \mathrm{Bi}(s_n))(\mathrm{Tr}\ \Theta)(\mathrm{Tr}\ (\Theta_n - \Theta)) \, \mathrm{d}t \right| \leq \\
&\leq \frac{\varepsilon}{2} \int_0^t ||(\mathrm{Bi}(s) - \mathrm{Bi}(s_n))\mathrm{Tr}\ \Theta||^2_{L^2(\partial\Omega)} \, \mathrm{d}t + \frac{1}{2\varepsilon} \int_0^t ||\mathrm{Tr}\ (\Theta_n - \Theta)||^2_{L^2(\partial\Omega)} \, \mathrm{d}t,
\end{aligned} \tag{3.71}
$$

Introducing the previous results in (3.68):

$$
\begin{aligned}
&||\Theta_n - \Theta||^2_{L^2(\Omega)} + \int_0^t ||\nabla(\Theta_n - \Theta)||^2_{L^2(\Omega;\mathbb{R}^n)} \, \mathrm{d}t - \frac{2}{\varepsilon} \int_0^t ||\mathrm{Tr}\ (\Theta_n - \Theta)||^2_{L^2(\partial\Omega)} \, \mathrm{d}t \leq \\
&||\Theta_n - \Theta||^2_{L^2(\Omega)} + \int_0^t ||\nabla(\Theta_n - \Theta)||^2_{L^2(\Omega;\mathbb{R}^n)} \, \mathrm{d}t - \frac{2C_1}{\varepsilon} \int_0^t ||\Theta_n - \Theta||^2_{H^1(\Omega)} \, \mathrm{d}t \leq \\
&\leq C_2 \Bigg[\int_0^T ||(k(s) - k(s_n))\nabla\Theta||^2_{L^2(\Omega;\mathbb{R}^n)} \, \mathrm{d}t + \int_0^T ||\sigma(s_n)\mathcal{V}_n\nabla\mathcal{V}_n - \sigma(s)\mathcal{V}\nabla\mathcal{V}||^2_{L^2(\Omega;\mathbb{R}^n)} \, \mathrm{d}t \\
&\quad + \int_0^T ||\nabla(\sigma(s_n)\mathcal{V}_n\nabla\mathcal{V}_n - \sigma(s)\mathcal{V}\nabla\mathcal{V})||^2_{L^2(\partial\Omega;\mathbb{R}^n)} \, \mathrm{d}t + \\
&\quad + \int_0^T ||(\mathrm{Bi}(s) - \mathrm{Bi}(s_n))\mathrm{Tr}\ \Theta||^2_{L^2(\partial\Omega)} \, \mathrm{d}t \Bigg],
\end{aligned} \tag{3.72}
$$

where ε is taken in (3.70) y (3.71) such that

$$
||\Theta_n - \Theta||^2_{L^2(\Omega)} + ||\nabla(\Theta_n - \Theta)||^2_{L^2(\Omega;\mathbb{R}^n)} - \frac{2C}{\varepsilon} ||\Theta_n - \Theta||^2_{H^1(\Omega)} > 0, \tag{3.73}
$$

that is:

$$||\Theta_n-\Theta||^2_{L^2(\Omega)}+||\nabla(\Theta_n-\Theta)||^2_{L^2(\Omega;\mathbb{R}^n)}-\frac{2C_1}{\varepsilon}\left(||\Theta_n-\Theta||^2_{L^2(\Omega)}+||\nabla(\Theta_n-\Theta)||^2_{L^2(\Omega;\mathbb{R}^n)}\right)>0, \quad (3.74)$$

from wich is deduced that $\varepsilon > 2C_1$.

As Θ_n is a relatively compact set of $B(0,R;L^2(0,\mathcal{T};L^2(\Omega))$, it suffices to prove that Θ is the only limit point for Θ_n. Let Θ^* that point:

$$\Theta^* = \lim_{n_k\to\infty}\Theta_{n_k} \ \text{ in } B(0,R;L^2(0,\mathcal{T};L^2(\Omega)), \quad (3.75)$$

and assuming that another subsequence of n_k has been extracted, which is denoted also as n_k, it can be assumed that

$$s_{n_k}\to s \ \ a.e. \text{ in } \Omega\times(0,\mathcal{T}). \quad (3.76)$$

Taking into account the previous results, as $|\nabla\Theta|^2 \in L^1(\Omega\times(0,\mathcal{T}))$ and by (3.76) it is satisfied that $|k(s)-k(s_n)|^2\to 0$ and $|(\mathrm{Bi}(s)-\mathrm{Bi}(s_n)|^2\to 0$ a.e., so making use of the dominated convergence theorem allows to deduce:

$$\int_0^{\mathcal{T}}||(k(s)-k(s_n))\nabla\Theta||_{L^2(\Omega;\mathbb{R}^n)}\,\mathrm{d}t=\int_0^{\mathcal{T}}\int_\Omega|k(s)-k(s_n))|^2|\nabla\Theta|^2\,\mathrm{d}x\,\mathrm{d}t\to 0, \quad (3.77)$$

$$\int_0^{\mathcal{T}}||(\mathrm{Bi}(s)-\mathrm{Bi}(s_n))\mathrm{Tr}\ \Theta||^2_{L^2(\partial\Omega)}\,\mathrm{d}t\le C\int_0^{\mathcal{T}}|(\mathrm{Bi}(s)-\mathrm{Bi}(s_n)|^2|\Theta|^2\,\mathrm{d}x\,\mathrm{d}t\to 0. \quad (3.78)$$

Now, on the one hand, the second integral of the second term on the right-hand side of the inequality (3.72) can be given a bound as a function of three new integrals:

$$\begin{aligned}
&\int_0^{\mathcal{T}}||\sigma(s_n)\mathcal{V}_n\nabla\mathcal{V}_n-\sigma(s)\mathcal{V}\nabla\mathcal{V}||^2_{L^2(\Omega;\mathbb{R}^n)}\,\mathrm{d}t\le\\
&\le\int_0^{\mathcal{T}}||\sigma(s_n)\mathcal{V}_n\nabla\mathcal{V}_n-\sigma(s_n)\mathcal{V}_n\nabla\mathcal{V}||^2_{L^2(\Omega;\mathbb{R}^n)}\,\mathrm{d}t+\\
&\quad+\int_0^{\mathcal{T}}||\sigma(s_n)\mathcal{V}_n\nabla\mathcal{V}-\sigma(s_n)\mathcal{V}\nabla\mathcal{V}||^2_{L^2(\Omega;\mathbb{R}^n)}\,\mathrm{d}t+\\
&\quad+\int_0^{\mathcal{T}}||\sigma(s_n)\mathcal{V}\nabla\mathcal{V}-\sigma(s)\mathcal{V}\nabla\mathcal{V}||^2_{L^2(\Omega;\mathbb{R}^n)}\,\mathrm{d}t=\\
&=I_4+I_5+I_6.
\end{aligned} \quad (3.79)$$

On the other hand, the following inequalities are satisfied:

$$I_4=\int_0^{\mathcal{T}}||\sigma(s_n)\mathcal{V}_n(\nabla\mathcal{V}_n-\nabla\mathcal{V})||^2_{L^2(\Omega;\mathbb{R}^n)}\,\mathrm{d}t\le C_4\int_0^{\mathcal{T}}\int_\Omega|\nabla(\mathcal{V}_n-\mathcal{V})|^2\,\mathrm{d}x\,\mathrm{d}t; \quad (3.80)$$

$$I_5 = \int_0^{\mathcal{T}} ||\sigma(s_n)\nabla\mathcal{V}(\mathcal{V}_n - \mathcal{V})||^2_{L^2(\Omega;\mathbb{R}^n)} \, \mathrm{d}t \leq C_5 \int_0^{\mathcal{T}} \int_\Omega |\mathcal{V}_n - \mathcal{V}|^2 |\nabla V|^2 \, \mathrm{d}x \, \mathrm{d}t; \tag{3.81}$$

$$I_6 = \int_0^{\mathcal{T}} ||(\sigma(s_n) - \sigma(s))^2\mathcal{V}\nabla\mathcal{V}||^2_{L^2(\Omega;\mathbb{R}^n)} \, \mathrm{d}t \leq C_6 \int_0^{\mathcal{T}} \int_\Omega |\sigma(s_n) - \sigma(s)|^2 |\nabla V|^2 \, \mathrm{d}x \, \mathrm{d}t. \tag{3.82}$$

Making use of (3.50) and (3.76) and the dominated convergence theorem it is deduced that $I_6 \to 0$. Furthermore, $\mathcal{V}_n$ solves (3.37) and (3.38), so it can be inferred that

$$\int_\Omega \sigma(s_n)\nabla\mathcal{V}_n \cdot \nabla(\mathcal{V}_n - \mathcal{V}) \, \mathrm{d}x = \int_\Omega \sigma(s)\nabla\mathcal{V} \cdot \nabla(\mathcal{V}_n - \mathcal{V}) \, \mathrm{d}x, \tag{3.83}$$

and

$$\int_\Omega \sigma(s_n)|\nabla(\mathcal{V}_n - \mathcal{V})|^2 \, \mathrm{d}x = \int_\Omega (\sigma(s) - \sigma(s_n))\nabla\mathcal{V} \cdot \nabla(\mathcal{V}_n - \mathcal{V}) \, \mathrm{d}x. \tag{3.84}$$

As a consequence of the previous results:

$$\int_\Omega |\nabla(\mathcal{V}_n - \mathcal{V})|^2 \, \mathrm{d}x \leq C \int_\Omega |\sigma(s) - \sigma(s_n)|^2 |\nabla\mathcal{V}|^2 \, \mathrm{d}x, \tag{3.85}$$

and substituting the previous result in (3.80) it is found that

$$I_4 \leq C_4 \int_0^{\mathcal{T}} \int_\Omega |\nabla(\mathcal{V}_n - \mathcal{V})|^2 \, \mathrm{d}x \, \mathrm{d}t \leq C_4 \int_\Omega |\sigma(s) - \sigma(s_n)|^2 |\nabla\mathcal{V}|^2 \, \mathrm{d}x \to 0 \tag{3.86}$$

Finally, as $\mathcal{V}_n - \mathcal{V} \in H_0^1(\Omega)$, Poincaré's inequality applies (Evans, §5.6, Theorem 3) to give:

$$\int_0^{\mathcal{T}} \int_\Omega |\mathcal{V}_n - \mathcal{V}|^2 \, \mathrm{d}x \, \mathrm{d}t \to 0, \tag{3.87}$$

so, up to an extracted subsequence:

$$\mathcal{V}_n \to \mathcal{V} \quad a.e. \text{ in } \Omega \times (0, \mathcal{T}), \tag{3.88}$$

and making use of the Dominated Convergence Theorem it is deduced that $I_5 \to 0$.

To conclude, as $\mathcal{V}_n = \mathcal{V} = \mathcal{V}_0$ on $\partial\Omega \times (0, T)$, the third integral of the term on the right-hand side of the inequality (3.72) is written as

$$\begin{aligned} &\int_0^{\mathcal{T}} ||\nabla(\sigma(s_n)\mathcal{V}_n\nabla\mathcal{V}_n - \sigma(s)\mathcal{V}\nabla\mathcal{V})||^2_{L^2(\partial\Omega;\mathbb{R}^n)} \, \mathrm{d}t = \\ &= \int_0^{\mathcal{T}} ||\nabla((\sigma(s_n) - \sigma(s))\mathcal{V}_0\nabla\mathcal{V}_0)||^2_{L^2(\partial\Omega;\mathbb{R}^n)} \, \mathrm{d}t = 0, \end{aligned} \tag{3.89}$$

where the hypothesis (3.33) has been used, that allows to deduce that the previous integral is zero. Consequently, $\Theta_n \to \Theta = \Theta^*$ in $L^2(0, \mathcal{T}; L^2(\Omega))$ and the proof is finished.

Proof of the measurability of $\mathcal{V}$. It will be shown that $\mathcal{V}$ is measurable in t with values in $H^1(\Omega)$. Firstly, it is important to note that $s \in C([0,\mathcal{T}]\times\bar{\Omega})$, so $\mathcal{V} \in C([0,\mathcal{T}], H^1(\Omega))$. Thus

$$\nabla\cdot(\sigma(s(t))\nabla\mathcal{V}(t)) = \nabla\cdot(\sigma(s(t'))\nabla\mathcal{V}(t')) = 0, \tag{3.90}$$

and therefore:

$$\int_\Omega \sigma(s(t))|\nabla(\mathcal{V}(t)-\mathcal{V}(t'))|^2\,\mathrm{d}x = \int_\Omega \sigma(s(t'))-\sigma(s(t))\nabla\mathcal{V}(t')\cdot\nabla(\mathcal{V}(t)-\mathcal{V}(t'))\,\mathrm{d}x \tag{3.91}$$

and

$$\int_\Omega |\nabla(\mathcal{V}(t)-\mathcal{V}(t'))|^2\,\mathrm{d}x \le C\int_\Omega |\sigma(s(t'))-\sigma(s(t))|^2|\nabla\mathcal{V}(t')|^2\,\mathrm{d}x \to 0, \tag{3.92}$$

where $t\to t'$ as a consequence of the dominated convergence theorem. Now, if $s\in L^2(0,\mathcal{T};L^2(\Omega))$, ethen there exists a sequence $s_n \in C([0,\mathcal{T}]\times\bar{\Omega})$ such that $s_n\to s$ in $L^2(0,\mathcal{T};L^2(\Omega))$, and almost everywhere in $\Omega\times[0,\mathcal{T}]$. From (3.85) it is deduced that

$$\int_\Omega |\nabla(\mathcal{V}_n-\mathcal{V})|^2\,\mathrm{d}x \to 0, \tag{3.93}$$

and, as $\mathcal{V}_n$ is measurable, also is $\mathcal{V}$. □

3.3.2 Optimal control.

Once the existence and uniqueness of the problem (3.4) - (3.8) has been shown, the last step consists of analysing if it is possible to obtain a control law after fixing an optimality condition. The dimensionless voltage $\mathcal{V}_0$ will be chosen as the control, being the cost functional as follows:

$$J(\mathcal{V}_0) = \int_0^{\mathcal{T}}\int_\Omega |\Theta-\Lambda|^2\,\mathrm{d}x\,\mathrm{d}t + \beta\int_0^{\mathcal{T}}|\mathcal{V}_0(t)|^2\,\mathrm{d}t, \tag{3.94}$$

that is, a modification of the one proposed in [Cimatti, 2007]; in this case, a temperature profile that is near a given function is looked for, $\Lambda(x,t)$, but without implying that the voltage is high. $\Lambda(x,t)\in L^2(0,\mathcal{T};L^2(\Omega))$ and $\beta>0$, and the the set of admissible controls is as follows:

$$\mathcal{A} = \{\mathcal{V}_0 \in W^{1,\infty}(\partial\Omega\times(0,\mathcal{T})) \mid 0<\mathcal{V}_0\le \mathcal{V}_{0\text{máx}}\}, \tag{3.95}$$

so the optimal control problem consists of finding $\mathcal{V}_0^*\in\mathcal{A}$ such that

$$J(\mathcal{V}_0^*) = \min_{\mathcal{V}_0\in\mathcal{A}} J(\mathcal{V}_0), \tag{3.96}$$

taking that minimum of the cost function in the class of solutions of (3.45) and (3.59) where $\Theta(x,0)=\Theta_0$. Now let $\mathcal{V}_{0n}$ a minimizing sequence, that is, it satisfies:

$$\lim_{n\to\infty} J(\mathcal{V}_{0n}) = \inf_{\mathcal{V}_0\in\mathcal{A}} J(\mathcal{V}_0), \tag{3.97}$$

while $\Theta_n = \Theta_n(\mathcal{V}_{0n})$ and $\mathcal{V}_n = \mathcal{V}_n(\mathcal{V}_{0n})$ are the corresponding solutions to

$$\int_0^{\mathcal{T}} \int_\Omega \sigma(\Theta_n) \nabla \Upsilon_n \cdot \nabla v \, \mathrm{d}x \, \mathrm{d}t = -\int_0^{\mathcal{T}} \int_\Omega \sigma(\Theta_n) \nabla \mathcal{V}_{0n} \cdot \nabla v \, \mathrm{d}x \, \mathrm{d}t, \quad \forall v \in H_0^1(\Omega), \tag{3.98}$$

$$\begin{aligned} &\int_0^{\mathcal{T}} \int_\Omega \Theta_n' v \, \mathrm{d}x \, \mathrm{d}t + \int_0^{\mathcal{T}} \int_\Omega k(\Theta_n) \nabla \Theta_n \cdot \nabla v \, \mathrm{d}x \, \mathrm{d}t + \\ &\quad + \int_0^{\mathcal{T}} \int_{\partial\Omega} \mathrm{Bi}(\Theta_n)(\mathrm{Tr}\ \Theta_n)(\mathrm{Tr}\ v) \, \mathrm{d}S \, \mathrm{d}t = \\ &= \int_0^{\mathcal{T}} \int_\Omega \sigma(\Theta_n) \mathcal{V}_n \nabla \mathcal{V}_n \cdot \nabla v \, \mathrm{d}x \, \mathrm{d}t, \quad \forall v \in H^1(\Omega). \end{aligned} \tag{3.99}$$

As it is shown in [Shi and Shillor, 1993], the term on the right-hand side of the equation (3.99) is equivalent to

$$\begin{aligned} \int_0^{\mathcal{T}} \int_\Omega \sigma(\Theta_n) \mathcal{V}_n \nabla \mathcal{V} \cdot \nabla v \, \mathrm{d}x \, \mathrm{d}t = &- \int_0^{\mathcal{T}} \int_\Omega \sigma(\Theta_n) \Upsilon_n \nabla \mathcal{V}_n \cdot \nabla v \, \mathrm{d}x \, \mathrm{d}t + \\ &+ \int_0^{\mathcal{T}} \int_\Omega (\sigma(\Theta_n) \nabla \mathcal{V}_n \cdot \nabla \mathcal{V}_{n0}) v \, \mathrm{d}x \, \mathrm{d}t, \end{aligned} \tag{3.100}$$

so (3.99) reads:

$$\begin{aligned} &\int_0^{\mathcal{T}} \int_\Omega \Theta_n' v \, \mathrm{d}x + \int_\Omega k(\Theta_n) \nabla \Theta_n \cdot \nabla v \, \mathrm{d}x \, \mathrm{d}t + \int_0^{\mathcal{T}} \int_{\partial\Omega} \mathrm{Bi}(\Theta_n)(\mathrm{Tr}\ \Theta_n)(\mathrm{Tr}\ v) \, \mathrm{d}S \, \mathrm{d}t = \\ &= \int_0^{\mathcal{T}} \int_\Omega \sigma(\Theta_n)(\mathcal{V}_{n0} - \mathcal{V}_n) \nabla \mathcal{V}_n \cdot \nabla v \, \mathrm{d}x \, \mathrm{d}t + \\ &\quad + \int_0^{\mathcal{T}} \int_\Omega (\sigma(\Theta_n) \nabla \mathcal{V}_n \cdot \nabla \mathcal{V}_{n0}) v \, \mathrm{d}x \, \mathrm{d}t, \quad \forall v \in H^1(\Omega). \end{aligned} \tag{3.101}$$

As the sequence $\mathcal{V}_{0n}$ is bounded in $H^1(0, \mathcal{T})$, there exists a constant $\tilde{\mathcal{V}}_0$ such that $|\mathcal{V}_{0n}(t)| \leq \tilde{\mathcal{V}}_0$. So, making use of (3.47):

$$||\mathcal{V}_n||_{L^\infty(\Omega)} \leq ||\mathcal{V}_{0n}||_{L^\infty(\partial\Omega)}, \tag{3.102}$$

Moreover, from the results obtained in the previous section, the following relationships are satisfied:

$$\mathcal{V}_n \text{ is bounded in } L^\infty(0, \mathcal{T}; H^1(\Omega) \cap L^\infty(\Omega)) \text{ as a consequence of (3.50);} \tag{3.103}$$

$$\Theta_n \text{ is bounded in } L^2(0, \mathcal{T}; H^1(\Omega)) \text{ as a consequence of (3.18);} \tag{3.104}$$

$$\Theta_n' \text{ is bounded in } L^2(0, \mathcal{T}; (H^1(\Omega))^*) \text{ as a consequence of (3.63),} \tag{3.105}$$

and from (3.104) it is inferred that

$$\mathrm{Tr}\ \Theta_n \text{ is bounded in } L^2(0, \mathcal{T}; L^2(\partial\Omega)). \tag{3.106}$$

Then, using (3.102) - (3.106) and taking into account that $\mathcal{V}_{0n}$ is bounded in $H^1(0,\mathcal{T})$, using well known compactness results subsequences of Θ_n, $\mathcal{V}_n$ and $\mathcal{V}_{0n}$ can be extracted such that:

$$\mathcal{V}_n \rightharpoonup \mathcal{V} \text{ in } L^2(\Omega\times(0,\mathcal{T})); \tag{3.107}$$

$$\nabla\mathcal{V}_n \rightharpoonup \nabla\mathcal{V} \text{ in } L^2(\Omega\times(0,\mathcal{T})); \tag{3.108}$$

$$\Theta_n \rightharpoonup \Theta \text{ in } L^2(0,\mathcal{T};H^1(\Omega)); \tag{3.109}$$

$$\text{Tr }\Theta_n \rightharpoonup \text{Tr }\Theta \text{ in } L^2(0,\mathcal{T};L^2(\Omega)); \tag{3.110}$$

$$\frac{\partial\Theta_n}{\partial t} \rightharpoonup \frac{\partial\Theta}{\partial t} \text{ in } L^2(0,\mathcal{T};(H^1(\Omega))^*); \tag{3.111}$$

$$\mathcal{V}_{0n} \rightharpoonup \mathcal{V}_0 \text{ uniformly in } [0,\mathcal{T}], \tag{3.112}$$

where the subindex n has been maintained for the subsequences. Moreover, up to a subsequence:

$$\Theta_n \to \Theta \text{ en } L^2(\Omega\times(0,\mathcal{T})); \tag{3.113}$$

$$\mathcal{V}_n \to \mathcal{V} \text{ en } L^2(\Omega\times(0,\mathcal{T})); \tag{3.114}$$

$$\nabla\mathcal{V}_n \to \nabla\mathcal{V} \text{ en } L^2(\Omega\times(0,\mathcal{T})), \tag{3.115}$$

where the Theorem 2.2 from [Temam, 1976] has been used in order to deduce (3.113) and from (3.87) and (3.93) to deduce (3.114) and (3.115), respectively. As a consequence, making use of (3.33) - (3.36):

$$k(\Theta_n)\to k(\Theta) \text{ y } \sigma(\Theta_n)\to\sigma(\Theta) \text{ en } L^\infty(\Omega\times(0,\mathcal{T})); \tag{3.116}$$

$$\text{Bi}(\text{Tr }\Theta_n)\to \text{Bi}(\text{Tr }\Theta) \text{ en } L^\infty(\partial\Omega\times(0,\mathcal{T})). \tag{3.117}$$

By (3.112), (3.115) y (3.116) it is inferred that:

$$\int_0^{\mathcal{T}}\int_\Omega \sigma(\Theta_n)\nabla\Upsilon_n\cdot\nabla v\ \mathrm{d}x\ \mathrm{d}t \to \int_0^{\mathcal{T}}\int_\Omega \sigma(\Theta)\nabla\Upsilon\cdot\nabla v\ \mathrm{d}x\ \mathrm{d}t; \tag{3.118}$$

$$-\int_0^{\mathcal{T}}\int_\Omega \sigma(\Theta_n)\nabla\mathcal{V}_{0n}\cdot\nabla v\ \mathrm{d}x\ \mathrm{d}t \to -\int_0^{\mathcal{T}}\int_\Omega \sigma(\Theta)\nabla\mathcal{V}_0\cdot\nabla v\ \mathrm{d}x\ \mathrm{d}t, \tag{3.119}$$

so it is possible to take limits in (3.98) to give

$$\int_0^{\mathcal{T}}\int_\Omega \sigma\nabla\Upsilon\cdot\nabla v\ \mathrm{d}x\ \mathrm{d}t = -\int_0^{\mathcal{T}}\int_\Omega \sigma\nabla\mathcal{V}_0\cdot\nabla v\ \mathrm{d}x\ \mathrm{d}t, \quad \forall v\in H_0^1(\Omega). \tag{3.120}$$

With regard to (3.101), by (3.109), (3.110), (3.111) and (3.116) it is found that:

$$\int_0^{\mathcal{T}}\int_\Omega \Theta_n' v\ \mathrm{d}x\ \mathrm{d}t \to \int_0^{\mathcal{T}}\int_\Omega \Theta' v\ \mathrm{d}x\ \mathrm{d}t, \tag{3.121}$$

$$\int_0^{\mathcal{T}}\int_\Omega k(\Theta_n)\nabla\Theta_n\cdot\nabla v\ \mathrm{d}x\ \mathrm{d}t \to \int_0^{\mathcal{T}}\int_\Omega k(\Theta)\nabla\Theta\cdot\nabla v\ \mathrm{d}x\ \mathrm{d}t, \tag{3.122}$$

$$\int_0^{\mathcal{T}}\int_{\partial\Omega} \text{Bi}(\Theta_n)(\text{Tr }\Theta_n)(\text{Tr }v)\ \mathrm{d}S\ \mathrm{d}t \to \int_0^{\mathcal{T}}\int_{\partial\Omega} \text{Bi}(\Theta)(\text{Tr }\Theta)(\text{Tr }v)\ \mathrm{d}S\ \mathrm{d}t. \tag{3.123}$$

while the proof of the convergence of the two terms on the right-hand side of (3.101) can be found in [Hrykiv, 2009].

$$\int_0^{\mathcal{T}} \int_\Omega \sigma(\Theta_n)(\mathcal{V}_{0n} - \mathcal{V}_n)\nabla\mathcal{V}_n \cdot \nabla v \, \mathrm{d}x \, \mathrm{d}t \to \int_0^{\mathcal{T}} \int_\Omega \sigma(\Theta)(\mathcal{V}_0 - \mathcal{V})\nabla\mathcal{V} \cdot \nabla v \, \mathrm{d}x \, \mathrm{d}t, \tag{3.124}$$

$$\int_0^{\mathcal{T}} \int_\Omega (\sigma(\Theta_n)\nabla\mathcal{V}_n \cdot \nabla\mathcal{V}_{0n})v \, \mathrm{d}x \, \mathrm{d}t \to \int_0^{\mathcal{T}} \int_\Omega (\sigma(\Theta)\nabla\mathcal{V} \cdot \nabla\mathcal{V}_0)v \, \mathrm{d}x \, \mathrm{d}t. \tag{3.125}$$

Based on the obtained results, $(\Theta^*, \mathcal{V}^*)$ is a weak solution associated to $\mathcal{V}_0^*$, that is, $\Theta^* = \Theta(\mathcal{V}_0^*)$ and $\mathcal{V}^* = \mathcal{V}(\mathcal{V}_0^*)$. To conclude, using the weak-lower-semicontinuity of $J(\mathcal{V}_0)$ with respect to the norm in L^2 it is deduced that the infimum is reached in $\mathcal{V}_0^*$.

Chapter 4

Conclusions

In this work an approximate model has been developed to study catheter ablation procedure. The initial system of 9 three-dimensional equations has been reduced to 4 two-dimensional equations by means of several approximations, where rotational symmetry plays an important role. The equations have been nondimensionalized, and a numerical scheme based on a spectral method for the spatial discretization and a Runge-Kutta method for the time discretization has been proposed. Moreover, it has been validated using a manufactured solution, and a study of the influence of the order of Chebyshev polynomials in the real problem has been conducted.

With respect to the obtained results, a parametric study of the procedure has been performed, deducing that catheters with amplitudes of 28 volts applied during 60 seconds produce maximum temperatures that are far from dangerous values. The speed of temperature growth decreases as time increases, and maximum temperatures reached at 45, 60 and 75 seconds are almost identical, even though the variations in the temperature distribution far from the catheter are important. One aspect worth pointing out is that reduced differences in the voltage amplitude cause important variations in the temperature distribution, and, if the esophagus is near the endocardium, small values of discharge times and high values of the voltage are the best choice. The last parameter of the procedure that has been analised is catheter radius, concluding that bigger catheters give rise to higher safe radii and lower maximum temperatures that are located further from the catheter surface. The consequences are just the opposite when catheter radius is lowered, caused by the decrease of heat transfer because of blood perfusion.

Focusing attention on the assumptions of the model, blood perfusion has been shown to be an effective cooling process. This fact allows to deduce that blood perfusion term is not negligible in the proposed system of equations. Furthermore, it has been demonstrated that temperature distribution does not depend on blood velocity except for the values on the catheter-blood interface. In connection with the previous idea, it has been proved that it is not necessary to include the equation of conservation of energy in the present approximate model. Keeping attention on the model, another step has consisted of studying the models for thermal and electrical conductivities. It has been deduced that a constant-thermal-conductivity model is a correct choice, while a temperature-dependent electrical conductivity is necessary. Moreover, it has been shown that it is possible to find a control law for a simplified system of equations such that a certain optimality condition is achieved.

The work presented here involves a first step towards a complete analysis of catheter ablation, and the proposed goals have been achieved. However, a more elaborate model is needed in order to obtain more accurate solutions. In fact, a restrictive hypothesis is to assume that catheters are refrigerated to the point where temperature remains in 37°C. This issue can be solved by

including the real geometry of the catheter in the model, and solving the system of equations also in it. As a first task, an homogeneous catheter could be considered.

The rotational symmetry assumption is clearly a good choice for an initial contact, but the real geometry of the cardiac tissue deviates from that, specially far from the catheter. The reason lies in the presence of the pulmonary veins, and also the esophagus, which is near the endocardium separated from it by a fat layer. The temperature distribution around these zones is not supposed to be accurate. In addition, blood moves longitudinally in the cardiac chamber, and the proposed model assumes that the trajectories are circles (as a consequence of the rotational symmetry). Consequently, future work has to be done based on a full three-dimensional model.

Finally, despite the fact that heat transfer due to the blood perfusion has been demostrated to be a dominant effect, it has been assumed that blood temperature remains constant and equal to human body temperature. This may not be the case, so further research is needed concerning this aspect.

Appendix A

Code

The code used to solve the system of equations (2.84) - (2.99) has been programmed in Fortran 90, and it consist of a main program, `catheter_ablation`, two modules, `nodesandmatrices_r` and `nodesandmatrices_phi` and six subroutines: `bweights`, `pmatrix`, `dmatrix_r`, `dmatrix_phi`, `elliptic` and `RK4`.

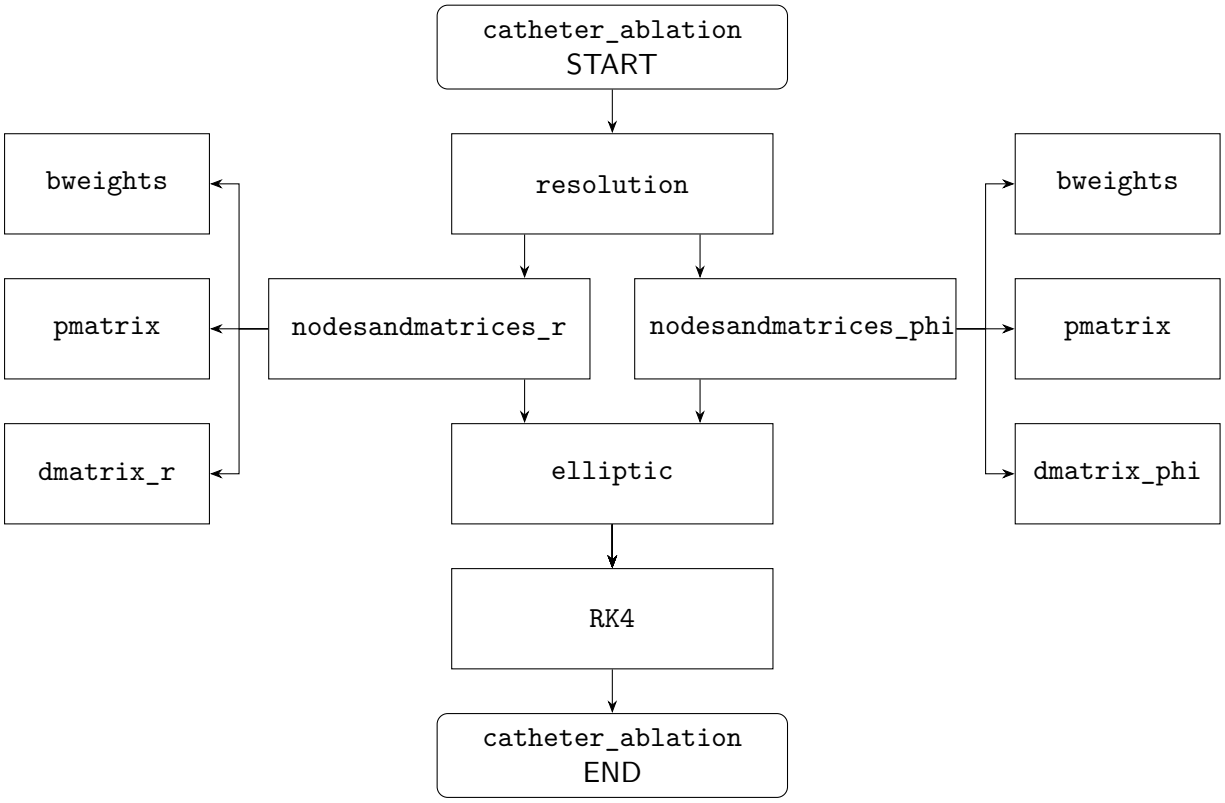

FIGURE A.1: Block diagram of the `catheter_ablation` program.

The structure of the program is as follows:

- The main subroutine is `resolution`. First of all, it calls `nodesandmatrices_r` and `nodesandmatrices_phi`, which allow to compute the nodes and the derivation matrices by means of four subroutines: `bweights`, `pmatrix`, `dmatrix_r` and `dmatrix_phi`.
- After defining the initial conditions, the subroutine `elliptic` solves the elliptic equations (2.87) - (2.89) and (2.93) - (2.95).

- Using the results given by `elliptic`, the subroutine RK4 solves the parabolic equations (2.84) - (2.86) and (2.90) - (2.92).

program catheter_ablation

```
!Master Thesis code
!Author: Aitor Amatriain Carballo
!June 2019

program catheter_ablation

use nodesandmatrices_r
use nodesandmatrices_phi

implicit none

!  ---------------
!  Local Variables
!  ---------------

integer                          :: N, i, j, k
real(kind=RP), allocatable       :: r_1(:), theta_1(:), r(:), ...
                                    theta(:), D_1r(:,:), ...
                                    D_1theta(:,:)
real(kind=RP), allocatable       :: D_r(:,:), D_2r(:,:), ...
                                    D2_r(:,:), D_theta(:,:), ...
                                    D_2theta(:,:), D2_theta(:,:)
real(kind=RP), allocatable       :: A_D2r(:,:), A_Dr(:,:), ...
                                    A_D2theta(:,:), A_Dtheta(:,:)

!  -------------------------------------
!  Polynomial order of the approximation
!  -------------------------------------

N = 14

!  ---------------
!  Allocate memory
!  ---------------

allocate(r_1(0:N), theta_1(0:N), r(1:N+1), theta(1:N+1))
allocate(D_1r(0:N,0:N), D_2r(0:N,0:N), D_1theta(0:N,0:N), ...
         D_2theta(0:N,0:N), D_theta(1:N+1,1:N+1))
allocate(D2_r(1:N+1,1:N+1), D2_theta(1:N+1,1:N+1), ...
         D_r(1:N+1,1:N+1))
```

```
41 allocate(A_D2r(N*N+2*N+1,N*N+2*N+1), A_Dr(N*N+2*N+1,N*N+2*N+1),
42           A_D2theta(N*N+2*N+1,N*N+2*N+1), ...
43           A_Dtheta(N*N+2*N+1,N*N+2*N+1))
44
45 !  ------------------------------------
46 !  Compute derivation matrix and nodes
47 !  ------------------------------------
48
49 call dmatrix_r(D_1r, r_1, N)
50 call dmatrix_phi(D_1theta, theta_1, N)
51
52 !  ---------------
53 !  Result file
54 !  ---------------
55
56 open (unit=1, file='results.dat')
57
58 !  ---------------------------------------
59 !  Compute first and second derivatives
60 !  ---------------------------------------
61
62 D_2r     = matmul(D_1r,D_1r)
63 D_2theta = matmul(D_1theta,D_1theta)
64
65 do i=1,N+1
66  do j=1,N+1
67       D_r(i,j) = D_1r(i-1,j-1)
68  end do
69 end do
70
71 do i=1,N+1
72  do j=1,N+1
73       D2_r(i,j) = D_2r(i-1,j-1)
74  end do
75 end do
76
77 do i=1,N+1
78  do j=1,N+1
79       D_theta(i,j) = D_1theta(i-1,j-1)
80  end do
81 end do
82
83 do i=1,N+1
84  do j=1,N+1
85       D2_theta(i,j) = D_2theta(i-1,j-1)
86  end do
```

```
87  end do
88
89  do k=1,N+1
90   do i=(k-1)*N+k,k*(N+1)
91    do j=(k-1)*N+k,k*(N+1)
92         A_Dr(i,j) = D_r(i-(k-1)*N-k+1,j-(k-1)*N-k+1)
93    end do
94   end do
95  end do
96
97  do k=1,N+1
98   do i=(k-1)*N+k,k*(N+1)
99    do j=(k-1)*N+k,k*(N+1)
100        A_D2r(i,j) = D2_r(i-(k-1)*N-k+1,j-(k-1)*N-k+1)
101   end do
102  end do
103 end do
104
105 do k=1,N+1
106  do i=1,N+1
107   do j=1,N+1
108        A_Dtheta((i-1)*(N+1)+k,(j-1)*(N+1)+k) = D_theta(i,j)
109   end do
110  end do
111 end do
112
113 do k=1,N+1
114  do i=1,N+1
115   do j=1,N+1
116        A_D2theta((i-1)*(N+1)+k,(j-1)*(N+1)+k) = D2_theta(i,j)
117   end do
118  end do
119 end do
120
121 do i=1,N+1
122     r(i) = r_1(i-1)
123 end do
124
125 do i=1,N+1
126     theta(i) = theta_1(i-1)
127 end do
128
129 call resolution(N, D_r, D_theta, D2_r, D2_theta, r, theta,
130                 A_D2r, A_Dr, A_D2theta, A_Dtheta)
131
132 end program catheter_ablation
```

module `nodesandmatrices_r`

```
module nodesandmatrices_r

use SMConstants
implicit none

contains

!  ------------------------------------------------------------
!  Compute the barycentric weights for polynomial interpolation
!  ------------------------------------------------------------

subroutine bweights(N, x, w)

!  ---------
!  Arguments
!  ---------

integer                                    :: N
real(kind=RP), dimension(0:N), intent(in)  :: x
real(kind=RP), dimension(0:N), intent(out) :: w

!  ---------------
!  Local Variables
!  ---------------

integer :: j, k

w = 1.0_RP
do j=1,N
 do k=0,j-1
      w(k) = w(k)*(x(k)-x(j))
      w(j) = w(j)*(x(j)-x(k))
 end do
end do

w = 1.0_RP/w

end subroutine bweights

!  ------------------------------
!  Compute the derivative matrix.
!  D(i,j) = \prime \ell_j(x_i)
!  ------------------------------
```

```
44
45 subroutine pmatrix(N, nodes, D)
46
47 !  ---------
48 !  Arguments
49 !  ---------
50
51 integer, intent(out)                              :: N
52 real(kind=RP), dimension(0:N), intent(out)       :: nodes
53 real(kind=RP), dimension(0:N,0:N), intent(out)   :: D
54
55 !  ---------------
56 !  Local Variables
57 !  ---------------
58
59 integer                            :: i, j
60 real(kind=RP), dimension(0:N)      :: baryWeights
61
62 call BarycentricWeights(N,nodes,baryWeights)
63
64 do i=0,N
65 D(i,i) = 0.0_RP
66   do j=0,N
67    if(j /= i)  then
68     D(i,j)=baryWeights(j)/(baryWeights(i)*(nodes(i)-nodes(j)))
69     D(i,i) = D(i,i)-D(i,j)
70    end if
71   end do
72 end do
73
74 end subroutine pmatrix
75
76 !  -------------------------------------------------------------
77 !  Compute the derivative matrix for the Chebyshev Rational
78 !  polynomials
79 !  -------------------------------------------------------------
80
81 subroutine dmatrix_r(Dmapped1, xmapped1, N)
82
83 !  ---------
84 !  Arguments
85 !  ---------
86
87 integer, intent(in)                                :: N
88 real(kind=RP), dimension(0:N)                      :: xmapped
89 real(kind=RP), dimension(0:N,0:N)                  :: Dmapped
```

```
90  real(kind=RP), dimension(0:N), intent(out)      :: xmapped1
91  real(kind=RP), dimension(0:N,0:N), intent(out) :: Dmapped1
92
93  !  ---------------
94  !  Local Variables
95  !  ---------------
96
97  integer:: i
98  real(kind=RP), dimension(0:N)      :: x
99  real(kind=RP), dimension(0:N,0:N) :: D
100
101 !  ----------------------------
102 !  Compute Chebyshev Gauss nodes
103 !  ----------------------------
104
105 do i=0,N
106     x(N-i) = dcos((2d0*i+1d0)*PI/(2d0*N+2d0))
107 end do
108
109 !  ----------------------------
110 !  Compute Derivate Matrix for
111 !  Chebyshev Gauss nodes
112 !  ----------------------------
113
114 call pmatrix(N, x, D)
115
116 !  ---------------------------------------
117 !  Map nodes from [-1,1] to [0,inf]
118 !  ---------------------------------------
119
120 do i=0,N
121     xmapped(i) = (1d0+x(i))/(1d0-x(i))
122 end do
123
124 !  -----------------------------------------------
125 !  Use chain rule to generate the Derivative Matrix
126 !  for Chebyshev rational polynomials
127 !  -----------------------------------------------
128
129 do i=0,N
130     Dmapped(i,:) = D(i,:)*0.5d0*(-1d0+x(i))**2d0
131 end do
132
133 do i=0,N
134     xmapped1(i) = xmapped(i)+1d0
135 end do
```

```
136
137 do i=0,N
138     Dmapped1(i,:) = Dmapped(i,:)
139 end do
140
141 end subroutine dmatrix_r
142
143 end module nodesandmatrices_r
```

module nodesandmatrices_phi

```
1  module nodesandmatrices_phi
2
3  use SMConstants
4  implicit none
5
6  contains
7
8  !  ------------------------------------------------------------
9  !  Compute the barycentric weights for polynomial interpolation
10 !  ------------------------------------------------------------
11
12 subroutine bweights(N, x, w)
13
14 !  ---------
15 !  Arguments
16 !  ---------
17
18 integer                                        :: N
19 real(kind=RP), dimension(0:N), intent(in)  :: x
20 real(kind=RP), dimension(0:N), intent(out) :: w
21
22 !  ---------------
23 !  Local Variables
24 !  ---------------
25
26 integer :: j, k
27
28 w = 1.0_RP
29 do j=1,N
30  do k=0,j-1
31       w(k) = w(k)*(x(k)-x(j))
32       w(j) = w(j)*(x(j)-x(k))
33  end do
34 end do
```

```
35
36 w = 1.0_RP/w
37
38 end subroutine bweights
39
40 !  ------------------------------
41 !  Compute the derivative matrix.
42 !  D(i,j) = \prime \ell_j(x_i)
43 !  ------------------------------
44
45 subroutine pmatrix(N, nodes, D)
46
47 !  ---------
48 !  Arguments
49 !  ---------
50
51 integer                              , intent(out) :: N
52 real(kind=RP), dimension(0:N)        , intent(out) :: nodes
53 real(kind=RP), dimension(0:N,0:N), intent(out) :: D
54
55 !  ---------------
56 !  Local Variables
57 !  ---------------
58
59 integer                              :: i, j
60 real(kind=RP), dimension(0:N)   :: baryWeights
61
62 call BarycentricWeights(N,nodes,baryWeights)
63
64 do i=0,N
65 D(i,i) = 0.0_RP
66  do j=0,N
67   if(j /= i)  then
68    D(i,j)=baryWeights(j)/(baryWeights(i)*(nodes(i)-nodes(j)))
69    D(i,i) = D(i,i)-D(i,j)
70   end if
71  end do
72 end do
73
74 end subroutine pmatrix
75
76 !  ------------------------------------------------------------
77 !  Compute the derivative matrix for the Chebyshev Rational
78 !  polynomials
79 !  ------------------------------------------------------------
80
```

```
81  subroutine dmatrix_phi(Dmapped, xmapped, N)
82
83  !  ---------
84  !  Arguments
85  !  ---------
86
87  integer, intent(in)                                :: N
88  real(kind=RP), dimension(0:N), intent(out)         :: xmapped
89  real(kind=RP), dimension(0:N,0:N), intent(out) :: Dmapped
90
91  !  ---------------
92  !  Local Variables
93  !  ---------------
94
95  integer :: i
96  real(kind=RP), dimension(0:N)      :: x
97  real(kind=RP), dimension(0:N,0:N) :: D
98
99  !  -----------------------------
100 !  Compute Chebyshev Gauss nodes
101 !  -----------------------------
102
103 do i=0,N
104     x(N-i) = dcos((2d0*i+1d0)*PI/(2d0*N+2d0))
105 end do
106
107 !  -----------------------------
108 !  Compute Derivate Matrix for
109 !  Chebyshev Gauss nodes
110 !  -----------------------------
111
112 call PDerivativeMatrix( N, x, D )
113
114 !  ---------------------------------------
115 !  Map nodes from [-1,1] to [0,pi]
116 !  ---------------------------------------
117
118 do i=0,N
119     xmapped(i) = (pi/2d0)*(x(i)+1d0)
120 end do
121
122 !  -------------------------------------------------
123 !  Use chain rule to generate the Derivative Matrix
124 !  for Chebyshev rational polynomials
125 !  -------------------------------------------------
126
```

```
127 do i=0,N
128     Dmapped(i,:) = (2d0/pi)*D(i,:)
129 end do
130 
131 end subroutine dmatrix_phi
132 
133 end module nodesandmatrices_phi
```

subroutine resolution

```
1  subroutine resolution(N, D_r, D_theta, D2_r, D2_theta , r, ...
2                        theta, A_D2r, A_Dr,A_D2theta,A_Dtheta)
3  
4  use nodesandmatrices_r
5  use nodesandmatrices_phi
6  
7  implicit none
8  
9  !  ---------------
10 !  Arguments
11 !  ---------------
12 
13 integer, intent(in)         :: N
14 real(kind=RP), intent(in)  :: D2_r(1:N+1,1:N+1), r(1:N+1), ...
15                                 D2_theta(1:N+1,1:N+1), ...
16                                 theta(1:N+1)
17 real(kind=RP), intent(in)  :: D_r(1:N+1,1:N+1),
18                                 D_theta(1:N+1,1:N+1), ...
19                                 A_D2r(N*N+2*N+1,N*N+2*N+1)
20 real(kind=RP), intent(in)  :: A_Dr(N*N+2*N+1,N*N+2*N+1), ...
21                                 A_D2theta(N*N+2*N+1,N*N+2*N+1),
22                                 A_Dtheta(N*N+2*N+1,N*N+2*N+1)
23 
24 !  ---------
25 !  Local variables
26 !  ---------
27 
28 real(kind=RP)               :: t, dt, c, sigma_s, sigma_o, ...
29                                 kappa_s
30 real(kind=RP)               :: U(1:N+1,1:2*(N+1)), ...
31                                 V1(1:N+1,1:N+1), ...
32                                 V2(1:N+1,1:N+1)
33 real(kind=RP), parameter    :: rho=1d3, eps=1.3d-3, ...
34                                 c_p=3111d0, omega=5d5, ...
35                                 Vo=28d0/dsqrt(2d0), 5kappa_o=1d0
```

```
36 real(kind=RP), parameter   :: sigma_gs=2d-2, sigma_go=0.5d0, ...
37                               kappa_go=0.531d0, kappa_gs=1.4d-3
38 integer                    :: i, j, counter
39
40 !  ---------------------------------------
41 !  Function definition
42 !  ---------------------------------------
43
44 interface
45
46 function F (N, U, V1, V2, t, D_r, D_theta, D2_r, D2_theta, ...
47             r, theta)
48
49 use nodesandmatrices_r
50 use nodesandmatrices_theta
51
52 integer, intent(in)         :: N
53 real(kind=RP), intent(in)   :: t, U(1:N+1,1:2*(N+1)), ...
54                                r(1:N+1), theta(1:N+1), ...
55                                V1(1:N+1,1:N+1)
56 real(kind=RP), intent(in)   :: D2_r(1:N+1,1:N+1), ...
57                                D2_theta(1:N+1,1:N+1), ...
58                                V2(1:N+1,1:N+1)
59 real(kind=RP), intent(in)   :: D_r(1:N+1,1:N+1), ...
60                                D_theta(1:N+1,1:N+1)
61 real(kind=RP)               :: F(1:N+1,1:2*(N+1))
62
63 end function F
64
65 end interface
66
67 c = kappa_go/(rho*eps**(2d0)*c_p)
68
69 dt  = 0.5*0.01d0*(1d0/(10*10))/4d0 !Time step
70
71 !  ---------------------------------------
72 !  Initial conditions
73 !  ---------------------------------------
74
75 t = 0d0
76
77 do i=1,N+1
78  do j=1,2*(N+1)
79      U(i,j) = 0d0
80  end do
81 end do
```

```
82
83 write (1,*) t, U(:,:)
84
85 !  ---------------------------------------
86 !  Integration of the system
87 !  ---------------------------------------
88
89 counter = 0
90
91 do while (t <= 60d0*c)
92    call eliptic(N, U, V1, V2, r, theta, A_D2r, A_Dr, ...
93                 A_D2theta,A_Dtheta, t, D_theta)
94    call RK4(N, U, V1, V2, t, F, dt, D_r, D_theta, D2_r, ...
95             D2_theta, r, theta)
96      counter = counter + 1
97       if (mod(counter,2000)==0) then
98         write (1,*) t, U(:,:)
99       end if
100 end do
101
102 end subroutine resolution
```

subroutine elliptic

```
1  subroutine elliptic(N, U, V1, V2, r, theta, A_D2r, A_Dr, ...
2                      A_D2theta, A_Dtheta, t, D_theta)
3
4  use nodesandmatrices_r
5  use nodesandmatrices_phi
6
7  implicit none
8
9  !  ---------------
10 !  Arguments
11 !  ---------------
12
13 integer, intent(in)         :: N
14 real(kind=RP), intent(in)  :: r(1:N+1), theta(1:N+1), ...
15                                 D_theta(1:N+1,1:N+1)
16 real(kind=RP), intent(in)  :: U(1:N+1,1:2*(N+1)), ...
17                                 A_D2r(1:N*N+2*N+1,1:N*N+2*N+1)
18 real(kind=RP), intent(in)  :: A_Dr(1:N*N+2*N+1,1:N*N+2*N+1),
19                               A_D2theta(1:N*N+2*N+1,1:N*N+2*N+1),
20                               A_Dtheta(1:N*N+2*N+1,1:N*N+2*N+1)
21 real(kind=RP),intent(out) :: V1(1:N+1,1:N+1), V2(1:N+1,1:N+1)
```

```
22
23 !  ---------------
24 !  Local variables
25 !  ---------------
26
27 real(kind=RP)              :: W(1:N*N+2*N+1), ...
28                                B(1:2*(N*N+2*N+1)), ...
29                               A(1:2*(N*N+2*N+1),1:2*(N*N+2*N+1))
30 real(kind=RP)              :: W_r(1:N*N+2*N+1), ...
31                                W_theta(1:N*N+2*N+1), ...
32                                sigma_o, sigma_s, kappa_s, c
33 real(kind=RP)              :: V_t, U_t(1:N+1,1:N+1)
34 real(kind=RP)              :: SOL1(1:N*N+2*N+1), ...
35                                SOL2(1:N*N+2*N+1)
36 real(kind=RP), parameter   :: rho=1d3, eps=1.3d-3, ...
37                                c_p=3111d0, omega=5d5, ...
38                                Vo=28d0/dsqrt(2d0)
39 real(kind=RP), parameter   :: sigma_gs=2d-2, sigma_go=0.5d0, ...
40                                kappa_go=0.531d0, ...
41                                kappa_gs=1.4d-3, kappa_o=1d0
42 integer                    :: i, j, l, m, p, q, INFO
43 integer                    :: LDA, LDB, NRHS,...
44                                IPIV(1:2*(N*N+2*N+1))
45
46 sigma_o = sigma_go*Vo*Vo/(kappa_go*(100d0-37d0))
47 sigma_s = sigma_gs*Vo*Vo/kappa_go
48 kappa_s = kappa_gs/kappa_go
49 c = kappa_go/(rho*eps**(2d0)*c_p)
50
51 V_t=1d0    !RMS Voltage
52
53 LDA=2*(N*N+2*N+1)
54 LDB=2*(N*N+2*N+1)
55 NRHS=1
56
57 do i=1,N+1
58  do j=1,N+1
59       U_t(i,j) = U(i,j)
60  end do
61 end do
62
63 W = reshape(U_t, (/N*N+2*N+1/) )
64
65 W_r = matmul(A_Dr,W)
66 W_theta = matmul(A_Dtheta,W)
67
```

```
68 !  ---------------------------------------
69 !  Cardiac tissue
70 !  ---------------------------------------
71
72 do i=1,2*(N*N+2*N+1)
73  do j=1,2*(N*N+2*N+1)
74       A(i,j) = 0d0
75  end do
76 end do
77
78 do i=1,2*(N*N+2*N+1)
79      B(i) = 0d0
80 end do
81
82 do i=1,N*N+2*N+1
83  do j=1,N*N+2*N+1
84
85    l=mod(i,N+1)
86    m=mod(j,N+1)
87    p=int(i/(N+1))+1
88    q=int(j/(N+1))+1
89
90   if (l==0) then
91     l=N+1
92     p=p-1
93   end if
94
95 !  ---------------------------------------
96 !  Compatibility condition
97 !  ---------------------------------------
98
99   if (p==1) then
100
101     A(i,j) = 0
102     A(i,i) = 1d0
103     A(i,i+N*N+2*N+1) = -1d0
104
105    else if (p==N+1) then
106
107     A(i,j) = 0
108     A(i,i) = 1d0
109     A(i,i+N*N+2*N+1) = -1d0
110
111    else
112
113   A(i,j) = (sigma_o+sigma_s*W(i))*(A_D2r(i,j)+ ...
```

```
114             (2d0/r(l))*A_Dr(i,j)+...
115             (1d0/(r(l)*r(l)))*A_D2theta(i,j)+ ...
116             (1d0/(r(l)*r(l)*dtan(theta(p))))*A_Dtheta(i,j)) +...
117             sigma_s*(W_r(i)*A_Dr(i,j)+...
118             (1d0/(r(l)*r(l)))*W_theta(i)*A_Dtheta(i,j))
119
120   end if
121
122   if (l==1) then
123
124     A(i,:) = 0
125
126    else if (l==N+1) then
127
128     A(i,:) = 0
129
130   end if
131
132  end do
133 end do
134
135
136 !  ---------------------------------------
137 !  Blood
138 !  ---------------------------------------
139
140
141 do i=N*N+2*N+2,2*(N*N+2*N+1)
142  do j=N*N+2*N+2,2*(N*N+2*N+1)
143
144    l=mod(i-(N*N+2*N+1),N+1)
145    m=mod(j-(N*N+2*N+1),N+1)
146    p=int((i-(N*N+2*N+1))/(N+1))+1
147    q=int((j-(N*N+2*N+1))/(N+1))+1
148
149   if (l==0) then
150     l=N+1
151     p=p-1
152   end if
153
154 !  ---------------------------------------
155 !  Compatibility condition
156 !  ---------------------------------------
157
158   if (p==1) then
159
```

```
160       A(i,j) = A_Dtheta(i-(N*N+2*N+1),j-(N*N+2*N+1))
161       A(i,j-(N*N+2*N+1)) = A_Dtheta(i-(N*N+2*N+1),j-(N*N+2*N+1))
162
163      else if  (p==N+1) then
164
165       A(i,j) = A_Dtheta(i-(N*N+2*N+1),j-(N*N+2*N+1))
166       A(i,j-(N*N+2*N+1)) = A_Dtheta(i-(N*N+2*N+1),j-(N*N+2*N+1))
167
168      else
169
170  A(i,j) = A_D2r(i-(N*N+2*N+1),j-(N*N+2*N+1))+...
171           (2d0/r(l))*A_Dr(i-(N*N+2*N+1),j-(N*N+2*N+1))+...
172    (1d0/(r(l)*r(l)))*A_D2theta(i-(N*N+2*N+1),j-(N*N+2*N+1))+...
173           (1d0/(r(l)*r(l)*dtan(theta(p))))* ...
174           A_Dtheta(i-(N*N+2*N+1),j-(N*N+2*N+1))
175
176    end if
177
178    if (l==1) then
179
180       A(i,:) = 0
181
182      else if (l==N+1) then
183
184       A(i,:) = 0
185
186      end if
187   end do
188  end do
189
190  !  ---------------------------------------
191  !  Boundary conditions
192  !  ---------------------------------------
193
194  do i=1,N*N+2*N+1
195   do j=1,N*N+2*N+1
196
197      l=mod(i,N+1)
198      m=mod(j,N+1)
199      p=int(i/(N+1))+1
200      q=int(j/(N+1))+1
201
202    if (l==0) then
203       l=N+1
204       p=p-1
205    end if
```

```
206
207    if (l==1) then
208      A(i,j) = 0
209      A(i,i) = 1d0
210      B(i) = V_t
211    end if
212
213    if (l==N+1) then
214      A(i,j) = 0
215      A(i,i) = 1d0
216      B(i) = 0d0
217    end if
218
219   end do
220  end do
221
222  do i=N*N+2*N+2,2*(N*N+2*N+1)
223   do j=N*N+2*N+2,2*(N*N+2*N+1)
224
225     l = mod(i-(N*N+2*N+1),N+1)
226     m = mod(j-(N*N+2*N+1),N+1)
227     p = int((i-(N*N+2*N+1))/(N+1))+1
228     q = int((j-(N*N+2*N+1))/(N+1))+1
229
230    if (l==0) then
231      l=N+1
232      p=p-1
233    end if
234
235    if (l==1) then
236      A(i,j) = 0
237      A(i,i) = 1d0
238      B(i) = V_t
239    end if
240
241    if (l==N+1) then
242      A(i,j) = 0
243      A(i,i) = 1d0
244      B(i) = 0d0
245    end if
246
247   end do
248  end do
249
250  call DGESV (2*(N*N+2*N+1), NRHS, A, LDA, IPIV, B, LDB, INFO)
251
```

```
252 do i=1,N*N+2*N+1
253     SOL1(i) = B(i)
254 end do
255
256 do i=N*N+2*N+2,2*(N*N+2*N+1)
257     SOL2(i-N*N-2*N-1) = B(i)
258 end do
259
260 V1 = reshape(SOL1, (/N+1,N+1/))
261 V2 = reshape(SOL2, (/N+1,N+1/))
262
263 end subroutine elliptic
```

subroutine RK4

```
1  subroutine RK4(N, U, V1, V2, t, F, dt, D_r, D_theta, D2_r, ...
2                 D2_theta, r, theta)
3
4  !  ---------------------------------------
5  !  4th order Runge-Kutta scheme
6  !  ---------------------------------------
7
8  use nodesandmatrices_r
9  use nodesandmatrices_phi
10
11 implicit none
12
13 !  ---------------------------------------
14 !  Function definition
15 !  ---------------------------------------
16
17 interface
18
19 function F ( N, U, V1, V2, t, D_r, D_theta, D2_r, D2_theta, ...
      r, theta)
20
21 use nodesandmatrices_r
22 use nodesandmatrices_theta
23
24 integer, intent(in)         :: N
25 real(kind=RP), intent(in)  :: t, U(1:N+1,1:2*(N+1)), ...
26                                r(1:N+1), theta(1:N+1)
27 real(kind=RP), intent(in)  :: D2_r(1:N+1,1:N+1), ...
28                                D2_theta(1:N+1,1:N+1)
29 real(kind=RP), intent(in)  :: D_r(1:N+1,1:N+1), ...
```

```
30                                  D_theta(1:N+1,1:N+1), ...
31                                  V1(1:N+1,1:N+1), V2(1:N+1,1:N+1)
32  real(kind=RP)                :: F(1:N+1,1:2*(N+1))
33
34  end function F
35
36  end interface
37
38  !  ---------------
39  !  Arguments
40  !  ---------------
41
42  integer, intent(in)            :: N
43  real(kind=RP), intent(in)      :: D2_r(1:N+1,1:N+1), ...
44                                    r(1:N+1), ...
45                                    D2_theta(1:N+1,1:N+1), ...
46                                    theta(1:N+1)
47  real(kind=RP), intent(in)      :: D_r(1:N+1,1:N+1), ...
48                                    D_theta(1:N+1,1:N+1)
49  real(kind=RP), intent(inout)   :: t, dt
50  real(kind=RP), intent(inout)   :: U(1:N+1,1:2*(N+1)), ...
51                                    V1(1:N+1,1:N+1), ...
52                                    V2(1:N+1,1:N+1)
53
54  !  ---------------
55  !  Local variables
56  !  ---------------
57
58  real(kind=RP) :: k1(1:N+1,1:2*(N+1)), k2(1:N+1,1:2*(N+1)), ...
59                   k3(1:N+1,1:2*(N+1)), k4(1:N+1,1:2*(N+1))
60  real(kind=RP) :: U_m1, U_m2
61  integer       :: i, j, k
62
63  !  ------------------------------------
64  !  Computation of the ks
65  !  ------------------------------------
66
67  k1 = F (N, U, V1, V2, t, D_r, D_theta, D2_r, D2_theta, r, ...
68          theta)
69  k2 = F (N, U + (dt*k1)/2d0,V1, V2, t + dt/2d0, D_r, ...
70          D_theta, D2_r, D2_theta, r, theta)
71  k3 = F (N, U + (dt*k2)/2d0, V1, V2, t + dt/2d0, D_r, ...
72          D_theta, D2_r, D2_theta, r, theta)
73  k4 = F (N, U + dt*k3, V1, V2, t + dt, D_r, ...
74          D_theta, D2_r, D2_theta, r, theta)
75
```

```
76  !  ---------------------------------------
77  !  Final value of U
78  !  ---------------------------------------
79
80  U = U + (dt/6d0)*(k1 + 2d0*k2 + 2d0*k3 + k4)
81
82  t=t+dt
83
84  !  ---------------------------------------
85  !  Compatibility conditions
86  !  ---------------------------------------
87
88  do i=1,N+1
89
90       U_m1=(U(i,1)+U(i,N+2))/2d0
91
92       U(i,1) = U_m1
93       U(i,N+2) =U(i,1)
94
95       U_m2 = (U(i,N+1)+U(i,2*(N+1)))/2d0
96
97       U(i,N+1) = U_m1
98       U(i,2*(N+1)) = U(i,N+1)
99
100 end do
101
102 !  ---------------------------------------
103 !  Dirichlet BCs at r=1 and r=inf
104 !  ---------------------------------------
105
106 do i=1,2*(N+1)
107      U(1,i) = 0d0
108      U(N+1,i) = 0d0
109 end do
110
111 end subroutine RK4
```

function F

```
1  function F (N, U, V1, V2, t, D_r, D_theta, D2_r, ...
2              D2_theta, r, theta)
3
4  !  ---------------------------------------
5  !  System of ODEs
6  !  ---------------------------------------
```

```
7
8  use nodesandmatrices_r
9  use nodesandmatrices_phi
10
11 integer, intent(in)        :: N
12 real(kind=RP), intent(in) :: t, U(1:N+1,1:2*(N+1)), ...
13                                 r(1:N+1), theta(1:N+1), ...
14                                 V1(1:N+1,1:N+1), ...
15                                 V2(1:N+1,1:N+1)
16 real(kind=RP)              :: F(1:N+1,1:2*(N+1)), ...
17                                 D_1ir(1:N+1), ...
18                                 D_1itheta(1:N+1), sigma_o, ...
19                                 sigma_s, c, kappa_s
20 real(kind=RP)              :: sigma_b, w, v, ...
21                                 V2_theta(1:N+1), v_r, ...
22                                 v_theta, k_b, c_b, rho_b, alpha_b
23 real(kind=RP)              :: U_r(1:N+1), D_2ir(1:N+1), ...
24                                 U_theta(1:N+1), ...
25                                 D_2itheta(1:N+1), V1_r(1:N+1), ...
26                                 V1_theta(1:N+1), V2_r(1:N+1)
27 real(kind=RP), intent(in) :: D2_r(1:N+1,1:N+1), ...
28                                 D2_theta(1:N+1,1:N+1)
29 real(kind=RP), intent(in) :: D_r(1:N+1,1:N+1), ...
30                                 D_theta(1:N+1,1:N+1)
31 real(kind=RP), parameter   :: rho=1d3, eps=1.3d-3, ...
32                                 c_p=3111d0, omega=5d5, ...
33                                 Vo=28d0/dsqrt(2d0), kappa_o=1d0
34 real(kind=RP), parameter   :: sigma_gs=2d-2, sigma_go=0.5d0, ...
35                                 kappa_go=0.531d0, kappa_gs=1.4d-3
36 real(kind=RP), parameter   :: rho_bo=1d3, c_bo=4180d0, ...
37                                 w_o=0.017d0, v_o=4.5d-2, ...
                                      sigma_bo=0.667d0, k_bo=0.541d0
38 integer                    :: i, j, k
39
40
41 sigma_o = sigma_go*Vo*Vo/(kappa_go*(100d0-37d0))
42 sigma_s = sigma_gs*Vo*Vo/kappa_go
43 kappa_s = kappa_gs/kappa_go
44 w = rho_bo*c_bo*eps*eps*w_o/kappa_go
45 sigma_b = sigma_bo*Vo*Vo/(k_bo*(100d0-37d0))
46 v = eps*v_o*rho_bo*c_bo/k_bo
47 k_b=k_bo/kappa_go
48 c_b=c_bo/c_p
49 rho_b=rho_bo/rho
50 alpha_b = k_b/(rho_b*c_b)
51
```

```
52 !  ---------------------------------------
53 !  Cardiac tissue
54 !  ---------------------------------------
55
56 do i=1,N+1
57  do j=1,N+1
58
59     do k=1,N+1
60         D_2ir(k) = D2_r(i,k)
61     end do
62
63     do k=1,N+1
64         D_1ir(k) = D_r(i,k)
65     end do
66
67     do k=1,N+1
68         D_1itheta(k) = D_theta(j,k)
69     end do
70
71     do k=1,N+1
72         D_2itheta(k) = D2_theta(j,k)
73     end do
74
75     do k=1,N+1
76         U_r(k) = U(k,j)
77     end do
78
79     do k=1,N+1
80         U_theta(k) = U(i,k)
81     end do
82
83     do k=1,N+1
84         V1_r(k) = V1(k,j)
85     end do
86
87     do k=1,N+1
88         V1_theta(k) = V1(i,k)
89     end do
90
91 F(i,j) = (kappa_o+kappa_s*U(i,j))*(dot_product(D_2ir,U_r)+...
92           (2d0/r(i))*dot_product(D_1ir,U_r) +...
93           (1d0/(r(i)*r(i)))*dot_product(D_2itheta,U_theta)+...
94           (1d0/(r(i)*r(i)*dtan(theta(j))))*...
95           dot_product(D_1itheta,U_theta))+...
96           kappa_s*(dot_product(D_1ir,U_r)**(2d0)+...
97     (1d0/(r(i)*r(i)))*dot_product(D_1itheta,U_theta)**(2d0))+...
```

```
98      (sigma_o+sigma_s*U(i,j))*(dot_product(D_1ir,V1_r)**(2d0)+...
99      (1d0/(r(i)*r(i)))*dot_product(D_1itheta,V1_theta)**(2d0))-...
100           w*U(i,j)
101   end do
102   end do
103
104   !  ---------------------------------------
105   !  Blood
106   !  ---------------------------------------
107
108   do i=1,N+1
109    do j=N+2,2*(N+1)
110
111      do k=1,N+1
112          D_2ir(k) = D2_r(i,k)
113      end do
114
115      do k=1,N+1
116          D_1ir(k) = D_r(i,k)
117      end do
118
119      do k=1,N+1
120          D_1itheta(k) = D_theta(j-N-1,k)
121      end do
122
123      do k=1,N+1
124          D_2itheta(k) = D2_theta(j-N-1,k)
125      end do
126
127      do k=1,N+1
128          U_r(k) = U(k,j)
129      end do
130
131      do k=1,N+1
132          U_theta(k) = U(i,k+N+1)
133      end do
134
135      do k=1,N+1
136          V2_r(k) = V2(k,j-N-1)
137      end do
138
139      do k=1,N+1
140          V2_theta(k) = V2(i,k)
141      end do
142
143      v_r = -v
```

```
144     v_theta = 0
145
146
147  F(i,j) = alpha_b*(-v_r*dot_product(D_1ir,U_r)-...
148        v_theta*(1d0/(r(i)))*dot_product(D_1itheta,U_theta)+
149        dot_product(D_2ir,U_r)+(2d0/r(i))*...
150        dot_product(D_1ir,U_r)+...
151        (1d0/(r(i)*r(i)))*dot_product(D_2itheta,U_theta)+...
152        (1d0/(r(i)*r(i)*dtan(theta(j-N-1))))*...
153        dot_product(D_1itheta,U_theta)+...
154        sigma_b*(dot_product(D_1ir,V2_r)**(2d0)+...
155        (1d0/(r(i)*r(i)))*dot_product(D_1itheta,V2_theta)**(2d0)))
156
157
158  end do
159  end do
160
161  end function F
```

Bibliography

[1] Almendral, J. and Barrio-López, M.T. (2015). «Pulmonary Vein Stenosis After Ablation: The Difference Between Clinical Symptoms and Imaging Findings, and the Importance of Definitions in This Context». *Revista Española de Cardiología, Vol. 68, No. 12, pp. 1085-1091.*

[2] Anfuso, L., Corsi, M and Fasano, A. (2018). «Esophageal Thermal Probes: How Fast Should They Be?». *Matthews Journal of Cardiology, Vol. 3, No. 1, pp. 1-5.*

[3] Antontsev, A.N. y Chipot, M. (1994). «The Thermistor Problem: Existence, Smoothness, Uniqueness, Blowup». *SIAM Journal in Mathematical Analysis, Vol. 25, No. 4, pp. 1128-1156.*

[4] Avitall, B., Mughal, K., Hare, J., Helms, R. and Krum, D. (1997). «The Effects of Electrode-Tissue Contact on Radiofrequency Lesion Generation». *Pacing and Clinigal Electrophysiology, Vol. 20, No. 1, pp. 2899-2910.*

[5] Benchimol, A., Desser, K.B. and Gartlan, J.C. (1972). «Bidirectional Blood Flow Velocity in the Cardiac Chambers and Great Vessels Studied with the Doppler Ultrasonic Flowmeter». *The American Journal of Medicine, Vol. 54, No. 4, pp. 467-473.*

[6] Benjamin, E.J. *et al.* (2019). «Heart Disease and Stroke Statistics - 2019 Update: A Report From the American Heart Association». *AHA Journal of Circulation, Vol. 139, No. 10.*

[7] Berjano, E.J. *et al.* (2006). «Theoretical Modeling for Radiofrequency Ablation: State of the Art and Challenges for the Future». *Biomedical Engineering Online, Vol. 5, No. 24.*

[8] Bodnár, T., Sequeira, A. and Prosi, M. (2011). «On the Shear-Thinning and Viscoelastic Effects of Blood Flow Under Various Flow Rates». *Applied Mathematics and Computation Vol. 217, No. 11, pp. 5055–5067.*

[9] Boyd, J.P.N. (2000). «Chebyshev and Fourier Spectral Methods». Dover Publications.

[10] Calkins *et al.* (1994). «Temperature Monitoring During Radiofrequency Catheter Ablation Procedures Using Closed Loop Control». *AHA Journal of Circulation, Vol. 90, No. 3, pp. 1279-1286.*

[11] Calkins *et al.* (2012). «RS/EHRA/ECAS Expert Consensus Statement on Catheter and Surgical Ablation of Atrial Fibrillation». *Europace, Vol. 14, pp. 528-606.*

[12] Carlson, J, Johansson, R. and Olsson, S.B. (2001). «Classification of Electrocardiographic P-Wave Morphology». *IEEE Transactions on Biomedical Engineering, Vol. 48, No. 4, pp. 401-405.*

[13] Cimatti, G. (2007). «Optimal Control for the Thermistor Problem with a Current Limiting Device». *IMA Journal of Mathematical Control and Information, Vol. 24, pp. 339-345.*

[14] Dautray, R. and Lions, J.L. (2000). «Mathematical Analysis and Numerical Methods for Science and Technology, Volume 5: Evolution Problems II». Springer.

[15] Deneke, T. *et al.* (2011). «Utility of Esophageal Temperature Monitoring During Pulmonary Vein Isolation for Atrial Fibrillation Using Duty-Cycled Phased Radiofrequency Ablation.». *Journal of Vascular Electrophysiology, Vol. 22, No. 3, pp. 255-261.*

[16] Draw it to Know it - Medical & Biological Sciences. «Why is the P wave smaller than the QRS complex?». `https://www.drawittoknowit.com/pop-quizzes/physiology/why-is-the-p-wave-smaller-than-the-qrs-complex`.

[17] Duck, F.A. (1990). «Physical Properties of Tissues. A Comprehensive Reference Book». Academic Press.

[18] Durrer, D., Schoo, L., Schuilenburg, R.M. and Wellens, H.J.J. (1967). «The Role of Premature Beats in the Initiation and the Termination of Supraventricular Tachycardia in the Wolff-Parkinson-White Syndrome». *AHA Journal of Circulation, Vol. 36, No. 5, pp. 644-662.*

[19] Evans, L.C. (2010). «Partial Differential Equations». American Mathematical Society.

[20] Fasano, A., Anfuso, L, Bozzi, S. and Pandozi, C. (2016). «Safety And Necessity Of Thermal Esophageal Probes During Radiofrequency Ablation For The Treatment Of Atrial Fibrillation». *Journal of Atrial Fibrillation, Vol. 9, No. 1, pp. 11-18.*

[21] Forster, K.R. and Schwan, H.P. (1989). «Dielectric Properties of Tissues and Biological Materials: A Critical Review.». *Critical Reviews in Biomedical Engineering, Vol. 17, No. 1, pp. 25-104.*

[22] Ghia, K.K. *et al.* (2009). «A Nationwide Survey on the Prevalence of Atrioesophageal Fistula After Left Atrial Radiofrequency Catheter Ablation». *Journal of Interventional Cardiac Electrophysiology, Vol. 24, pp. 33-36.*

[23] González-Suárez, A. and Berjano, E. (2016). «Comparative Analysis of Different Methods of Modeling the Thermal Effect of Circulating Blood Flow During RF Cardiac Ablation». *IEEE Transactions on Bio-Medical Engineering, Vol. 63, No. 2, pp. 250-259.*

[24] González-Suárez, A., Pérez, J.J. and Berjano, E. (2018). «Should Fluid Dynamics be Included in Computer Models of RF Cardiac Ablation by Irrigated-Tip Electrodes?». *Biomedical Engineering Online, Vol. 17, No. 1.*

[25] Gilbarg, D. and Trudinger, N.S. (2000). «Elliptic Partial Differential Equations of Second Order». Springer.

[26] Haemerich, D. and Webster, J.G. (2005). «Automatic Control of Finite Element Models for Temperature-Controlled Radiofrequency Ablation». *Biomedical Engineering Online, Vol. 4, No. 42, pp. 1-8.*

[27] Haïssaguerre, M. *et al.* (1998). «Spontaneous Initiation of Atrial Fibrillation by Ectopic Beats Originating in the Pulmonary Veins». *The New England Journal of Medicine, Vol. 339, No. 10, pp. 659-666.*

[28] Halm, U. *et al.* (2010). «Thermal eEsophageal Lesions After Radiofrequency Catheter Ablation of Left Atrial Arrhythmias». *American Journal of Gastroenterology, Vol. 105, No. 3, pp. 551-556.*

[29] Higuera, F.J., Liñán, A. and Rodríguez, M. (2005) «Mecánica de Fluidos - Lecciones 1 a 22». Sección de Publicaciones de la Escuela Técnica Superior de Ingeniería Aeronáutica y del Espacio.

[30] Hrynkiv, V. (2009). «Optimal Boundary Control for a Time Dependent Thermistor Problem». *Electronic Journal of Differential Equations, Vol. 2009, No. 83, pp. 1-22.*

[31] Jackman, W.M. *et al.* (1991). «Catheter Ablation of Accesory Atrioventricular Pathways by Radiofrequency Current». *The New England Journal of Medicine, Vol. 324, No. 23, pp. 1605-1611.*

[32] Joseph, J.P. and Rajappan, K. (2011). «Radiofrequency Ablation of Cardiac Arrhythmias: Past, Present and Future». *QJUM: An International Journal of Medicine, Vol. 105, No. 4, pp. 303-314.*

[33] Kaouk, Z., Vahid Shahidi, A., Savard, P. and Molin, F. (1996). «Modelling of Myocardial Temperature Distribution During Radio-Frequency Ablation». *Medical & Biological Engineering & Computing, Vol. 34, No. 2, pp. 165-170.*

[34] Knecht, S. *et al.* (2017). «Reliability of Luminal Oesophageal Temperature Monitoring During Radiofrequency ablation of atrial fibrillation: Insights from Probe Visualization and Oesophageal Reconstruction Using Magnetic Resonance Imaging». *Europace, Vol. 19, No. 7, pp. 1123-1131.*

[35] Kopriva, D.A. (2009). «Implementing Spectral Methods for Partial Differential Equations». Springer.

[36] Kuck, K-H. *et al.* (2012). «A Novel Radiofrequency Ablation Catheter Using Contact Force Sensing: Toccata Study». *Heart Rythhm Journal, Vol. 9, No. 1, pp. 18-23.*

[37] Kumagai, K. *et al.* (2004). «Electrophysiologic Properties of Pulmonary Veins Assessed Using a Multielectrode Basket Catheter». *Journal of the American College of Cardiology, Vol. 43, No. 12, pp. 2281-2289.*

[38] Landau, L.D. and Lifshitz, E.M. (1987). «Fluid Mechanics: Volume 6». Butterworth-Heineman.

[39] Landau, L.D. and Lifshitz, E.M. (1980). «The Classical Theory of Fields: Volume 2». Butterworth-Heineman.

[40] Langberg, J.J. *et al.* (1992). «Temperature Monitoring During Radiofrequency Catheter Ablation of Accessory Pathways». *AHA Journal of Circulation, Vol. 86, No. 5, pp. 1469-1474.*

[41] Martín-Garre, S., Pérez-Castellano, N., Quintanilla, J.G., Ferreiros, J. and Pérez-Villacastín, J. (2015). «Predictores de Pérdida Luminal de las Venas Pulmonares Tras Ablación por Radiofrecuencia». *Revista Española de Cardiología, Vol. 68, No. 12, pp. 1085-1091.*

[42] Morady, F. and Scheinman, M.M. (1984). «Transvenous Catheter Ablation of a Posteroseptal Accessory Pathway in a Patient with the Wolff–Parkinson–White Syndrome». *The New England Journal of Medicine, Vol. 310, No. 11, pp. 310-311.*

[43] The Netlib. «LAPACK Documentation». `http://www.netlib.org/lapack/explore-html/`.

[44] Ouyang, F. *et al.* (2004). «Complete Isolation of Left Atrium Surrounding the Pulmonary Veins: New Insights From the Double-Lasso Technique in Paroxysmal Atrial Fibrillation». *AHA Journal of Circulation, Vol. 110, No. 15, pp. 2090-2096.*

[45] Packer, D.L. *et al.* (2005). «Clinical Presentation, Investigation and Management of Pulmonary Vein Stenosis Complicating Ablation for Atrial Fibrillation». *AHA Journal of Circulation, Vol. 111, No. 5, pp. 546-554.*

[46] Pennes, H.H. (1948). «Analysis of Tissue and Arterial Blood Temperatures in the Resting Human Forearm». *Journal of Applied Physiology, Vol. 1, No. 2, pp. 93-122.*

[47] Qi, Z. *et al.* (2016). «Contact Force-Guided Catheter Ablation for the Trreatment of Atrial Fibrillation. a Meta Analysis of Randomized, Controlled Trials». *Brazilian Journal of Medical and Biological Research, Vol. 49, No. 3.*

[48] Rillig, A. *et al.* (2015). «Modified Energy Settings are Mandatory to Minimize Oesophageal Injury Using the Novel Multipolar Irigated Radiofrequency Ablation Catheter for Pulmonary Vein Isolation». *Europace, Vol. 17, No. 3, pp. 396-402.*

[49] Sánchez-Quintana, D. *et al.* (2005). «Anatomic Relations Between the Esophagus and Left Atrium and Relevance for Ablation of Atrial Fibrillation». *AHA Journal of Circulation, Vol. 112, No. 10, pp. 1400-1405.*

[50] Schutt, D., Berjano, E. and Haemmerich, D. (2009). «Effect of Electrode Thermal Conductivity in Cardiac Radiofrequency Catheter Ablation: A Computational Modeling Study». *International Journal of Hyperthermia Vol. 25, No. 2, pp. 99-107.*

[51] Shi, P. and Shillor, M. (1993). «Exisrence of a Solution to the Stefan Problem with Joule's Heating». *Journal of Differential Equations, Vol. 105, No. 2, pp. 239-263.*

[52] Temam, R. (1976). «Navier-Stokes Equations. Theory and Numerical Analysis». North-Holland.

[53] Tungjitkusolmun, S., Woo, E.J., Cao, H., Tsai, J.Z., Vorperian, V.R. and Webster, J.G. (2002). «Thermal—Electrical Finite Element Modelling for Radio Frequency Cardiac Ablation: Effects of Changes in Myocardial Properties». *Medical & Biological Engineering & Computing Vol. 38, No. 5, pp. 562-568.*

[54] University of Chicago Medical Center . «Arrhythmia Ablation Therapy». `https://www.uchicagomedicine.org/conditions-services/heart-vascular/arrhythmias/treatments/ablation-therapy`.

[55] Valvano, J.W. and Bhabaraju, J.C. (1999). «Thermophysical Properties of Swine Myocardium». *International Journal of Thermophysics, Vol. 20, No. 2, pp. 665-676.*

[56] Yokoyama, S. *et al.* (2008). «Novel Contact Force Sensor Incorporated in Irrigated Radiofrequency Ablation Catheter Predicts Lesion Size and Incidence of Stream Pop and Thrombus». *Circulation, Arrhythmmia and Electrophysiology, Vol. 1, No. 5, pp. 155-159.*

[57] Zellerhoff, S. *et al.* (2010). «Damage to the Esophagus After Atrial Fibrillation Ablation Just the Tip of the Iceberg? High Prevalence of Mediastinal Changes Diagnosed by Endosonography». *Circulation, Arrhythmmia and Electrophysiology, Vol. 3, No. 2, pp. 155-159.*